Theses and Dissertations	1. Thesis and Dissertation Collection, all items

1970-04

Simplified numerical models for the generation of synthetic reflection profiling seismograms and synthetic reflection/refraction seismograms.

Lodge, Charles David

Monterey, California. Naval Postgraduate School

http://hdl.handle.net/10945/15160

SIMPLIFIED NUMERICAL MODELS FOR THE
GENERATION OF SYNTHETIC REFLECTION
PROFILING SEISMOGRAMS AND SYNTHETIC
REFLECTION/REFRACTION SEISMOGRAMS

by

Charles David Lodge

United States
Naval Postgraduate School

THESIS

SIMPLIFIED NUMERICAL MODELS FOR THE GENERATION OF

SYNTHETIC REFLECTION PROFILING SEISMOGRAMS AND

SYNTHETIC REFLECTION/REFRACTION SEISMOGRAMS

by

Charles David Lodge

T132823

April 1970

Simplified Numerical Models for the Generation of

Synthetic Reflection Profiling Seismograms and

Synthetic Reflection/Refraction Seismograms

by

Charles David Lodge
Lieutenant Commander, United States Navy
B.A., Rice University, 1962

Submitted in partial fulfillment of the
requirements for the degree of

MASTER OF SCIENCE IN OCEANOGRAPHY

from the
NAVAL POSTGRADUATE SCHOOL
April 1970

ABSTRACT

Two numerical models were developed which generate synthetic
seismograms in formats similar to those of records obtained in field
exploration. The models solve the hyperbolic wave equations in one
and two dimensions by finite difference approximations in initially
undeformed solution domains of transversely-isotropic layered media
subjected to a time varying, dilatational forcing stress applied at
the surface. A velocity attenuation term was included in the models
to inhibit strong boundary reflections.

The one-dimensional model produces synthetic reflection profiling
seismograms for arbitrary horizontal or dipping layers. The two-
dimensional model generates synthetic reflection/refraction seismograms
for horizontal layered media with arbitrary distribution of wave
velocities, Poisson's ratio and density. Several sample records were
produced for some representative velocity structures. The synthetic
seismograms were interpreted and gross correlation was carried out
as if they were actual field records.

TABLE OF CONTENTS

3

LIST OF TABLES

LIST OF FIGURES

ACKNOWLEDGEMENTS

I. INTRODUCTION

A major problem in exploration geology is the determination of
structural relationships for areas in which the rocks cannot be directly
examined. This is usually a subjective process, involving the extra-
polation of lithologic facies from a region where control is available,
such as surface outcrops, mines or wells, across an unknown or
inaccessible area to another point with known structure. Indications
of subsurface structure, including magnetic, seismic and gravity
measurements as well as interpretation of surface morphological
features, are frequently relied upon to aid this process.

The problem becomes particularly acute in oceanic regions where
the only available control may be continental outcrops several hundreds
of miles away, a few bottom grab samples and shallow sediment cores
and a rough bottom topography. Remote measurements may then become
the only method of initial structure determination.

Frequent use is made of the manner in which the ocean bottom and
sub-bottom rocks reflect and transmit acoustic or seismic energy, not
only for the correlation of near-shore with on shore structures, but
also for initial determination of sub-bottom structures. When con-
ducting seismic exploratory operations, the information obtained is
usually presented as a two-dimensional graph (seismogram) on which
three variables are shown. These variables are: horizontal distance,
time and intensity of energy received. Depth information may be
inferred from the time scale with a known or assumed vertical distri-
bution of sonic velocity. A high level of intensity is usually
assumed to represent a point or surface at which the physical

11

parameters of the media change more or less abruptly, reflecting energy or providing a surface along which energy might be propagated.

Interpretation of the seismograms and the development of a subsurface structure can be aided by the use of a mathematical model of the supposed structure which would produce a synthetic seismogram. The synthetic seismogram could be compared with the field record for correlation.

This paper presents the development of two numerical models which produce synthetic seismograms for layered media subjected to an initial time varying, compressional (dilatational) stress input applied at the surface. The models were designed to have fairly wide variability while remaining simple enough to preclude the use of inordinate computer time and storage requirements. The one-dimensional model produces a reflection profiling seismogram. It is applicable to the case of vertically incident dilatational waves reflected and transmitted by arbitrary bottom profile and sub-bottom layered structure of horizontal or dipping interfaces. The two-dimensional model yields a set of seismograms applicable to a reflection/refraction problem where the receivers are distributed in a horizontal array. Both dilatational and shear stresses are treated. The region modeled is one of horizontal layered media with arbitrary distribution of shear and dilatational wave velocities and of density.

No attempt was made here to include the wide variability of possible media which is an integral part of the large SLAM (Stress waves in LAyered Media) code model developed at the Illinois Institute of Technology (IIT) [Constantino 1969] primarily to treat the neighborhood of high energy (nuclear) explosively generated ground shocks.

12

The IIT model has the capability of simulating a wide variety of conditions but requires a large amount of computing time and space in order to produce a single trace. It is felt that the two models presented here have a greater applicability to marine and terrestrial seismic exploration problems.

These models were developed on the basis of numerical approximations to the solutions of the wave equations in one and two dimensions by finite difference methods. The computer programs were written in the FORTRAN IV language and were run on a dual IBM 360/67 system. The plotting subroutines used to drive a CALCOMP 765 plotter were prepared by the staff of the United States Naval Postgraduate School Computer Facility [1969] .

II. THE SEISMIC REFLECTION PROFILING MODEL

The problem of synthetic seismic profile generation was approached as one of repeated transmission of normally incident longitudinal (dilatational) disturbances through transversely-isotropic media. The seismogram was developed by changing the velocity structure in the solution domain between pulse transmissions, corresponding to a change in position of the shot point as the profiling vessel moves across an area of changing water depth and sub-bottom structure. The solutions are presented as successive traces as though from a pressure hydrophone located at any depth below the shot point.

A. THE MATHEMATICAL MODEL

It was assumed that the wave velocity (C) is continuous throughout the domain and either varies linearly with depth (x) or is constant. Additionally, it was assumed that in transition zones, where the wave velocity does change, density remains constant. Under these assumptions, the equation of motion in one dimension for dilatational waves can be written (modified from Wolf [1937]):

$$E: \qquad \frac{\partial^2 u}{\partial t^2} = \frac{\partial}{\partial x}\left(C^2 \frac{\partial u}{\partial x}\right) + A \frac{\partial u}{\partial t} , \qquad (1)$$

where u is longitudinal particle displacement and A is a velocity attenuation parameter which is a function of x. Carrying out the indicated differentiation of the right side of equation (1) yields:

$$E: \qquad \frac{\partial^2 u}{\partial t^2} = C^2 \frac{\partial^2 u}{\partial x^2} + 2C \frac{\partial c}{\partial x} \frac{\partial u}{\partial x} + A \frac{\partial u}{\partial t} . \qquad (2)$$

14

Four collateral conditions are required in order to complete a well-posed problem. The following conditions were selected:

initial conditions:

I1:
$$U(x, 0) = 0 ,$$
(3)

I2:
$$U_t(x, 0) = 0 ,$$
(4)

boundary conditions:

B1:
$$(L, t) = 0 .$$
(5)

B2:
$$U_x(0, t) = F(t) , \qquad t \leqslant t_1 ,$$
(6a)

$$U_x(0, t) = \qquad , \qquad t > t_1 ,$$
(6b)

where L is the distance to the lower boundary.

The initial conditions allow the solution domain to be initially undeformed and at rest. The first boundary condition requires that displacements are zero for all time at the lower boundary, which then becomes perfectly reflective. The second boundary condition allows a variable stress to be applied to the upper boundary for $t \leqslant t_1$. For $t > t_1$, normal stresses are not transmitted across this boundary. It then becomes a free surface.

The second term on the right side of equation (1), $A \frac{\partial u}{\partial t}$, represesents an attenuation factor, dependent on depth and particle velocity, which was used to reduce the magnitude of the disturbance in the lower regions of the domain so that reflections from the lower boundary would not mask late arriving multiple reflections from points nearer to the surface. The function A(x) is assumed to be zero in the region from which reflections are to be studied.

B. THE SOLUTION DOMAIN

The solution domain (Fig. 1) is divided by N equally spaced mesh points into N-1 subintervals each of length δx. A sample wave velocity distribution is shown in the figure. The upper boundary (x = 0) is shown on the left. In the region $0 \leqslant x \leqslant x_1$, the wave velocity is constant and equal to C1. For $x_2 \leqslant x \leqslant L$, the velocity is equal to C2. In the transition zone, $x_1 < x < x_2$, the velocity varies linearly from C1 to C2.

The time-depth mesh is an array of N by M mesh points. Each rectangular mesh area is then of size δx by δt. This mesh is the full solution domain and the objective of the model is to find a solution of equation (2) at each mesh point under the collateral conditions, equations (3) through (6).

C. THE DIFFERENCE EQUATIONS

A central difference form for each of the partial derivatives in equation (2) can be written in terms of the (i,j) mesh point [Smith 1965]. Figure 2 shows the (i,j) and neighboring mesh points. The required derivatives, in central difference form, become:

$$\frac{\partial u}{\partial t} \doteq \frac{U_{i,j+1} - U_{i,j-1}}{2\delta t} \quad ; \qquad \frac{\partial^2 u}{\partial t^2} \doteq \frac{U_{i,j+1} - 2U_{i,j} + U_{i,j-1}}{\delta t^2} \quad ;$$

$$\frac{\partial u}{\partial x} \doteq \frac{U_{i+1,j} - U_{i-1,j}}{2\delta x} \quad ; \qquad \frac{\partial^2 u}{\partial x^2} \doteq \frac{U_{i+1,j} - 2U_{i,j} + U_{i-1,j}}{\delta x^2} \quad ;$$

$$\frac{\partial c}{\partial x} \doteq \frac{C_{i+1} - C_{i-1}}{2\delta x} \quad .$$
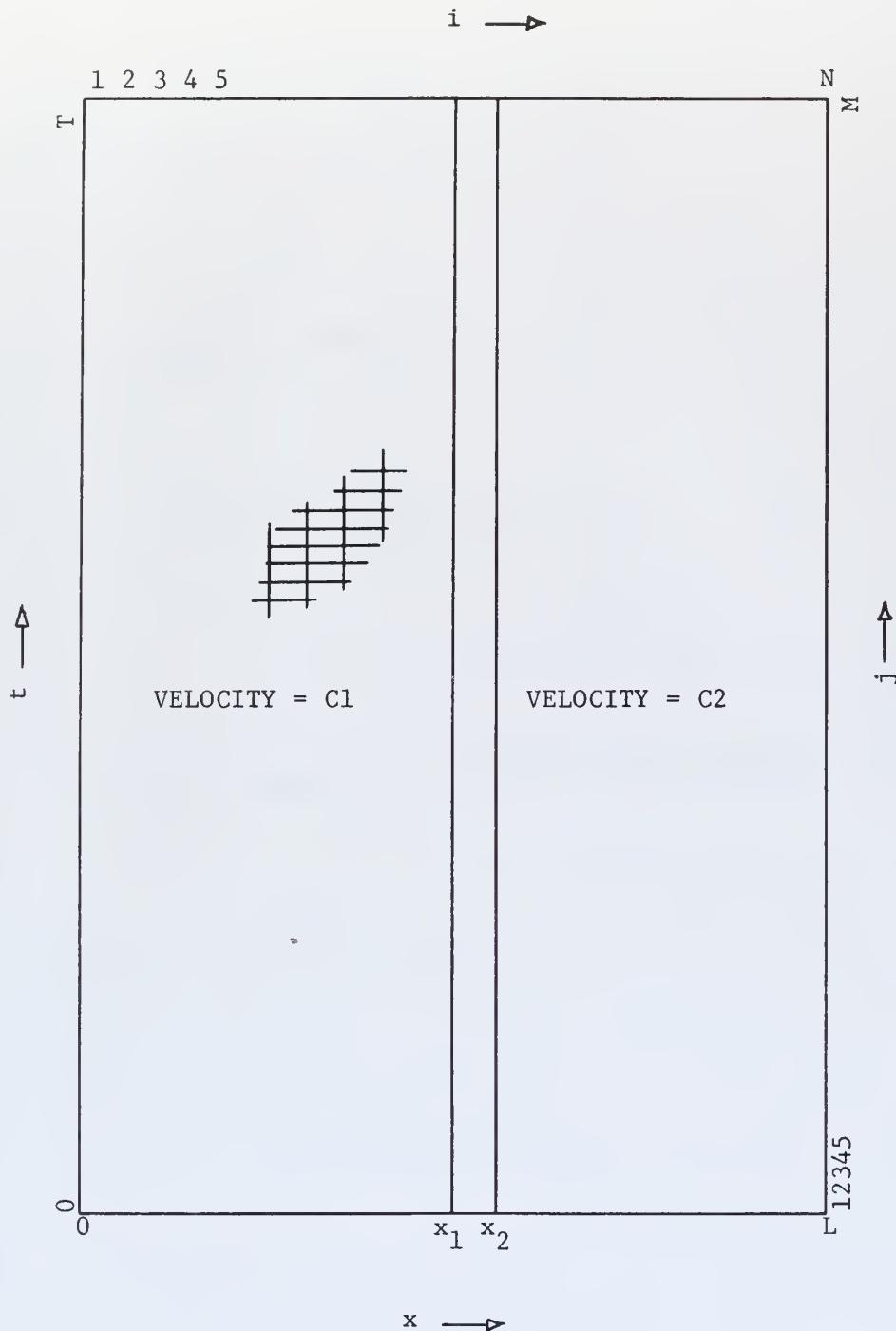
Figure 1. The solution domain
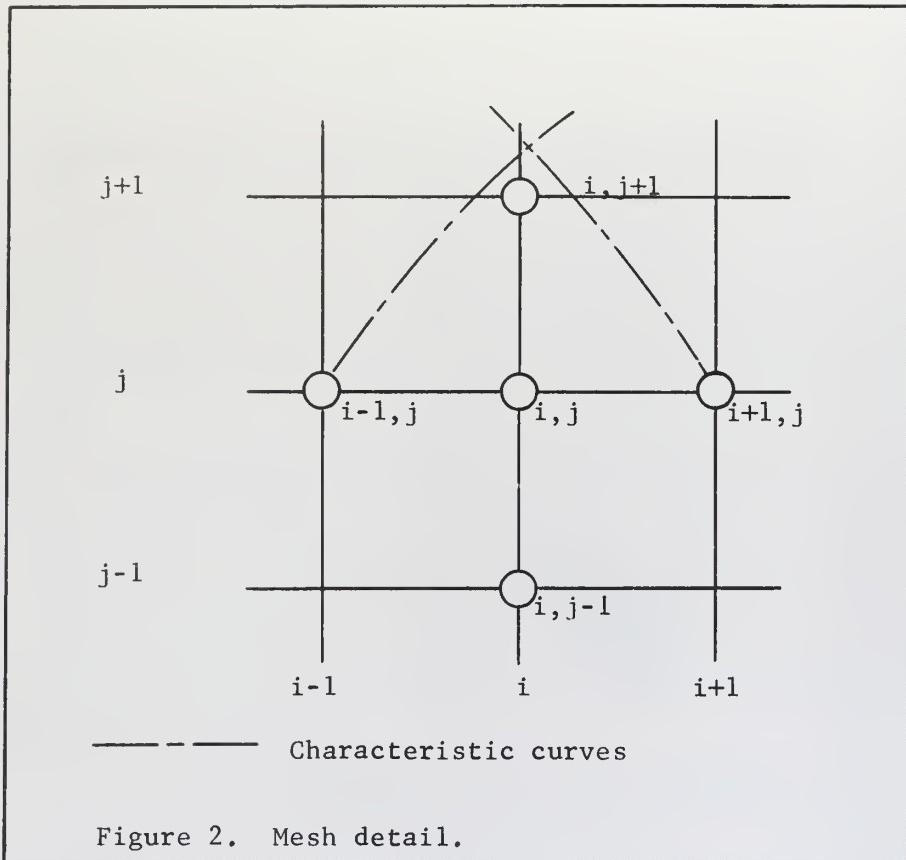
Figure 2. Mesh detail.

Substituting these into equation (2) gives the difference equation of motion for the (i,j) mesh point:

$$\frac{u_{i,j+1} - 2u_{i,j} + u_{i,j-1}}{\delta t^2} = c_i^2 \left(\frac{u_{i+1,j} - 2u_{i,j} + u_{i-1,j}}{\delta x^2} \right)$$

$$+ 2c_i \left(\frac{c_{i+1} - c_{i-1}}{2\delta x} \right) \left(\frac{u_{i+1,j} - u_{i-1,j}}{2\delta x} \right) + A_i \left(\frac{u_{i,j+1} - u_{i,j-1}}{2\delta t} \right) . \tag{7}$$

The collateral conditions become:

I1: $\qquad u_{i,1} = 0$, $\tag{8}$

I2: $\qquad \dfrac{u_{i,2} - u_{i,0}}{2\delta t} = 0$. $\tag{9}$

B1: $\qquad u_{N,j} = 0$. $\tag{10}$

B2: $\qquad \dfrac{u_{2,j} - u_{0,j}}{2\delta x} = F_j$. $\tag{11}$

where $\qquad F_j = F(t)$, $0 \leqslant t \leqslant t_1$,

$$F_j = 0 \quad , \quad t > t_1 .$$

Solving equation (7) for $u_{i,j+1}$ gives:

E: $\quad u_{i,j+1} = \Big[2u_{i,j} \left(1 - c_i^2 R^2 \right) + u_{i+1,j} \left(c_i^2 R^2 + \tfrac{1}{2} c_i (c_{i+1} - c_{i-1}) R^2 \right)$

$$+ u_{i-1,j} \left(c_i^2 R^2 - \tfrac{1}{2} c_i (c_{i+1} - c_{i-1}) R^2 \right)$$

$$- u_{i,j-1} \left(1 + \tfrac{1}{2} A_i \delta t \right) \Big] \Big/ \Big[1 - \tfrac{1}{2} A_i \delta t \Big] \quad , \tag{12}$$

where: $\qquad R^2 = \left(\dfrac{\delta t}{\delta x} \right)^2$.

Writing equation (12) for $j=1$ and substituting $u_{i,0}$ from equation (9) yields the initial conditions:

I1: $\qquad u_{i,1} = 0$. $\tag{8}$

I2: $\qquad u_{i,2} = 0$. $\tag{13}$

Writing equation (12) for i=1 and substituting $u_{o,j}$ from equation (11)

yields the boundary conditions:

B1: $\qquad\qquad U_{N,j+1} = 0$, $\qquad\qquad\qquad\qquad$ (10a)

B2: $\qquad U_{1,j+1} = \left[2 U_{1,j} (1 - C_1^2 R^2) + 2 U_{2,j} (C_1^2 R^2) \right.$

$\qquad\qquad - U_{1,j-1} (1 + \tfrac{1}{2} A_1 \delta t) + F_j \delta t^2 \left(\tfrac{C_1^2}{\delta x} \right) \Big] / \left[1 - \tfrac{1}{2} A_1 \delta t \right]$. $\qquad$ (14)

The equations (12), (8), (13), (10a) and (14) then form a well-

posed problem for numerical solution. Initially, the j=1 and j=2 rows

are set to zero following equations (8) and (13). The j+1 row can then

be solved utilizing equation (10a) for the lower boundary (i=N),

(14) for the upper boundary (i=1) and (12) for the interior points.

Note that the value of u anywhere along the interior of the j+1 row is

dependent only on the values of u at three points along the j row and

one on the j-1 row (shown as circles in Fig. 2).

D. STABILITY AND CONVERGENCE

1. Stability

Because of the large number of arithmetic operations involved

(approximately 10^9 for the solution spaces used), it is necessary to

insure that there is a stable decay of errors introduced in the various

computations. Studies of the stability of the centered difference

formulation of the basic wave equation:

$$\frac{\partial^2 u}{\partial t^2} = C^2 \frac{\partial^2 u}{\partial x^2} , \qquad\qquad (15)$$

have been carried out by several investigators [Smith 1965] . Smith

investigated the stability by the Fourier series method and showed

20

that the centered difference formulation is stable for the mesh ratio:

$$\frac{\delta t}{\delta x} \leqslant \frac{1}{c} . \tag{16}$$

The addition of the velocity gradient and velocity attenuation terms in equation (2) alters the stability conditions somewhat. A large velocity gradient, approaching discontinuous velocity change, generates instability in the gradient region. Investigation of the stability conditions showed that if the condition:

$$\Delta c_i = c_{i+1} - c_{i-1} \leqslant c_i , \tag{17}$$

were imposed on the gradient regions, the requirement on the mesh ratio [equation (16)] becomes:

$$\frac{\delta t}{\delta x} \leqslant \frac{0.89}{c} . \tag{18}$$

The addition of a negative attenuation term tends to decrease the right side of equation (18). This would lead to a more stringent requirement on the mesh ratio. This effect was found to be quite small for the values of $A(x)$ necessary to damp lower boundary reflections. Empirically, it was found that stability would be assured by requiring that:

$$\frac{\delta t}{\delta x} \leqslant \frac{0.95}{c} . \tag{19}$$

2. Convergence

A finite difference scheme is said to be convergent if the exact solution of the difference equations approaches the exact solution of the partial differential equations as δx and δt

21

approach zero together. Forsythe and Wasow [1967] have shown that convergence of a finite difference scheme such as equation (12) with boundary conditions such as equations (8), (13), (10a) and (14) is convergent as long as the mesh ratio is such that the (i, j+1) mesh point lies within the intersection of the characteristics through the (i-1, j) and (i+1, j) mesh points (see Fig. 2). The equation defining the characteristics for equation (2) is:

$$\left(\frac{dx}{dt}\right)^2 = c^2 . \tag{20}$$

This leads to:

$$\frac{dx}{dt} = \pm c . \tag{21}$$

Convergence is then assured for:

$$\frac{\delta t}{\delta x} \leqslant \frac{1}{c} . \tag{16}$$

It is apparent then that as long as equation (19) holds, the finite difference formulation will be both stable and convergent.

E. DESCRIPTION OF THE PROGRAM

The program requires 140K bytes of main core storage. An average run with a 251x1800 mesh grid with 41 shot points requires approximately 13 min of main run time exclusive of output time required for the plotting subroutines.

1. Distribution parameters

The advantage of this model lies in the wide variability of the conditions which may be easily simulated. The primary parameters used to model various conditions are the distribution parameters. They are:

a. wave velocity distribution, C(x,t),

22

b. forcing function, F(t),

c. attenuation parameter, A(x).

The forcing function and the attenuation parameter are put into the model as single-valued, continuous, polygonal line functions of the indicated dependent variable. The wave velocity is put into the model as a two-dimensional array of points which describe the depths to isovelocity layers at successive horizontal stations. Figure 3 shows a sample distribution of isovelocity horizons with horizontal stations and shot points indicated. Horizontal station distances and the velocity defining array for this sample are shown in Tables I and II. At each shot point, the wave velocity is a single-valued, continuous polygonal line function of depth. An example of wave velocity distribution at a single shot point is shown in Fig. 4 along with a sample attenuation parameter and forcing function. The polygons for A(x) and F(t) are defined in Tables III and IV.

2. Numerical parameters

The numerical parameters, which remain constant throughout the problem, are used to control the computation of the distribution parameters and to set the arrangement and size of the solution domain. They are:

a. mesh size in the x direction, (DX),

b. mesh size in the t direction, (DT),

c. horizontal distance between successive solution stations (shot point spacing), (DK),

d. number of total x mesh points, (N),

e. number of total t mesh points, (M),

f. number of solution stations, (KK),

23
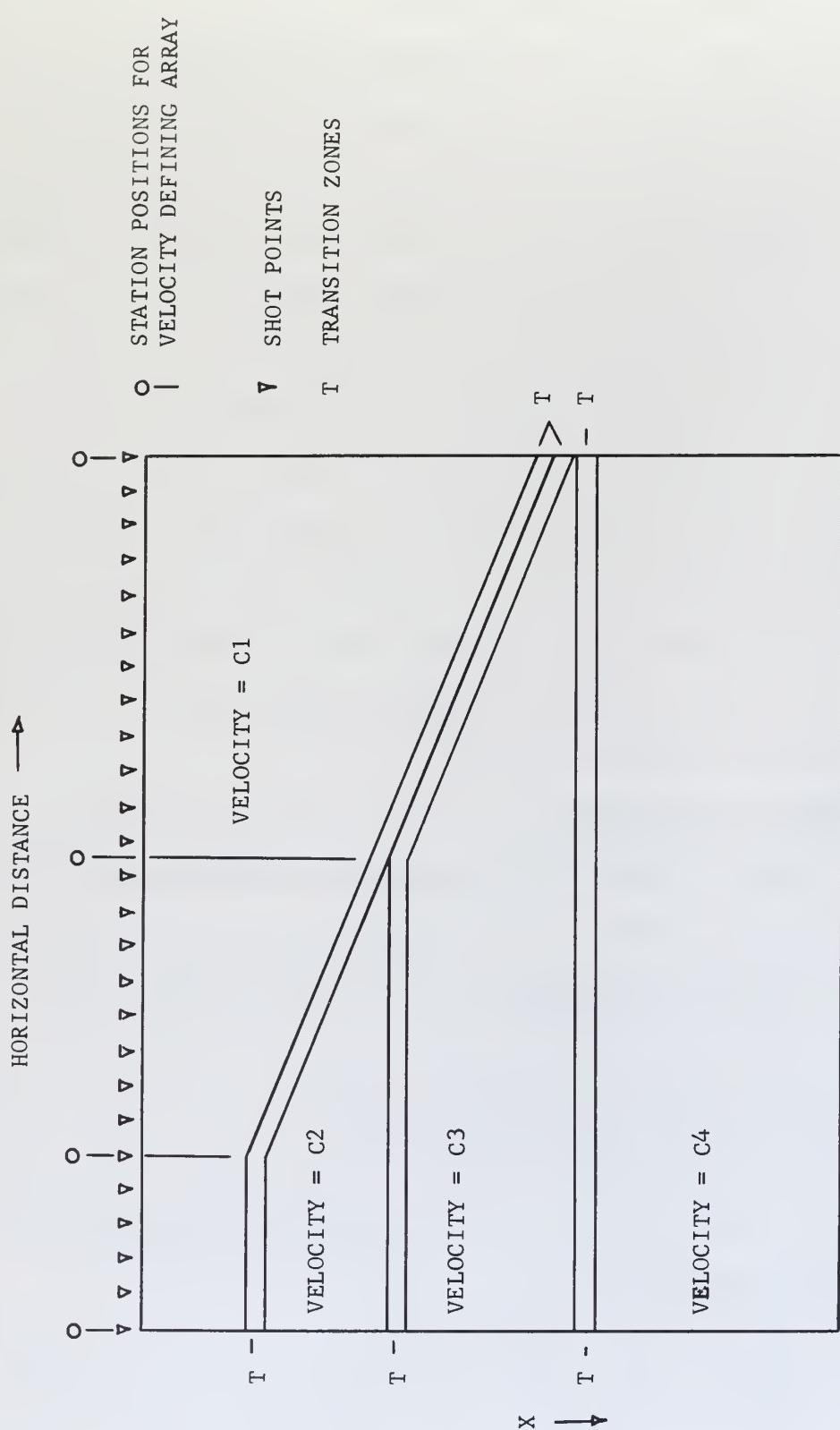
Figure 3. Sample velocity structure for seismic profiling
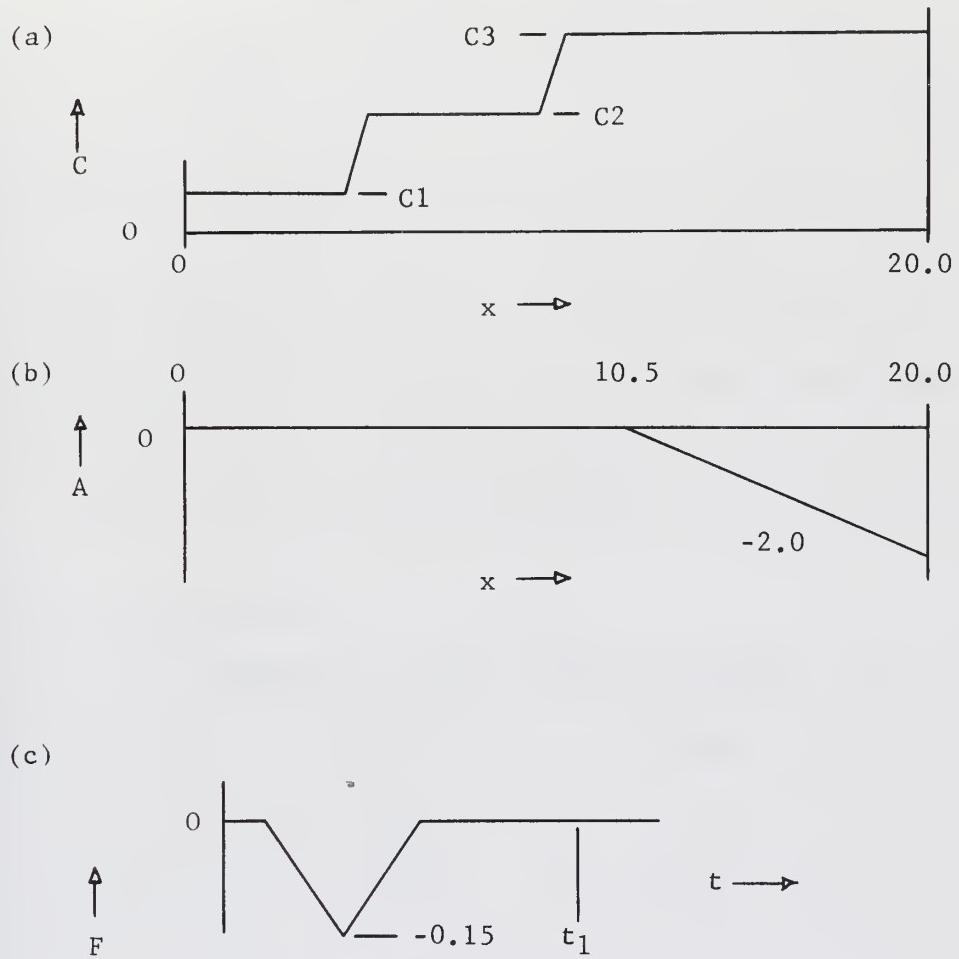
Figure 4. Sample distribution parameters

(a) Wave velocity at one shot point.
(b) Attenuation parameter.
(c) Forcing function.

g. number of points defining the distribution parameter
polygons:

      (1) wave velocity polygon, (NC),

      (2) attenuation parameter polygon, (NA),

      (3) forcing function polygon, (NF),

h. number of horizontal stations in the velocity defining
array, (NG),

i. mesh point at which the output stress is to be measured,
(IP),

j. horizontal distance to the first shot point, (EEE).

Additional numerical parameters are put into the program which
control the size, scale and arrangement of the output traces. For
details of their use see the explanatory notes in the program.

Table I.

Sample horizontal station distances

Station	Distance
1	0.0
2	2.0
3	10.5
4	20.0

Table II.

Sample velocity defining array

| | Station Numbers | | | | |
	1	2	3	4	Velocity
Depth	0.0	0.0	0.0	0.0	C1
to	2.0	2.0	4.5	9.8	C1
isovelocity	2.2	2.2	4.7	10.0	C2
horizons	4.7	4.7	4.7	10.0	C2
	4.9	4.9	4.9	10.2	C3
	20.0	20.0	20.0	20.0	C3

Table III.

Sample attenuation parameter polygon

Depth	A(x)
0.0	0.0
10.5	0.0
20.0	-2.0

Table IV

Sample forcing function polygon

Time	F(t)
0.0	0.0
0.10	0.0
0.40	-0.15
0.70	0.0
2.0	0.0

F. SCALING THE PROBLEM

All wave velocities and depths were put into the model in non-dimensional form. The wave velocity in the upper layer and the depth to the first transition zone were chosen as the definitive values for non-dimensionalizing the problem. Non-dimensional time was then determined by these values through the mesh ratio. Practically, the scale of the problem is determined by the wave velocity values and one of the mesh sizes. In general, the wave velocity is entered as C distance units per time unit. For a mesh ratio of:

$$\frac{\delta t}{\delta x} = \frac{0.025}{0.10} = \frac{1}{4} \quad , \qquad (22)$$

the stability condition [equation (19)] allows the wave velocity to vary from 0.0 to 3.4 distance units per time unit. If a value of C of 0.8 is to represent dilatational wave velocity in water (1.5 km/sec),

then the scale of the problem would depend on a choice of either time
or depth mesh size, chosen in view of the definition desired.   Table V
shows some scales where the time mesh size was specified.

Table V.

Scales available for   C = 0.8 = 1.5 km/sec

Numerical parameters: N = 251, M = 2000

Mesh Size x (m)	t (sec)	Distance Unit (m)	Time Unit (sec)	Seismogram Length (sec)	Depth to Lower Boundary (m)
187.5	.025	1875	1.0	50	46800
75	.010	750	0.4	20	18750
18.75	.0025	187.5	0.1	5	4680
7.5	.001	75	0.04	2	1875
1.875	.00025	18.75	0.01	0.5	468
0.75	.0001	7.5	0.004	0.2	187.5

III.   THE REFLECTION/REFRACTION MODEL

Synthetic reflection/refraction seismogram generation requires solution of the wave equation in at least two dimensions. A rectangular solution space was chosen with three rigid, reflective boundaries and one free boundary corresponding to the air-water or air-ground interface. In order to produce a model with wide variability as well as one that may be easily manipulated without inordinate computer time and storage requirements, it was assumed that the media in the solution space is horizontally isotropic. The y-derivatives of density and Lamé's constants (and hence of shear and dilatational wave velocities) will then be zero.

A.   THE MATHEMATICAL MODEL

It was assumed that density, ρ , and Lame's constants, λ and μ , are continuous throughout the solution domain. Further, it was assumed that density and the dilatational and shear wave velocities, C and S, are either constant or vary linearly with depth. Under these assumptions, the equations of motion in two dimensions for the propagation of shear and dilatational disturbances can be written (modified from Officer [1958] and Takeuchi [1966]):

E1:
$$\rho \frac{\partial^2 u}{\partial t^2} = \frac{\partial}{\partial x}\left[\lambda\left(\frac{\partial u}{\partial x} + \frac{\partial v}{\partial y}\right) + 2\mu\frac{\partial u}{\partial x}\right]$$
$$+ \frac{\partial}{\partial y}\left[\mu\left(\frac{\partial v}{\partial x} + \frac{\partial u}{\partial y}\right)\right] + B\frac{\partial u}{\partial t} , \tag{23}$$

E2:
$$\rho \frac{\partial^2 v}{\partial t^2} = \frac{\partial}{\partial y}\left[\lambda\left(\frac{\partial u}{\partial x} + \frac{\partial v}{\partial y}\right) + 2\mu\frac{\partial v}{\partial y}\right]$$
$$+ \frac{\partial}{\partial x}\left[\mu\left(\frac{\partial v}{\partial x} + \frac{\partial u}{\partial y}\right)\right] + B\frac{\partial u}{\partial t} , \tag{24}$$

where u and v are the particle displacements in the x and y directions and B is a velocity attenuation factor. The stresses are:

Dilatational stress: $\lambda\left(\dfrac{\partial u}{\partial x} + \dfrac{\partial v}{\partial y}\right)$.

Shear stress: $\mu\left(\dfrac{\partial v}{\partial x} + \dfrac{\partial u}{\partial y}\right)$.

These stresses are computed in the program and are used, in addition to displacements, to form the seismograms.

Carrying out the indicated differentiation on the right side of equations (23) and (24) and collecting terms yields:

E1:
$$\frac{\partial^2 u}{\partial t^2} = \left(\frac{\lambda+2\mu}{\rho}\right)\frac{\partial^2 u}{\partial x^2} + \left(\frac{\lambda+\mu}{\rho}\right)\frac{\partial^2 v}{\partial x\partial y} + \frac{\mu}{\rho}\frac{\partial^2 u}{\partial y^2}$$

$$+ \frac{1}{\rho}\frac{\partial\lambda}{\partial x}\left(\frac{\partial u}{\partial x} + \frac{\partial v}{\partial y}\right) + \frac{2}{\rho}\frac{\partial\mu}{\partial x}\frac{\partial u}{\partial x} + \frac{B}{\rho}\frac{\partial u}{\partial t} , \tag{25}$$

E2:
$$\frac{\partial^2 v}{\partial t^2} = \left(\frac{\lambda+2\mu}{\rho}\right)\frac{\partial^2 v}{\partial y^2} + \left(\frac{\lambda+\mu}{\rho}\right)\frac{\partial^2 u}{\partial x\partial y} + \frac{\mu}{\rho}\frac{\partial^2 v}{\partial x^2}$$

$$+ \frac{1}{\rho}\frac{\partial\mu}{\partial x}\left(\frac{\partial v}{\partial x} + \frac{\partial u}{\partial y}\right) + \frac{B}{\rho}\frac{\partial u}{\partial t} , \tag{26}$$

where it has been assumed that:

$$\frac{\partial\lambda}{\partial y} = \frac{\partial\mu}{\partial y} = 0 ,$$

$$\frac{\partial^2 u}{\partial x\partial y} = \frac{\partial^2 u}{\partial y\partial x} , \qquad\qquad \frac{\partial^2 v}{\partial x\partial y} = \frac{\partial^2 v}{\partial y\partial x} .$$

The eight collateral conditions chosen to complete a well-posed problem were:

initial conditions:

I1:
$$U(x,y,0) = 0 \quad , \tag{27}$$

I2:
$$V(x,y,0) = 0 \quad . \tag{28}$$

I3:
$$U_t(x,y,0) = 0 \quad , \tag{29}$$

I4:
$$V_t(x,y,0) = 0 \quad , \tag{30}$$

boundary conditions:

B1:
$$U(x,0,t) = 0 \quad ,$$
$$U(L,y,t) = 0 \quad ,$$
$$U(x,M,t) = 0 \quad , \tag{31}$$

B2:
$$V(x,0,t) = 0 \quad ,$$
$$V(L,y,t) = 0 \quad ,$$
$$V(x,M,t) = 0 \quad , \tag{32}$$

B3:
$$U_x(0,y,t) + V_y(0,y,t) = F(y,t) \quad , \tag{33}$$

where: $F(y,t) = 0$ for $t > t_1$

B4:
$$U_y(0,y,t) + V_x(0,y,t) = 0 \quad . \tag{34}$$

The initial conditions allow the solution space to be initially unde-
formed and at rest. The first two boundary conditions (B1 and B2)
require that displacements are zero for all time at the subsurface
boundaries, which then become perfectly reflective. The other boundary
conditions (B3 and B4) allow the x=0 boundary to become a free surface.
Shear and dilatational stresses are not transmitted across the surface
for all time except for an externally applied, time-varying dilatational
stress, applied at a point or combination of points for $t < t_1$.

As in the one-dimensional model, an attenuation term was included
in the equations of motion (E1 and E2) in order to keep boundary

32

reflections from masking multiple reflections in the central regions. The function $B(x,y)$ is non-zero only in the vicinity of the three rigid boundaries and is zero in areas where disturbances are to be studied.

B. THE SOLUTION DOMAIN

The solution domain is a three-dimensional rectangular array of L by M by N mesh points dividing the domain into (L-1) by (M-1) by (N-1) equal subdivisions, each of size δx by δy by δt. Figure 5 shows the x-y solution space. The total solution domain is formed from N successive solution spaces or planes. A detail of the distance-depth-time mesh in the vicinity of mesh point (i,j,k) is shown in Fig. 6.

C. THE DIFFERENCE EQUATIONS

As in the one-dimensional model, a centered difference form for each partial derivative in equations (25) and (26) can be written. Making use of the definitions for wave velocities:

$$c^2 = \frac{\lambda + 2\mu}{\rho} \, , \tag{35}$$

$$s^2 = \frac{\mu}{\rho} \, , \tag{36}$$

finite difference forms of equations (25) and (26) may be written in terms of wave velocities and their derivatives. Carrying out this substitution and solving for the time leading $(i,j,k+1)$ term for u and v yields:

E1: $\quad U_{i,j,k+1} = \left[2U_{i,j,k} \left(1 - c_i^2 RA - s_i^2 RC \right) + U_{i+1,j,k} \left(c_i^2 + \frac{DL}{4} + \frac{DM}{2} \right) RA \right.$

$\quad + U_{i-1,j,k} \left(c_i^2 - \frac{DL}{4} - \frac{DM}{2} \right) RA + \left(U_{i,j+1,k} + U_{i,j-1,k} \right) s_i^2 RC + VA \left(c_i^2 - s_i^2 \right) RB \qquad (37)$

$\quad + \left(V_{i+1,j,k} - V_{i-1,j,k} \right) RE\, DL - U_{i,j,k-1} \left(1 + \frac{B_{ij}}{2\rho_i} \delta t \right) \right] / \left[1 - \frac{B_{ij}}{2\rho_i} \delta t \right] \, ,$
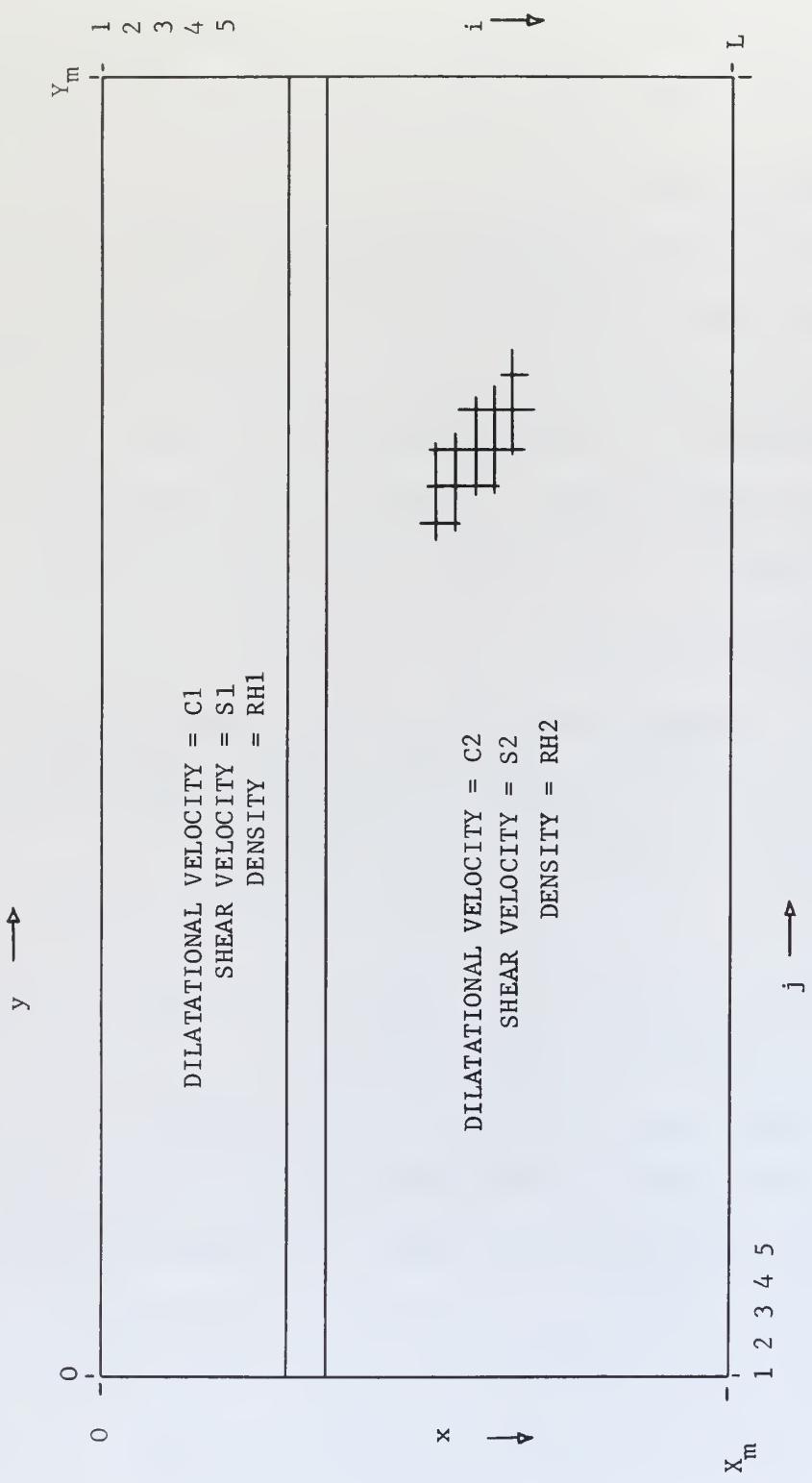
Figure 5. The x-y solution space.

34
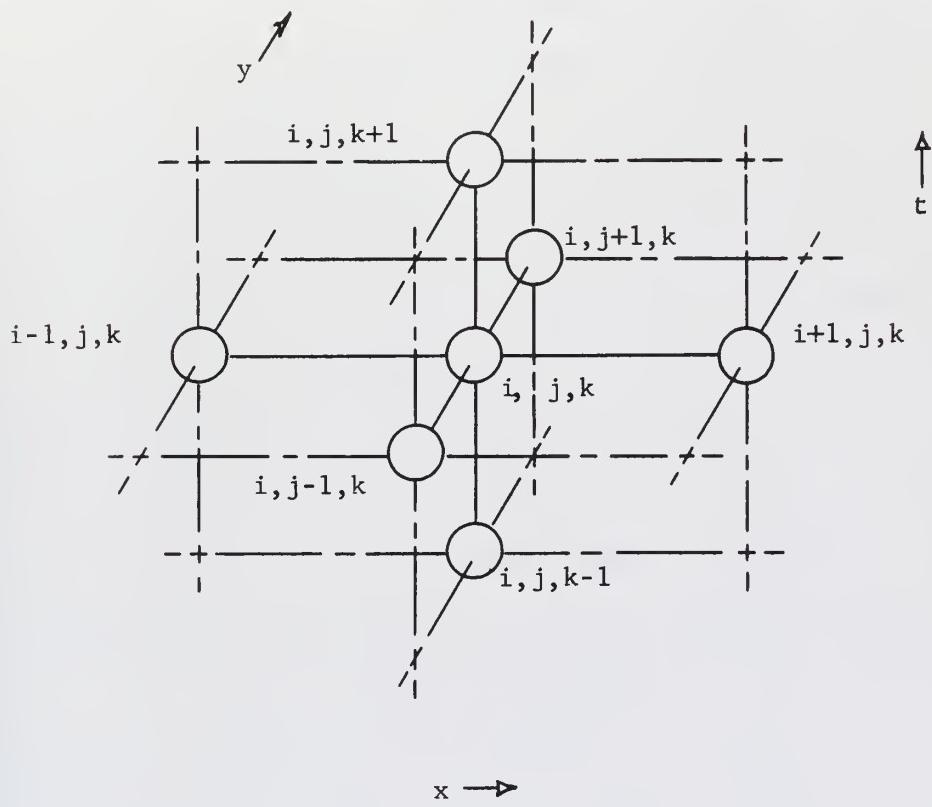
Figure 6. Isometric detail of three-dimensional mesh.

E2: $V_{i,j,k+1} = \left[2V_{i,j,k}(1-c_i^2 RC - s_i^2 RA) + V_{i+1,j,k}\left(s_i^2 + \frac{DM}{4}\right)RA\right.$

$+ V_{i-1,j,k}\left(s_i^2 - \frac{DM}{4}\right)RA + (V_{i,j+1,k}+V_{i,j-1,k})c_i^2 RC + UA(c_i^2-s_i^2)RB$

$\left. + (U_{i,j+1,k}-U_{i,j-1,k})RB\,DM - V_{i,j,k-1}\left(1+\frac{B_{i,j}}{2\rho_i}\delta t\right)\right]\Big/\left[1-\frac{B_{i,j}}{2\rho_i}\delta t\right]$,   (38)

where: $RA = \left(\frac{\delta t}{\delta x}\right)^2$, $RB = \frac{\delta t^2}{4\,\delta x\,\delta y}$, $RC = \left(\frac{\delta t}{\delta y}\right)^2$,

$DL = \frac{1}{\rho_i}(\lambda_{i+1}-\lambda_{i-1})$, $DM = \frac{1}{\rho_i}(\mu_{i+1}-\mu_{i-1})$,

$VA = V_{i+1,j+1,k} + V_{i-1,j-1,k} - V_{i+1,j-1,k} - V_{i-1,j+1,k}$,

$UA = U_{i+1,j+1,k} + U_{i-1,j-1,k} - U_{i+1,j-1,k} - U_{i-1,j-1,k}$.

The collateral conditions become:

I1: $U_{i,j,1} = 0$,   (39)

I2: $V_{i,j,1} = 0$,   (40)

I3: $U_{i,j,2} = 0$,   (41)

I4: $V_{i,j,2} = 0$,   (42)

B1: $U_{i,1,k} = 0$,

$U_{L,j,k} = 0$,   (43)

$U_{i,M,k} = 0$,

B2: $V_{i,1,k} = 0$,

$V_{L,j,k} = 0$,   (44)

$V_{i,M,k} = 0$,

B3: $U_{1,j,k+1} = \left[2U_{1,j,k}(1-c_1^2 RA - s_1^2 RC) + U_{2,j,k}(2c_1^2 RA)\right.$

$+ (U_{1,j+1,k}+U_{1,j-1,k})s_1^2 RC + (V_{1,j+1,k}-V_{1,j-1,k})DL\,RB$

$\left. - \left(c_1^2 RA - \frac{DL}{4} - \frac{DM}{2}\right)(2\delta x\,F_{j,k}) - U_{1,j,k-1}\left(1+\frac{B_{1,j}}{2\rho_1}\delta t\right)\right]\Big/\left[1-\frac{B_{1,j}}{2\rho_1}\delta t\right]$,   (45)

B4: $V_{1,j,k+1} = \left[2V_{1,j,k}(1-c_1^2 RC - s_1^2 RA) + V_{2,j,k}(2s_1^2 RA)\right.$

$+ (V_{1,j+1,k}+V_{1,j-1,k})c_1^2 RC + (U_{1,j+1,k}-U_{1,j-1,k})DM\,RB$

$\left. + (c_1^2-s_1^2)(F_{j+1,k}-F_{j-1,k})(2\delta x\,RB) - V_{1,j,k-1}\left(1+\frac{B_{1,j}}{2\rho_1}\delta t\right)\right]\Big/\left[1-\frac{B_{1,j}}{2\rho_1}\delta t\right]$.   (46)

36

A well-posed problem for numerical solution is then formed by
equations (37) and (38) with collateral conditions (39) through (46).
Initially, the k=1 and k=2 planes are set to zero following equations
(39) through (42). The k+1 plane can then be solved using equations
(43) through (46) for the boundaries and equations (37) and (38) for
the interior mesh points.

D. STABILITY AND CONVERGENCE

1. Stability

Under the conditions that the attenuation and velocity gradient
terms are zero and that $\delta x = \delta y$, the difference equations (37) and
(38) reduce to those for which a stability analysis was carried out by
Alterman and Karal [1968] , and Alterman and Rotenberg [1969] .
The former paper showed that the stability criterion is given by:

$$\frac{\delta t}{\delta x} < \frac{1}{C}\left[1 + \left(\frac{S}{C}\right)^2\right]^{-\frac{1}{2}} .$$

(47)

In the latter paper, the authors indicated that stability was guaranteed
under the condition that:

$$\frac{\delta t}{\delta x} < 0.86 ,$$

(48)

with the assumption that S/C = 0.55, corresponding to a Poisson's ratio
of 0.28. Poisson's ratio is defined in terms of wave velocities as:

$$\sigma = \frac{\frac{1}{2}\left(\frac{C}{S}\right)^2 - 1}{\left(\frac{C}{S}\right)^2 - 1} .$$

(49)

Empirically, it was found that the addition of attenuation and
velocity gradient terms reduced the right side of equation (47), while

37

an increase in δy ($\delta y > \delta x$) reduced the left side. An approximate
stability criterion was established, given by:

$$\frac{\delta t^2}{\delta x \delta y} \quad < \quad \frac{0.75}{C^2}\left[1 + \left(\frac{S}{C}\right)^2\right]^{-1} \quad , \tag{50}$$

under the condition that the restrictions on velocity gradients (for C
and S) given by equation (17) apply.

2. Convergence

Following the methods of Forsythe and Wasow [1967] and of
Fox et al. [1962] , it was assumed that convergence would be assured as
long as the mesh ratios were sufficiently small to insure that the
(i,j,k+1) mesh point lies within the characteristic surfaces through
adjacent mesh points in the k plane. Fox equated the characteristic
surfaces with successive positions of a wave front. The most restrictive
condition on convergence is then given by the maximum dilatational
wave velocity in the solution space. This would give a less stringent
mesh ratio condition than the stability condition. Therefore, as
long as equation (49) holds, the method will be convergent as well as
stable.

E. DESCRIPTION OF THE PROGRAM

The program produces a set of four seismograms: shear and dilata-
tional stress and vertical and horizontal displacement. The data is
written on a temporary storage device (tape, disk or drum). A second
program then reads the data and plots the seismograms. An average run
with a 71x81 grid, 800 time mesh points and 25 detectors requires 278K
bytes of main core storage and a run time of 18 min. The output
requires 325K bytes of temporary storage space. The primary limiting

factor on a given problem is the time required for input/output to and from the temporary storage device.

1. Distribution Parameters

As in the one-dimensional model, the distribution parameters are used to model the physical conditions in the solution space. They are:

    a.   dilatational wave velocity, $C(x)$,

    b.   shear wave velocity, $S(x)$,

    c.   density, $RH(x)$,

    d.   forcing function, $F(y,t)$,

    e.   attenuation parameter, $B(x,y)$.

Wave velocities and density are put in the program as single-valued, continuous, polygonal line functions of depth. The forcing function is put in as was done in the one-dimensional model along with horizontal stations at which F is to be applied. The attenuation parameter is put into the program as two single-valued, continuous, polygonal parameters. They are:

    e1. vertical attenuation parameter, $BA(x)$,

    e2. horizontal attenuation parameter, $BB(y)$.

The full attenuation parameter, $B(x,y)$, is then computed as follows:

$$B(x,y) = \text{MAX}\left[BA(x), BB(y)\right] . \tag{51}$$

Tables VI through VIII give sample numerical input used to describe the various distribution parameters. Their distributions in the solution domain are shown graphically in Fig. 7 through 9.

Table VI.

Sample wave velocity and density polygons

Depth	C(x)	S(x)	RH(x)
0.0	0.6	0.0	1.0
3.0	0.6	0.0	1.0
3.3	1.2	0.82	2.1
7.0	1.2	0.82	2.1

Table VII.

Sample forcing function polygon

Time	F(t)
0.0	0.0
0.1	0.0
0.7	-0.15
1.30	0.0
2.50	0.0

Table VIII.

Sample attenuation parameter polygons

Depth	BA(x)	Distance	BB(y)
0.0	0.0	0.0	-2.5
4.0	0.0	1.0	-1.0
7.0	-2.5	2.0	0.0
		10.0	0.0
		11.0	-1.0
		12.0	-2.5

y ⟶

C = 0.60
S = 0.0
RH = 1.0

C = 1.20
S = 0.82
RH = 2.10

x ⟶
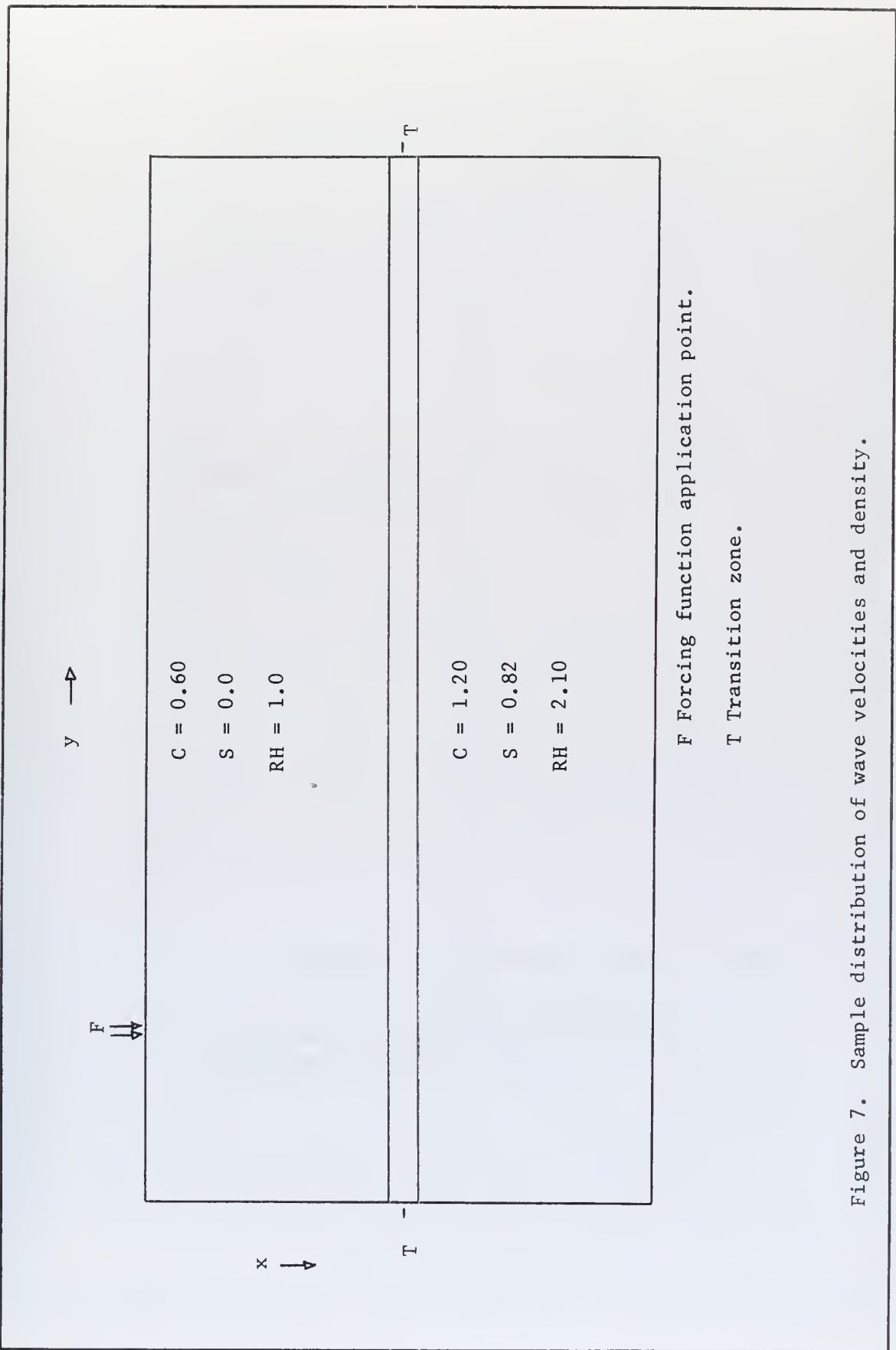
F Forcing function application point.

T Transition zone.

Figure 7. Sample distribution of wave velocities and density.
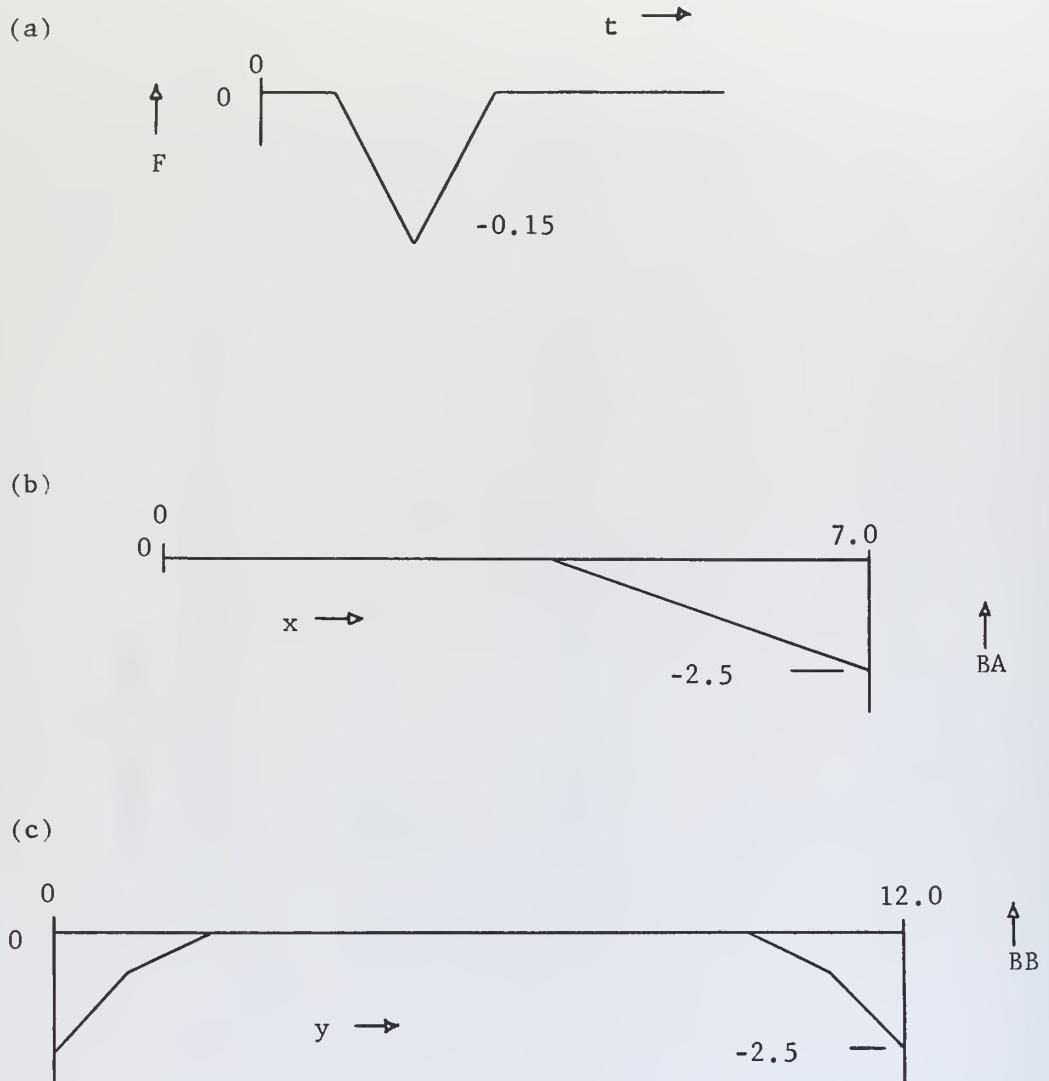
Figure 8. Sample distribution parameters.

(a) Forcing function
(b) Vertical attenuation parameter
(c) Horizontal attenuation parameter
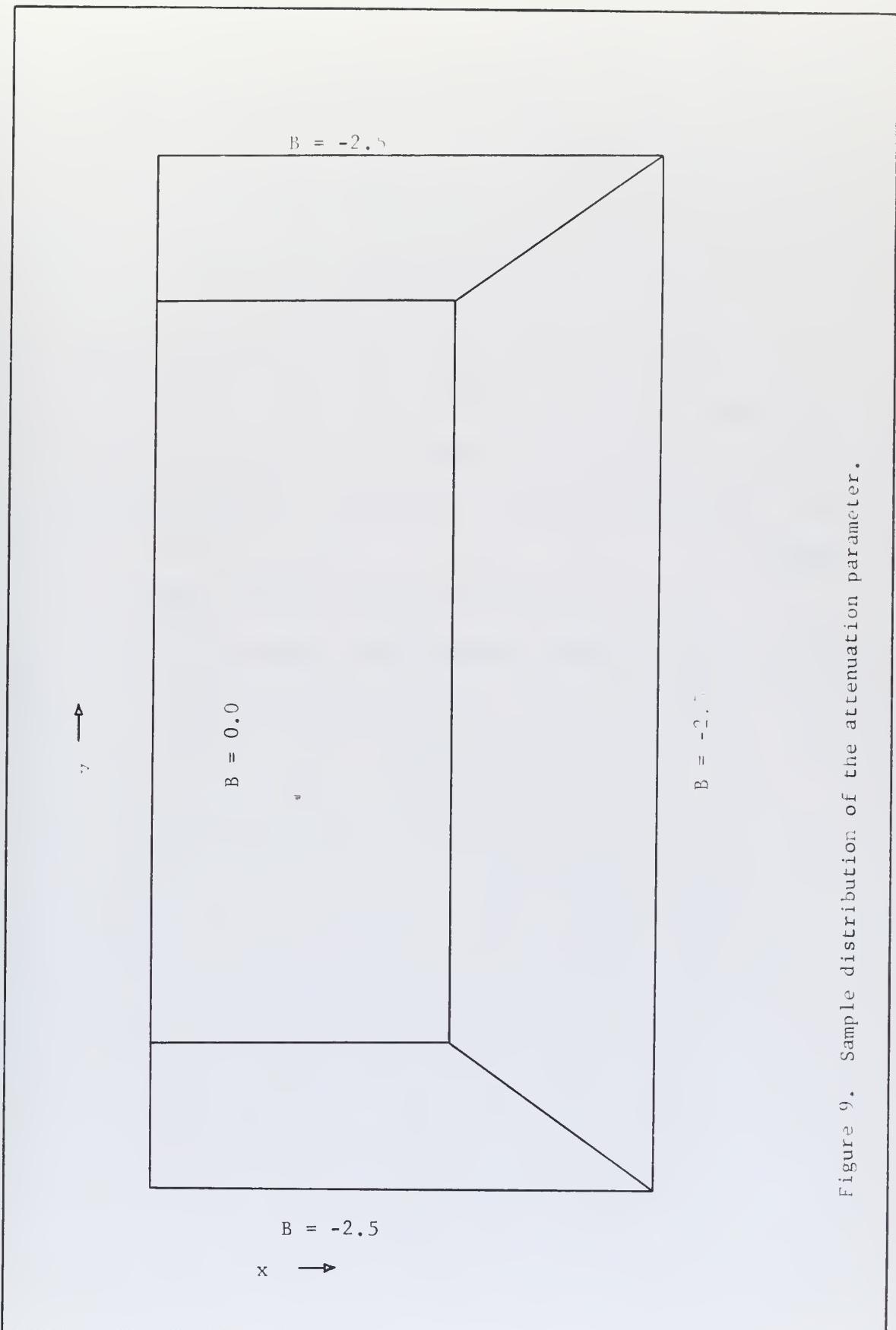
Figure 9. Sample distribution of the attenuation parameter.

2. Numerical Parameters

These parameters are used to control the computation of the distribution parameters and to set the arrangement and size of the solution domain. They are:

 a. mesh size in the x direction, (DX),

 b. mesh size in the y direction, (DY),

 c. mesh size in the t direction, (DT),

 d. number of total x mesh points, (L),

 e. number of total y mesh points, (M),

 f. number of total t mesh points, (N),

 g. number of points defining the distribution parameter polygons:

  (1) wave velocity and density polygons, (NC),

  (2) forcing function polygon, (NF),

  (3) attenuation parameter polygons:

   (a) vertical, (NBA),

   (b) horizontal, (NBB),

 h. x mesh point at which the output is measured:

  (1) stress, (IA),

  (2) displacement, (ID),

 i. number of horizontal output stations, (KK),

 j. y index of the first output station, (JB),

 k. mesh increment between output stations, (JJ),

 l. shot point or area location:

  (1) first shot mesh point, (MA),

  (2) last shot mesh point, (MB),

 m. last time mesh point at which $F(y,t)$ is to be applied, (LL).

F. SCALING THE PROBLEM

The scale of the problem is determined by choices of wave velocity
values and either δt or δx and δy. For mesh ratios of:

$$\frac{\delta t}{\delta x} = \frac{0.05}{0.10} = \frac{1}{2} \quad , \tag{52a}$$

$$\frac{\delta t}{\delta y} = \frac{0.05}{0.15} = \frac{1}{3} \quad , \tag{52b}$$

and under the condition on shear velocity that $S = C/\sqrt{3}$ ($\sigma = 0.25$),
the dilatational wave velocity may vary from 0.0 to 1.86 distance units
per time unit, and shear wave velocity may not exceed 1.07 distance
units per time unit. If a value of C = 0.60 is to represent dilata-
tional wave velocity in water of 1.5 km/sec, then the scale of the
problem would depend upon a choice of either time or distance mesh
size. Table IX shows scales available for various distance mesh sizes
specified.

45

Table IX.

Scales available for C = 0.60 = 1.5 km/sec

Numerical parameters: L = 71; M = 81; N = 800

| Mesh sizes | | | Units | | | Seismogram | Solution Space | |
x (m)	y (m)	t (sec)	Distance x (m)	y (m)	Time t (sec)	Length (sec)	Size x (m)	y (m)
100	150	.02	1000	1500	.4	16	7000	12000
10	15	.002	100	150	.04	1.6	700	1200
1	1.5	.0002	10	15	.004	.16	70	120

46

IV. INTERPRETATION

The synthetic seismic records produced by the two models presented in this paper were interpreted first in the manner of actual field records without direct reference to the structural profiles used. Extensive use was made of gross seismic interpretation techniques presented by Grant and West [1965] , Dobrin [1960] , and Bullen [1959] . Interpretation of the reflection and transmission of incident pulses was aided by the results of Alterman and Karal [1968] , Alterman and Rotenberg [1969] , Gupta [1966a and 1966b] , Sengbush, Lawrence and McDonal [1961] and Tooley, Spencer and Sagoci [1965] .

A. THE REFLECTION PROFILING SEISMOGRAMS

Each reflection profile produced by the model is designated by an alpha-numeric sequence. For example, C3H F7 A14 identifies the exact structure (C3H), forcing function (F7) and attenuation parameter (A14) used.

Six profiles were developed using three basic structures. The structures, shown in Fig. 10 through 15, can be described in terms of marine geology as follows:

(1) Shelf break with horizontal layers.

    (a) Increasing velocity in each successive layer (C3H).

    (b) With one low velocity layer (C4D).

(2) Flat bottom with double wedge.

    (a) High velocity wedge (C5A).

    (b) Low velocity wedge (C6C).

(3) Flat bottom, horizontal layering, penetrated unconformably by a dipping bed.
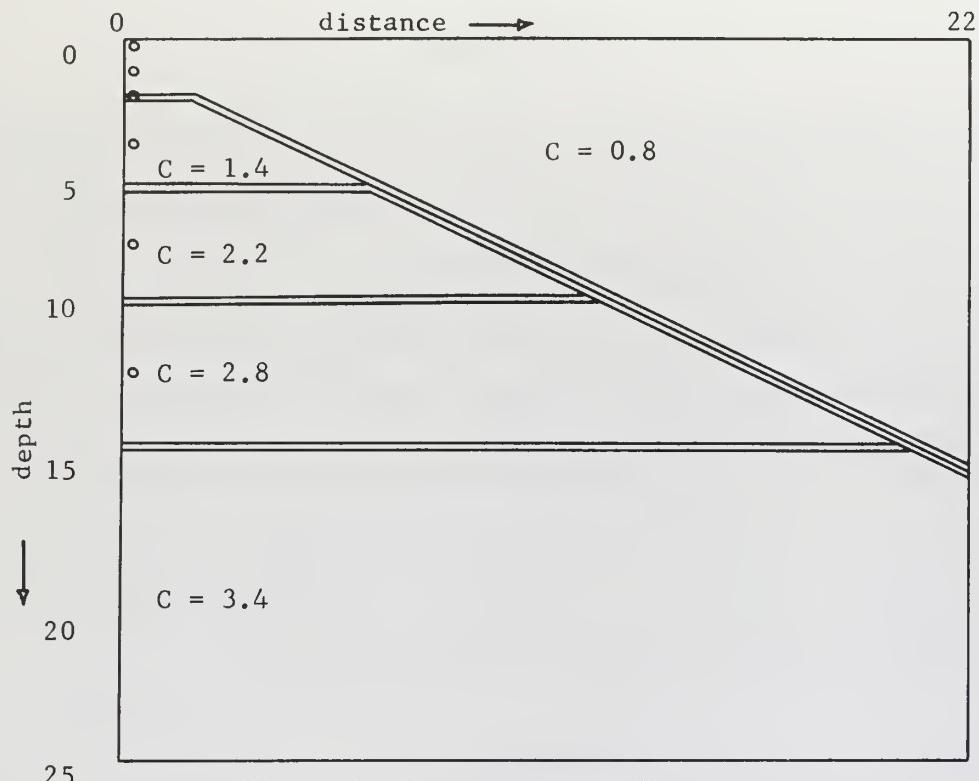
Figure 10. Velocity structure C3H
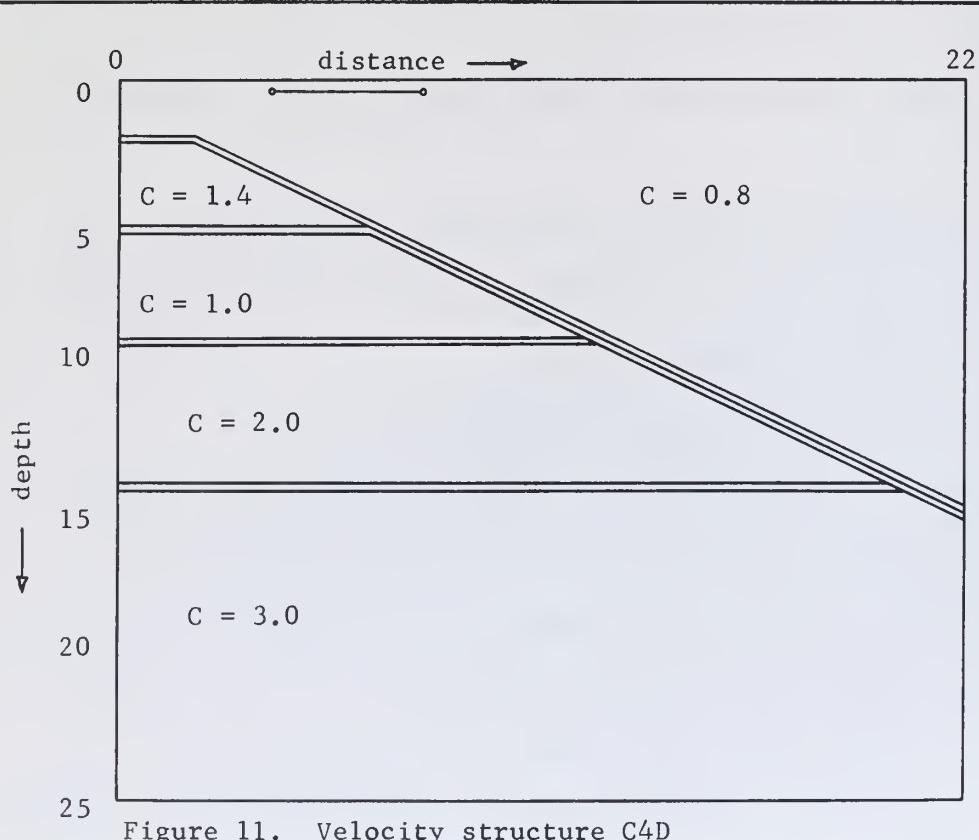
Figure 11. Velocity structure C4D
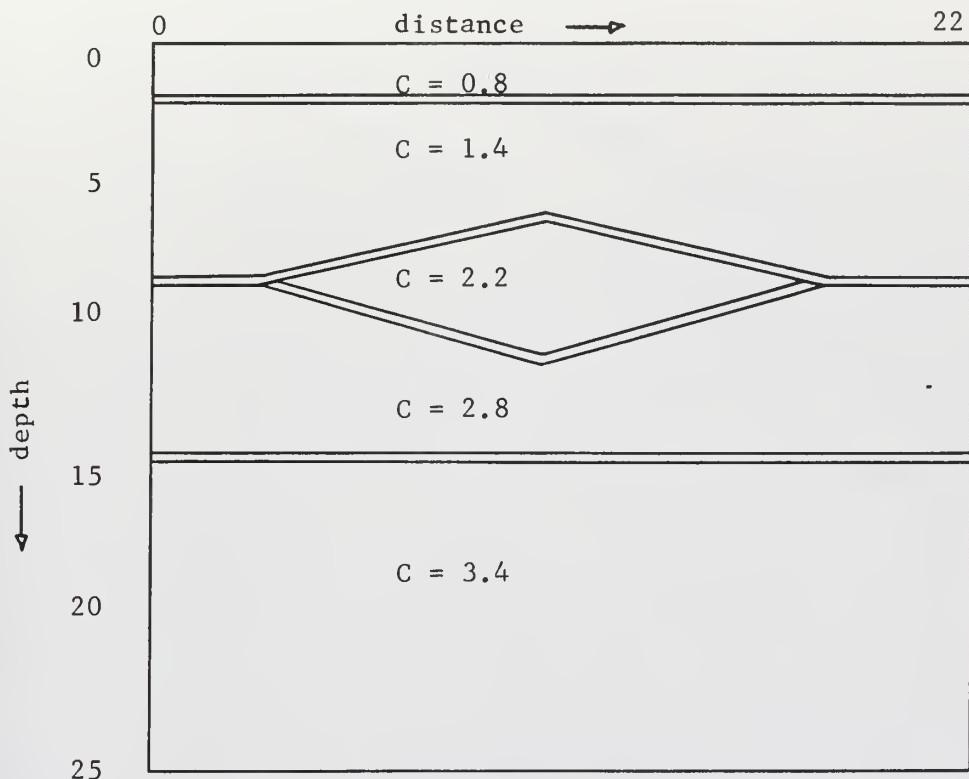
Figure 12. Velocity structure C5B
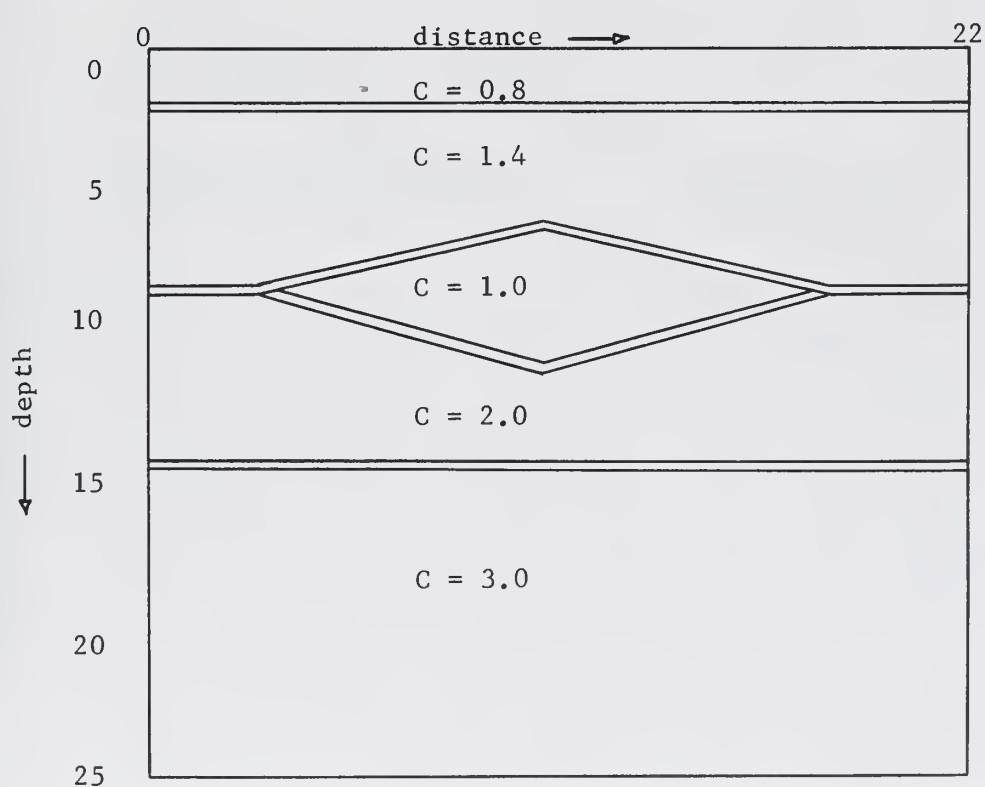
Figure 13. Velocity structure C6C
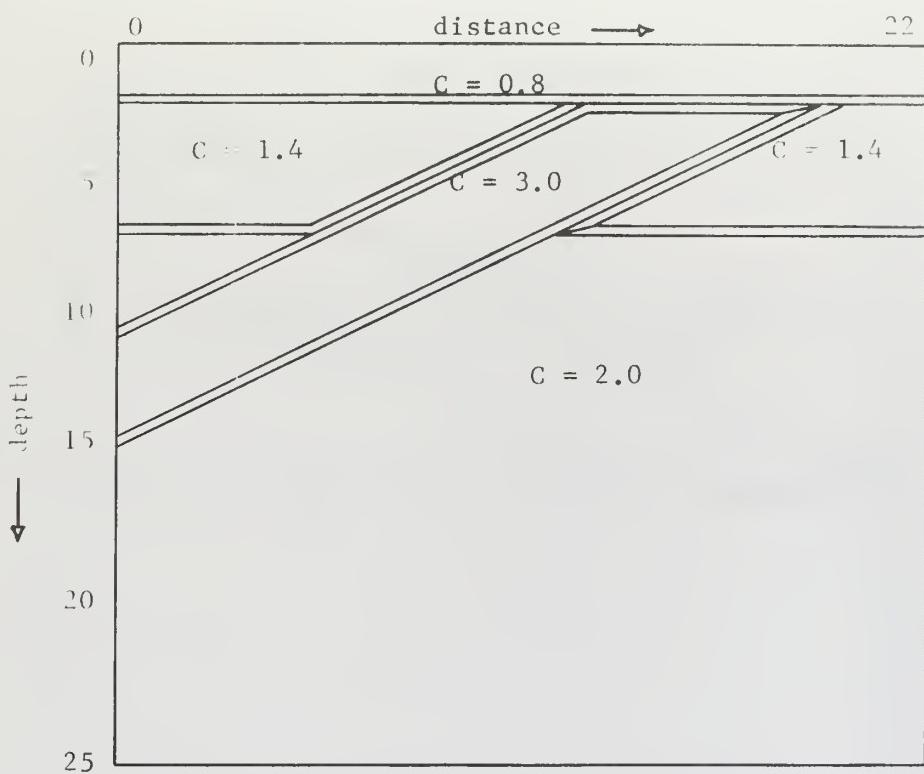
Figure 14. Velocity structure C7A
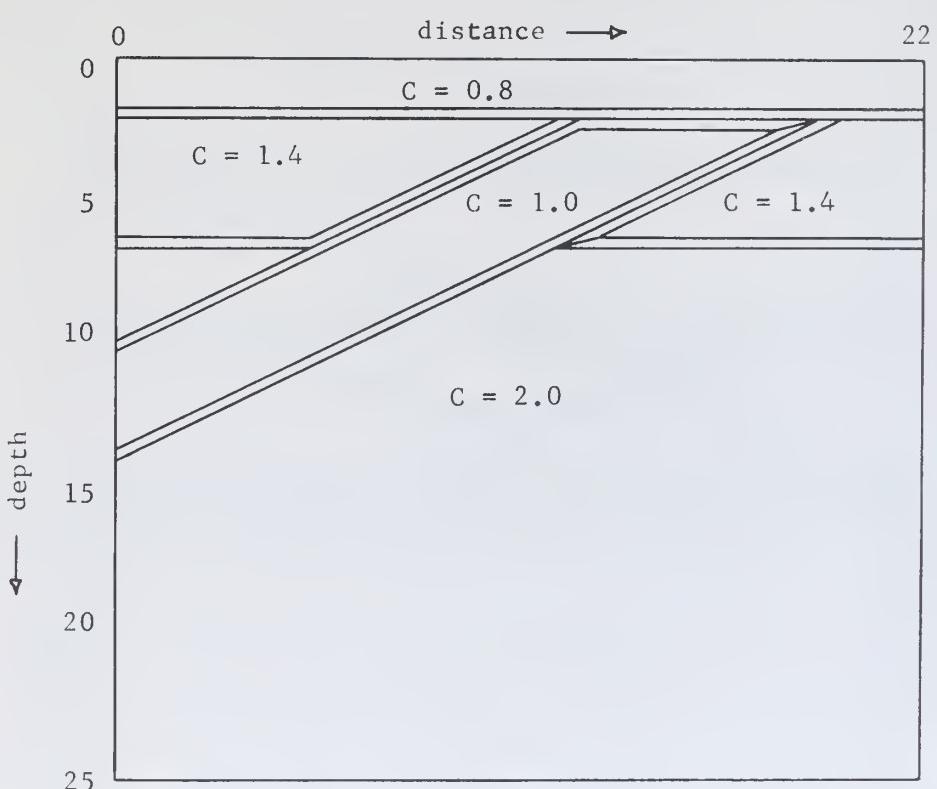
Figure 15. Velocity structure C8A

(a) High velocity bed (C7A).

(b) Low velocity bed (C8A).

All traces utilized forcing function F7 (Fig. 16) and attenuation parameter A14 (Fig. 17).

1. Variable Depth Records

As an aid to interpretation, several single traces were developed with a single velocity structure, where the depth of the detection point was varied between traces. The traces are shown in Fig. 18 along with the mesh point at which each was computed. These various detection points are shown as circles in Fig. 10. The traces were generated using a source located at a horizontal distance of 0.5 units for the problem designated C3H F7 A14. The first disturbance in each trace, designated d, is the direct wave. P_1 and P_2 designate the reflected pulses from the first and second transition zones, while the first primary multiple (P_1 reflected from the free surface) is shown by P_1P_s. Other multiples are marked in a similar manner.

These traces show clearly the development of a train of alternating negative and positive pulses behind the main pulse. The change in pulse shape is also quite evident. As the pulse progresses, the amplitude decreases and the pulse width increases. Additionally, the base and tip of the pulse form tends to become more rounded. These are primarily mesh effects and are dependent on mesh size (DX). When one particle is unloaded as the pulse passes by, the adjacent particle is still under stress, causing a reverse stress between the particles. In gradient zones, where the derivative of C is non-zero, there is also an elastic rebound effect which reinforces the pulse train.
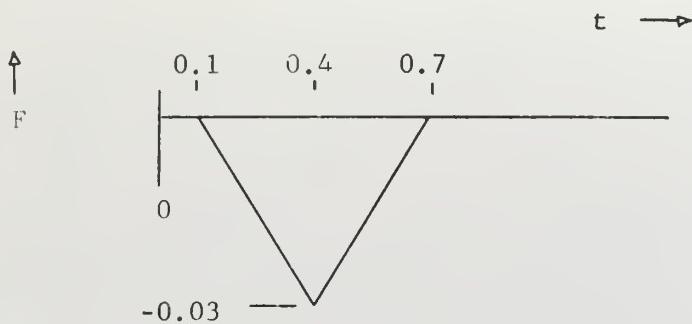
Figure 16. Forcing function F7
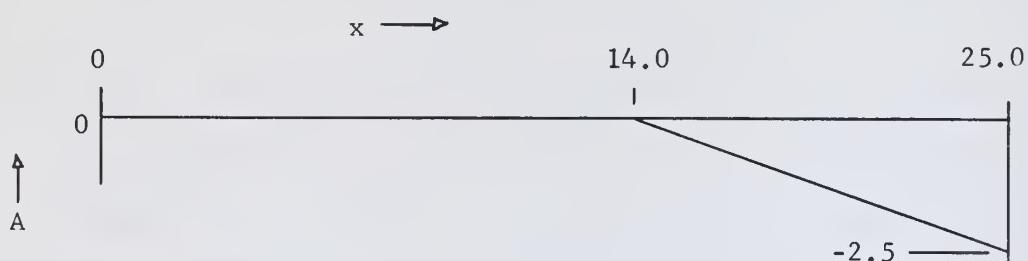
Figure 17. Attenuation parameter A14

52
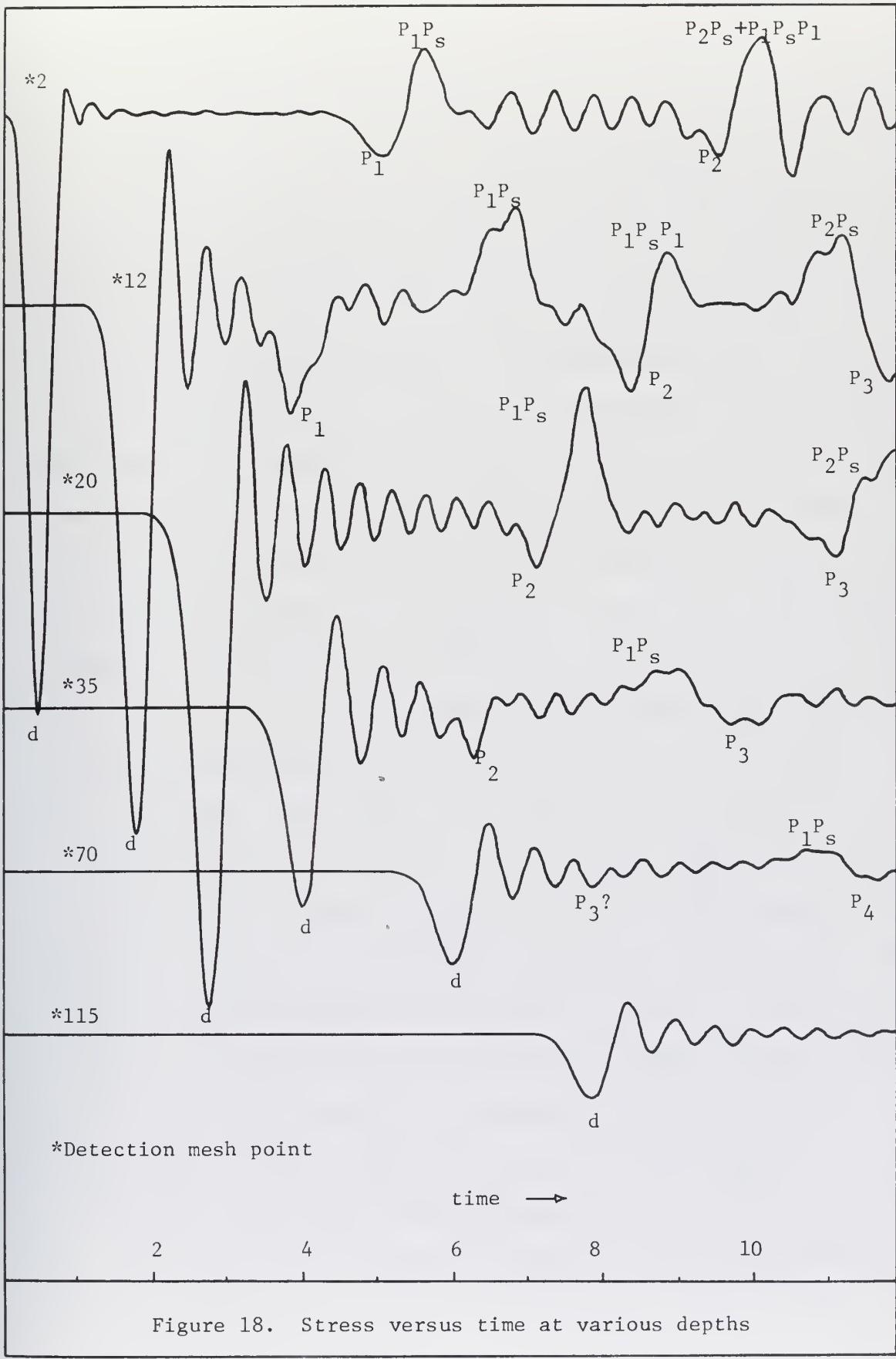
Figure 18. Stress versus time at various depths

2. The reflection profiling seismograms

Synthetic reflection profiling seismograms are shown in Fig. 19 through 26. Figure 19 is an uncorrelated version of Fig. 20, included so that lineations may be observed without the influence of correlation lines shown on the remaining figures. Solid lines on the seismograms mark lineations which were correlated with first reflections from a particular horizon. Dashed lines indicate multiple reflections which, if used as primary reflections, might lead to erroneous interpretations of structure. For each correlation, a particular phase was chosen and followed laterally through successive traces. Figures 20 and 21 show clearly the false dips introduced by the sloping bottom, increasing the pulse travel time in the lower velocity upper layer. The bottom slope causes a change in thickness of the top two layers (water and the first subbottom layer). The false dip introduced is a function of the bottom slope and the ratio of velocities involved. Note that there is a change in dip at each point where a layer pinches out.

Figures 22 and 23 show similar false dips and horizons introduced by variations in the thickness of a single layer. The high velocity wedge causes a doming up to be introduced into a horizontal transition zone below, while the low velocity wedge has the reverse effect. The most obvious feature of the records for velocity structures C7A and C8A (Fig. 24 and 25) is the relatively high amplitudes in the records in the areas where the dipping beds pinch out against the flat bottom. This is caused by a combination of factors. In velocity structure C7A (Fig. 24), there is a sharp change in velocity contrast across the bottom as the dipping bed outcrops. The steeper gradient then reflects more energy, causing an increase in amplitude in both

Figure 19

Uncorrelated reflection profile C3H F7 A14

DX: 0.10   DT: 0025   DK: 0.50

N: 251   M: 1800   IP: 2

Horizontal distance (d)

versus

time (t)

Figure 19. Uncorrelated reflection profile C3H F7 A14

56

Figure 20

Reflection profile C3H F7 A14

DX: 0.10   DT: 0.025   DK: 0.50

N: 251   M: 1800   IP: 2

Horizontal distance (d)

versus

time (t)

————————   First reflections
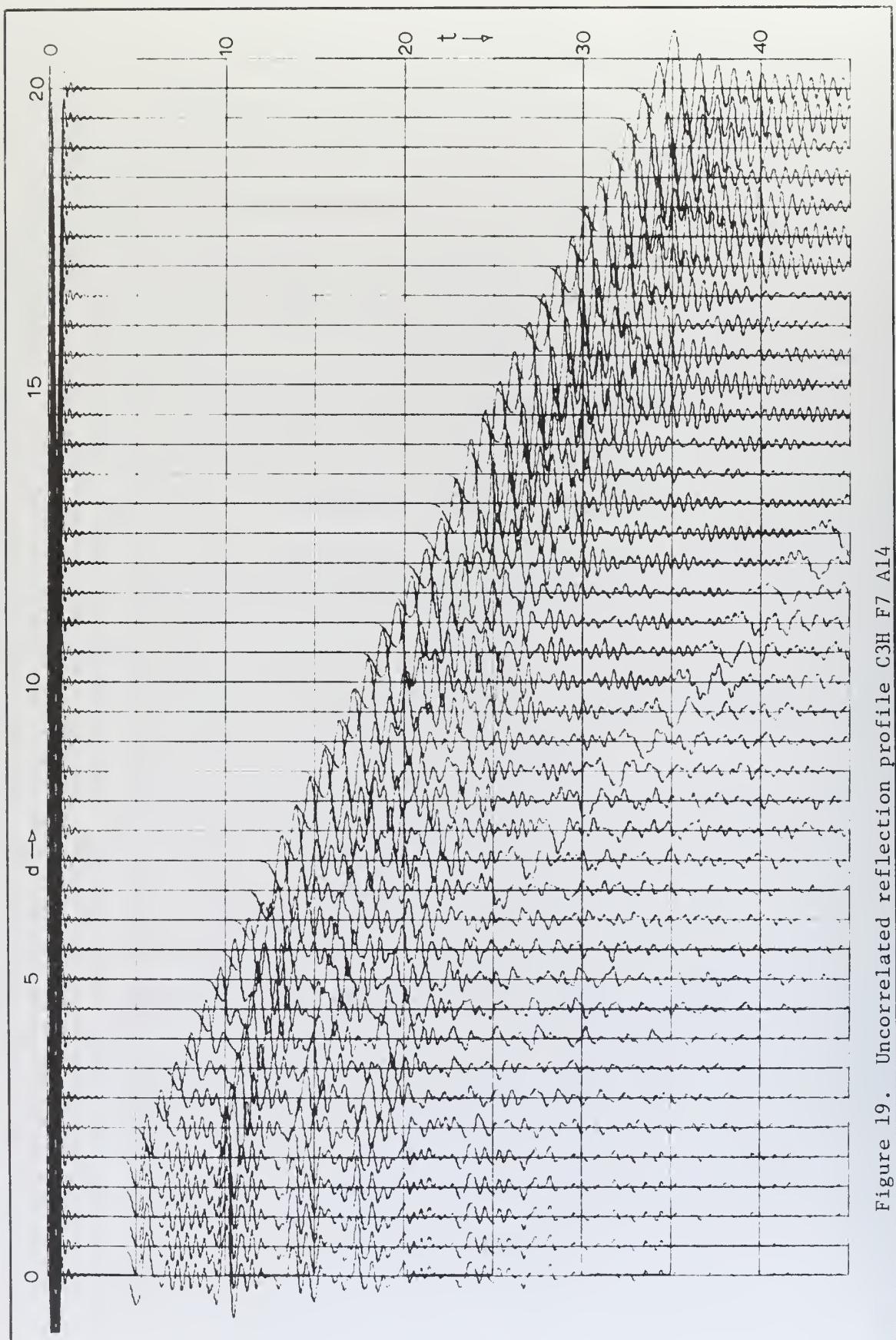
— — — —   Multiple reflections

Figure 20. Reflection profile C3H F7 A14

Figure 21

Reflection profile C4D F7 A14

DX: 0.10   DT: 0.025   DK: 0.50

N: 251   M: 1800   IP: 2

Horizontal distance (d)

versus

time (t)

———————   First reflections

— — — —   Multiple reflections

•———————•   Location of precision trace (Fig. 26)

Figure 21. Reflection profile C4D F7 A14

60
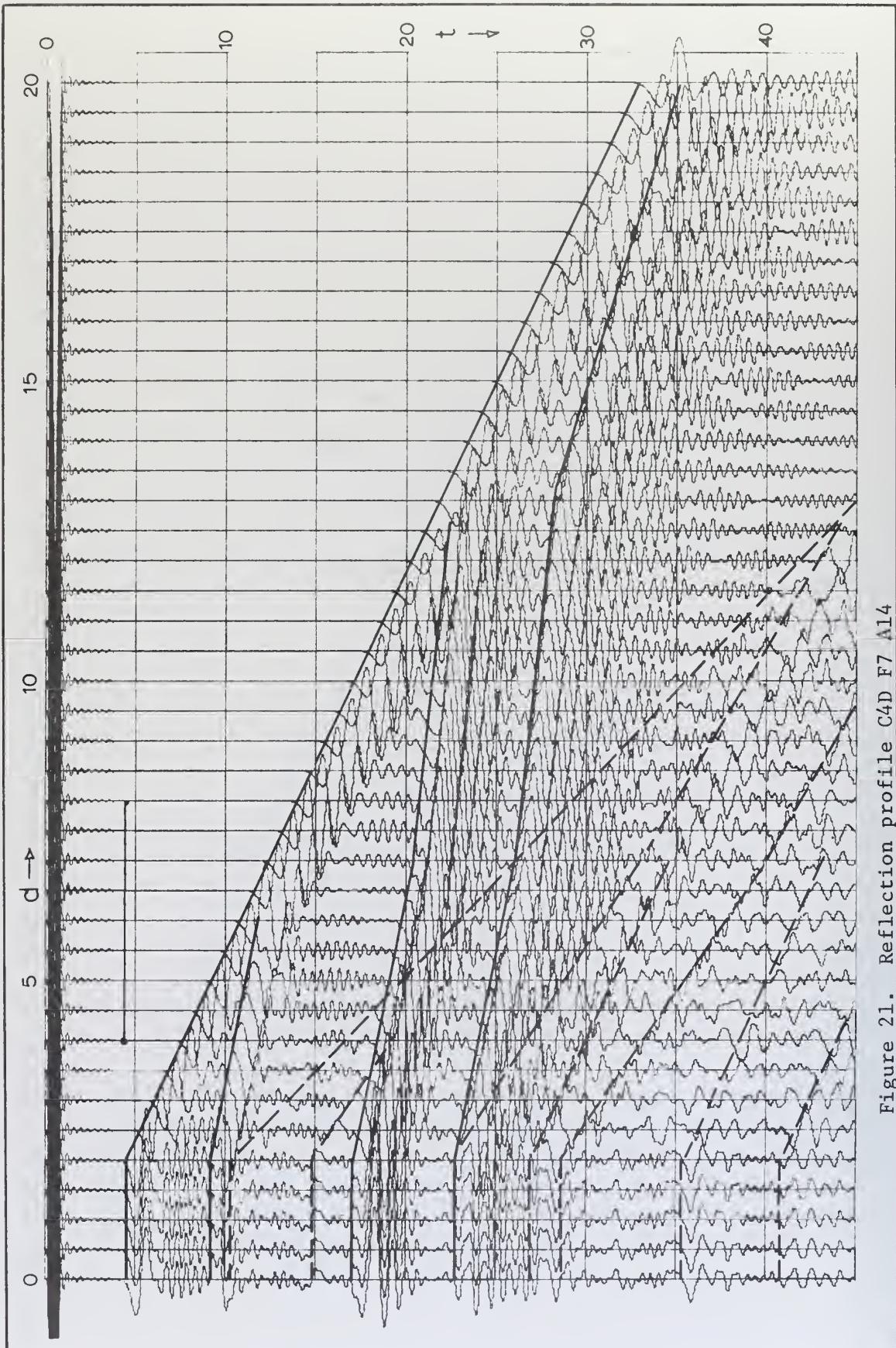
Figure 22

Reflection profile C5B F7 A14

DX: 0.10   DT: 0.025   DK: 0.50

N: 251   M: 1800   IP: 2

Horizontal distance (d)

versus

time (t)

————————   First reflections

— — — –   Multiple reflections
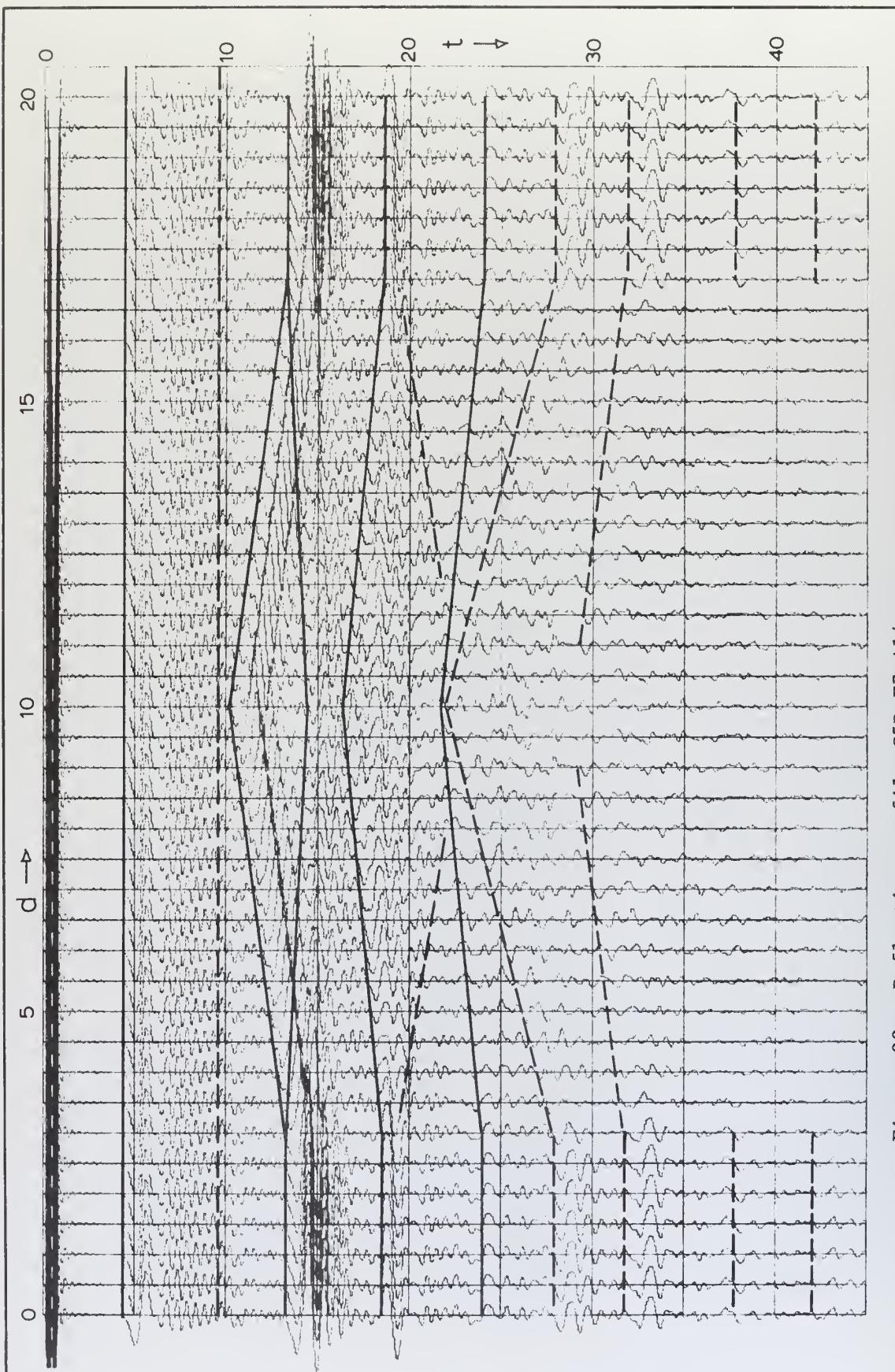
Figure 22. Reflection profile C5B F7 A14

Figure 23

Reflection profile C6C F7 A14

DX: 0.10   DT: 0.025   DK: 0.50

N: 251   M: 1800   IP: 2

Horizontal distance (d)

versus

time (t)

———————— First reflections

— — — Multiple reflections
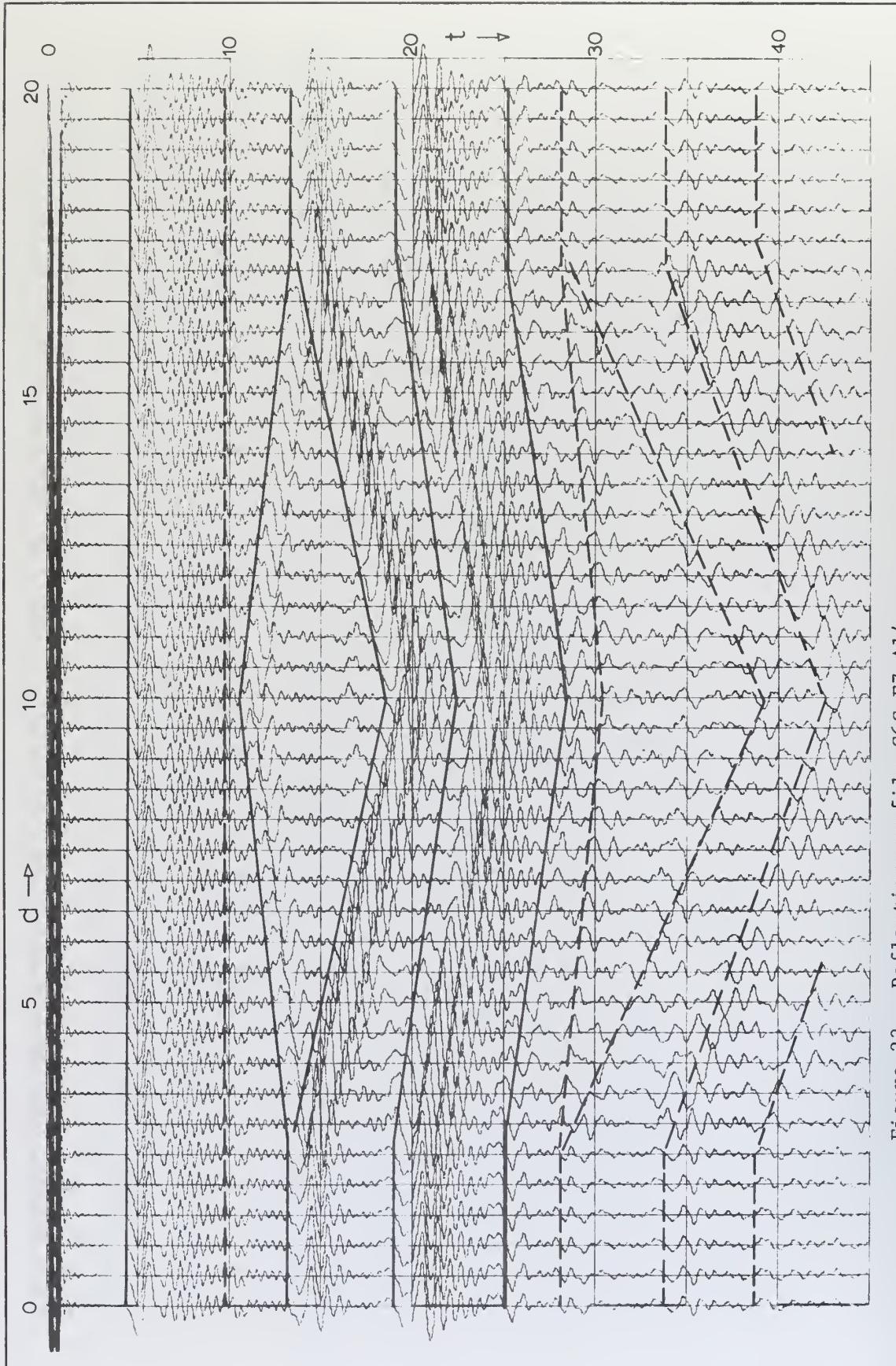
Figure 23. Reflection profile C6C F7 A14

Figure 24

Reflection profile C7A F7 A14

DX: 0.10   DT: 0.025   DK: 0.50

N: 251   M: 1800   IP: 2

Horizontal distance (d)

versus

time (t)

———————— First reflections

— — — Multiple reflections
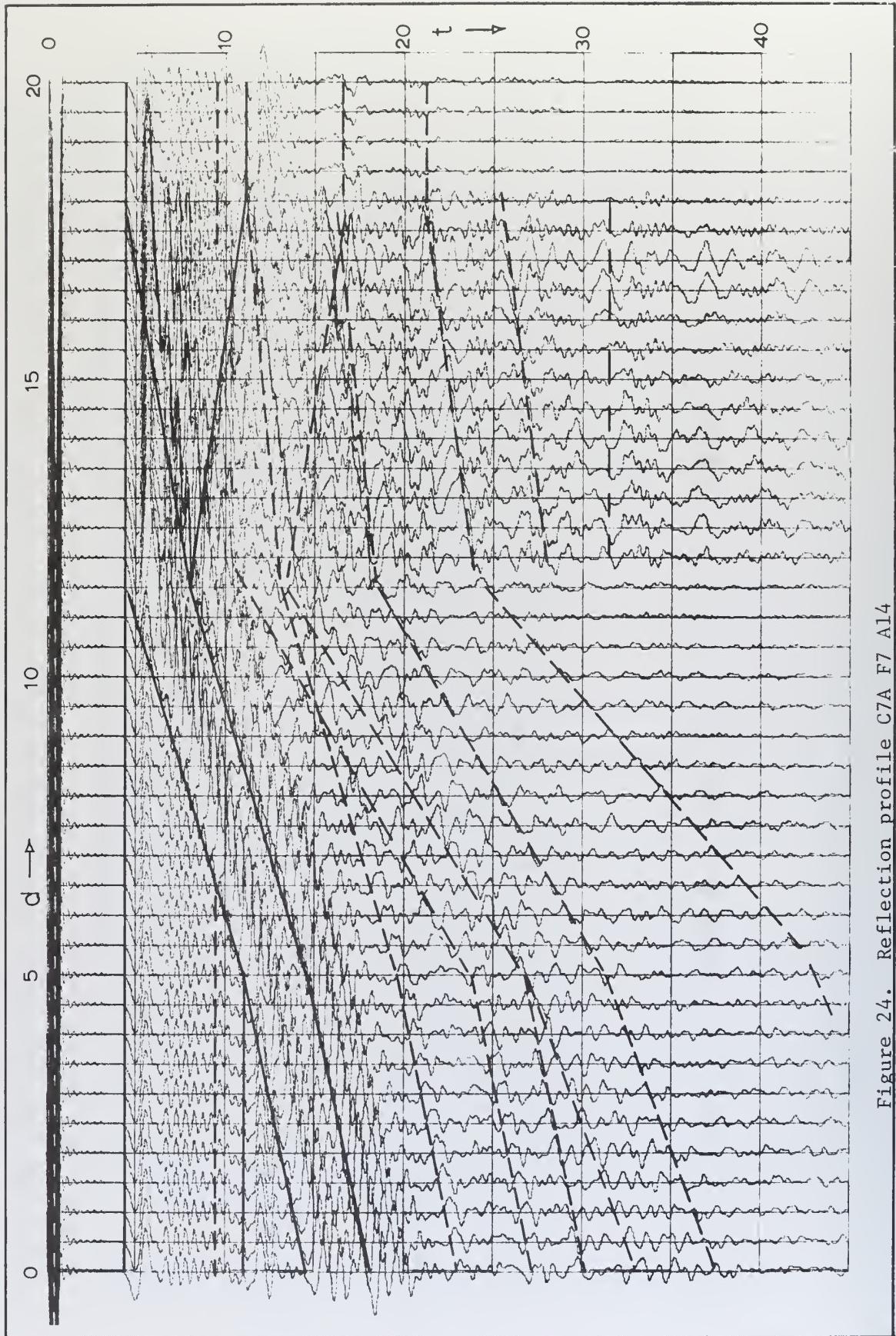
Figure 24. Reflection profile C7A F7 A14

Figure 25

Reflection profile C8A F7 A14

DX: 0.10   DT: 0.025   DK: 0.50

N: 251   M: 1800   IP: 2

Horizontal distance (d)

versus

time (t)

————— First reflections

— — — Multiple reflections
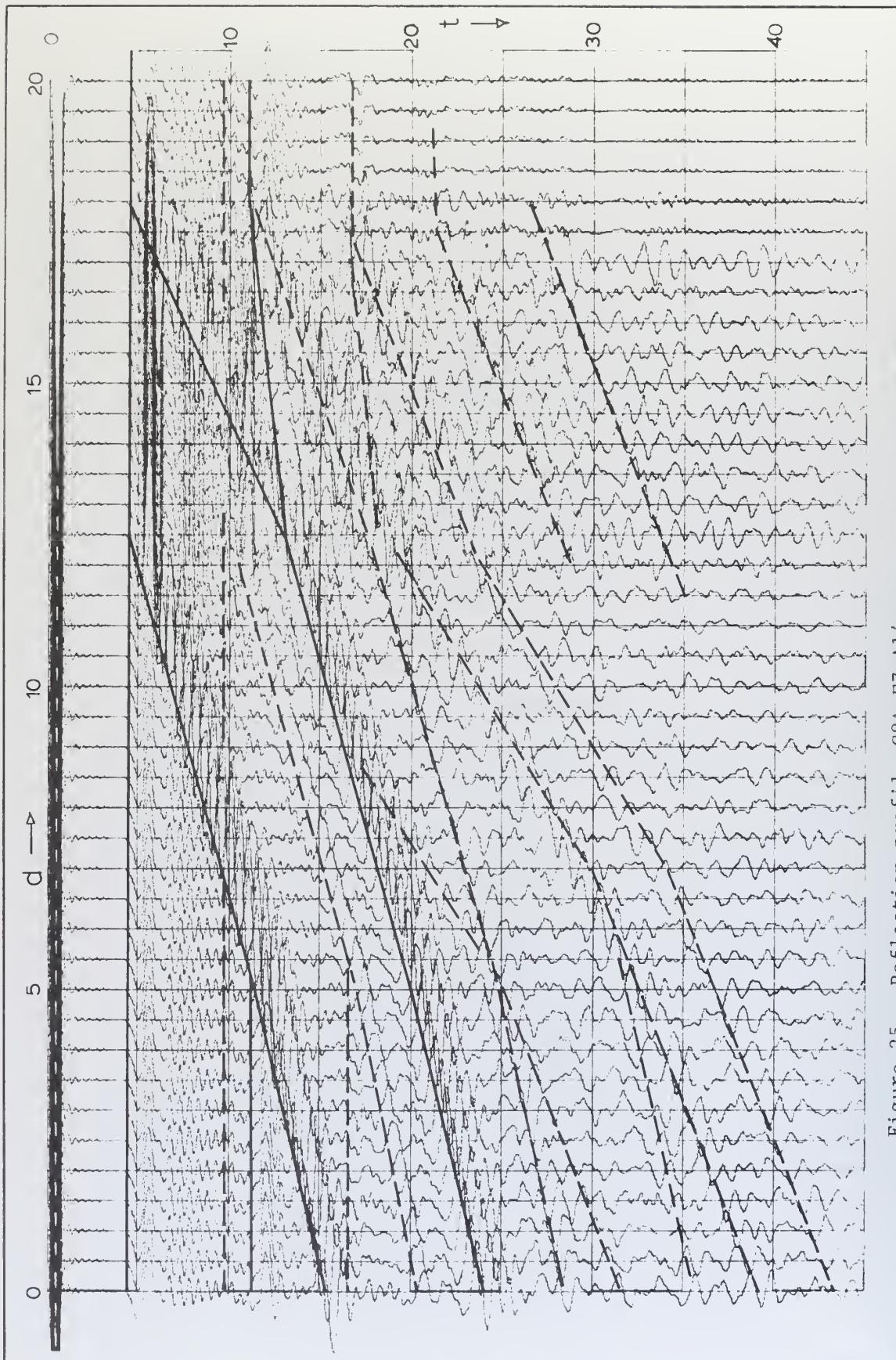
Figure 25. Reflection profile C8A F7 A14

Figure 26

Precision reflection profile C4D F7 A14

DX: 0.10   DT: 0.025   DK: 0.10   EEE: 4.0

N: 251   M: 1800   IP: 2

Horizontal distance (d)

versus

time (t)

————————   First reflections

— — —   Multiple reflections
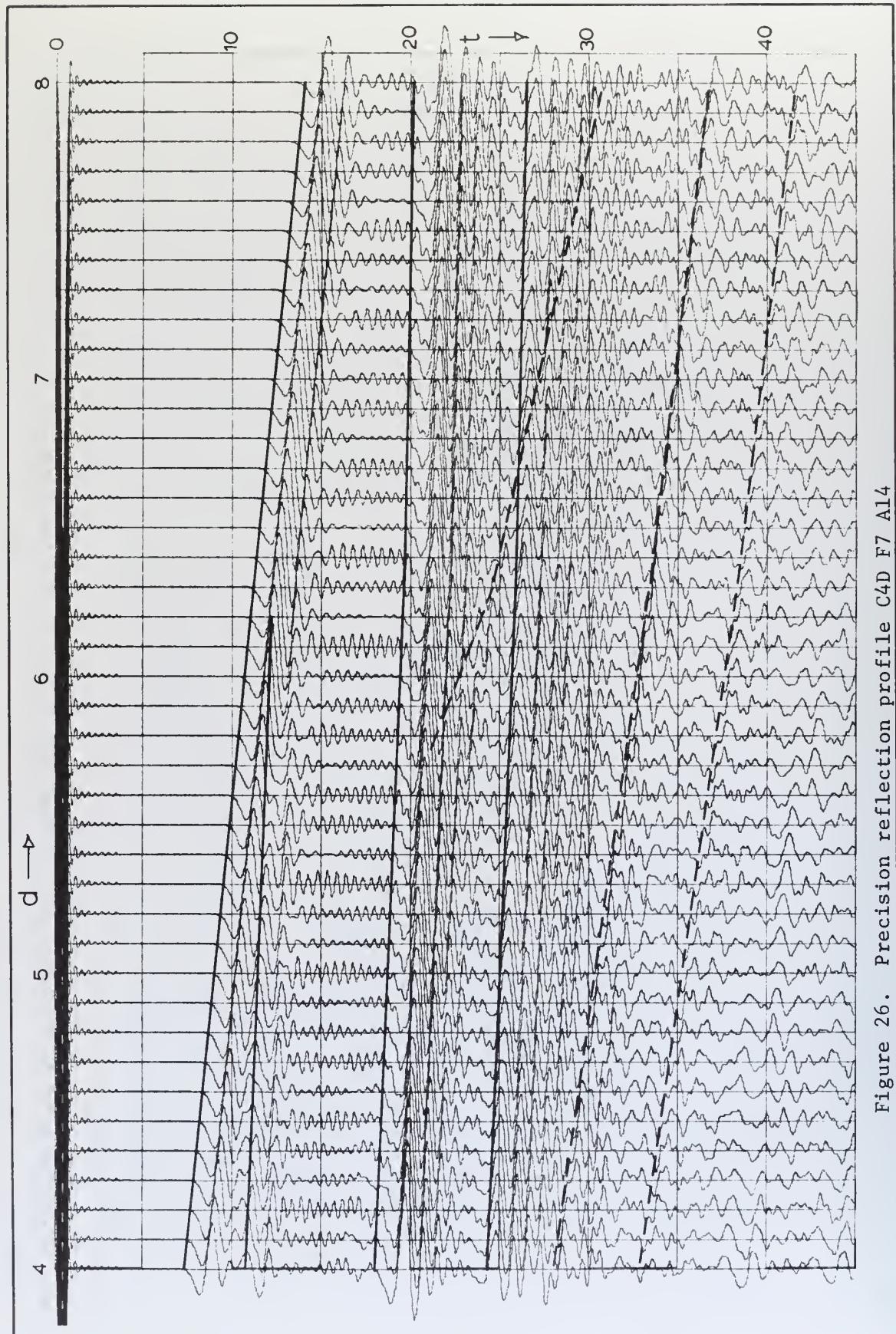
Figure 26. Precision reflection profile C4D F7 A14

first reflections and multiples. Additionally, there is a resonance effect of the large number of multiples being generated. This resonance effect is also present in velocity structure C8A (Fig. 25). There is also a tuning effect due to the relationship between the thickness of the transition zone and the primary period of the incident pulse [Sengbush, Lawrence and McDonal 1961] which would lead to high amplitude reflected pulses. The possibility that instabilities were introduced in these high gradient areas was considered. All parameters, however, are well within stability criteria established in Section II.

Figure 26 is an example of a "precision trace" that may be produced by the model. This seismogram presents a section of a record obtained with the same velocity structure as that shown in Fig. 21 (C4D F7 A14) with an expanded horizontal scale. The horizontal distance covered includes the region where the first sub-bottom layer pinches out. This area (from 4.0 to 8.0) is marked on Fig. 21 with a horizontal line in the record. The "precision trace" was obtained by reducing the shot point spacing (DK).

B. THE REFLECTION/REFRACTION SEISMOGRAMS

Each set of synthetic seismograms developed by the model is designated by a letter-number sequence similar to that used in the reflection profiling model. CA F5A B3 L2 identifies the exact wave velocity and density structure (CA), forcing function (F5A), attenuation parameter (B3) and shot point location (L2) used to generate the records. The seismograms presented in this section were developed using the following velocity structures (Fig. 27 through 29):

(1) Two elastic layers, (CA).

71
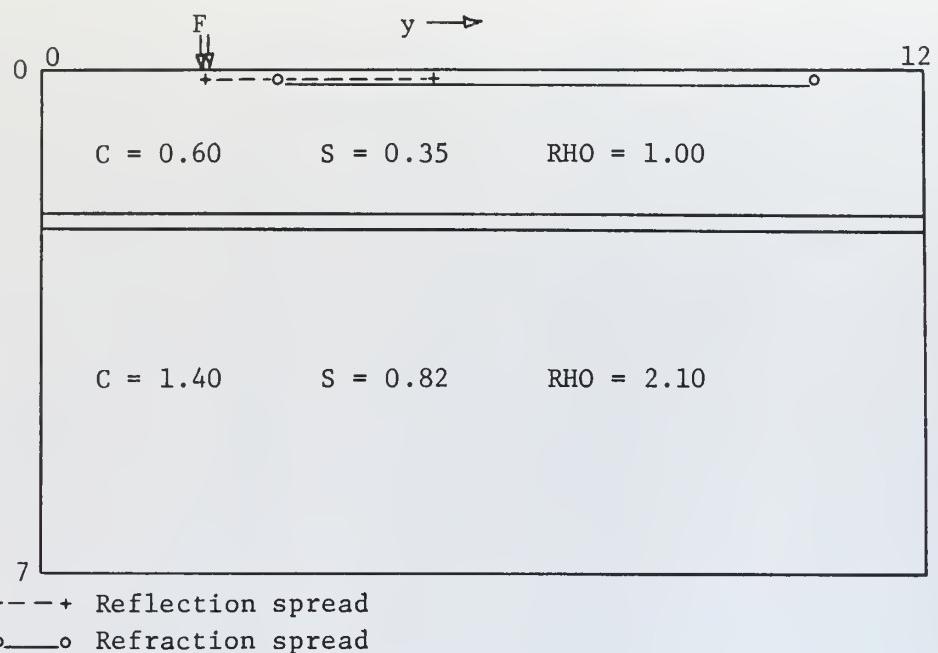
Figure 27. Velocity structure CA
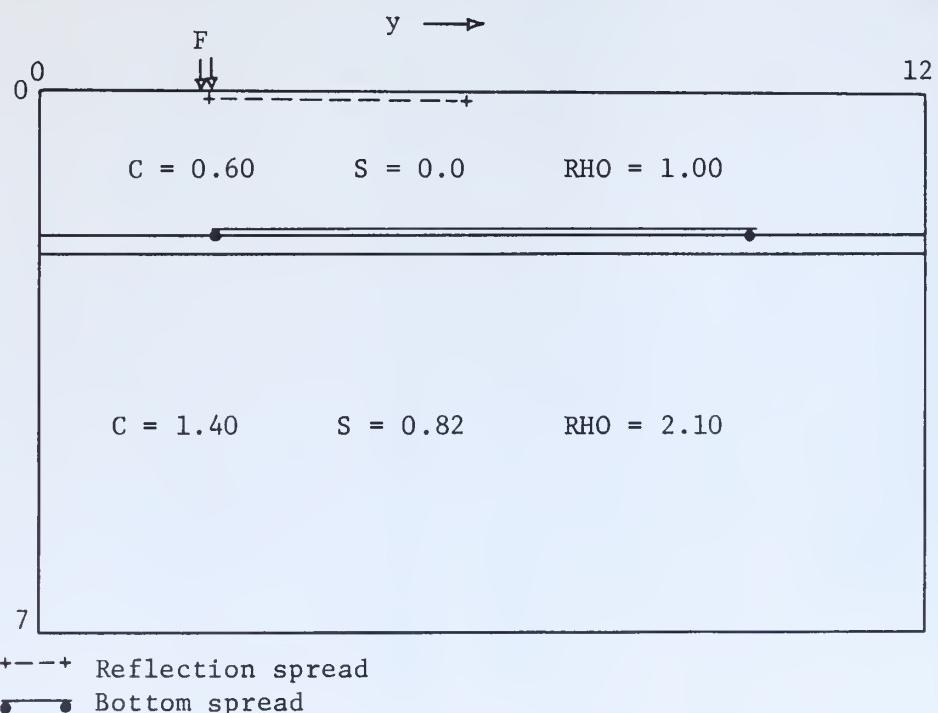
Figure 28. Velocity structure CB
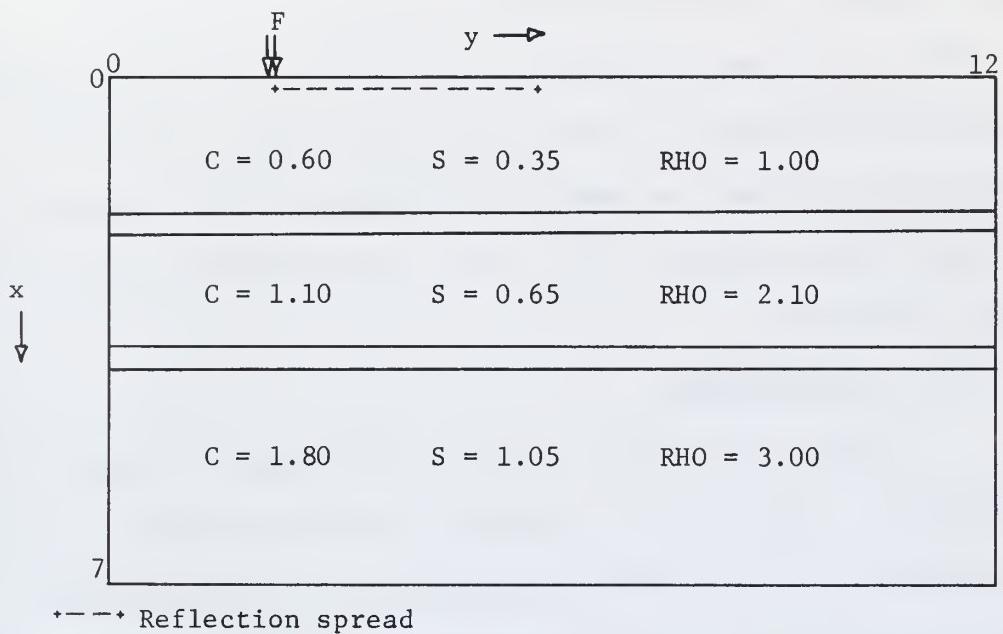
Figure 29. Velocity structure CC

(2)   Water layer over elastic layer, (CB).

(3)   Three elastic layers, (CC).

With the exception of the water layer in CB, all velocity structures
were designed with Poisson's ratio of 0.25.

All traces were produced utilizing forcing function F5A (Fig. 30),
attenuation parameter B3 (Fig. 31) and shot point location L2. At this
shot point location, the surface dilatational forcing stress is applied
at mesh points j=15 and j=16. This is marked by the letter "F" in
Fig. 27 through 29.

1.   The Seismograms

Selected correlated synthetic seismograms are shown in Fig. 32
through 36. Figure 32 is a complete set of four synthetic seismic
records for a close (reflection) spread of 25 surface detectors for
velocity structure CA. The detector spread is shown in Fig. 27. Com-
parison of these records shows the interdependence of the displacements
and stresses. Actual land field records would include only vertical
and/or horizontal displacements, or particle velocity, while marine
records would only consist of the dilatational (pressure) record. The
additional synthetic seismograms enable the proper phase arrivals to be
quickly identified. A set of theoretical time-distance curves was
developed for velocity structures CA and CB (Fig. 37), where it was
assumed that the width of the transition zone was zero. There is good
agreement between these theoretical arrival times and correlated linea-
tions on the synthetic records.

The first trace on the dilatation record corresponds to a
normally incident wave. It bears a very close resemblance to traces
obtained with the one-dimensional model for similar velocity structures.

74
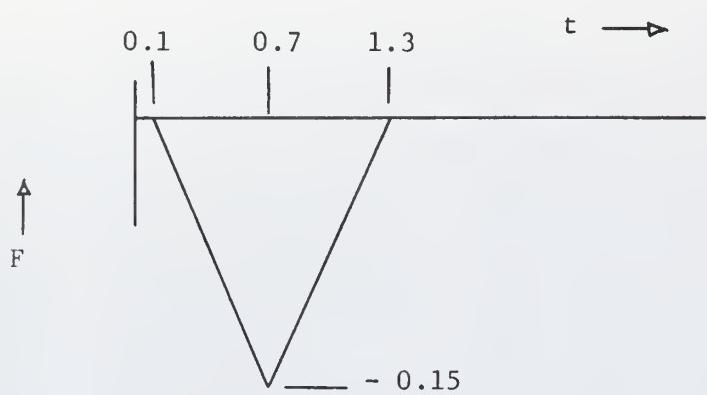
Figure 30. Forcing function F5A
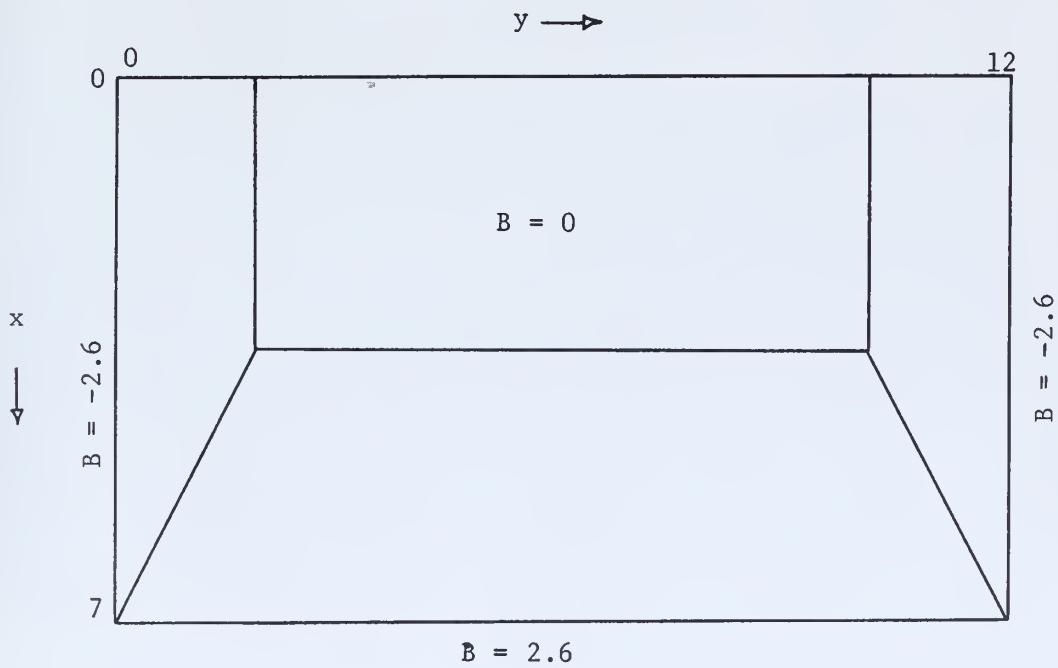
Figure 31. Attenuation parameter B3

Figure 32

Reflection seismogram CA F5A B3 L2

A: Dilatational stress

B: Shear stress

C: Vertical displacement

D: Horizontal displacement

DX: 0.10   DY: 0.15   DT: 0.05

L: 71   M: 81   N: 800

IA: 2   ID: 1   JB: 16   JJ: 1

Horizontal distance (d)

versus

time (t)

———o   Direct wave arrivals

————   First reflections

— — —   Multiple reflections

——–—   Shear-dilatation conversion wave

Figure 32A. Reflection Seismogram CA F5A B3 L2: Dilatational Stress
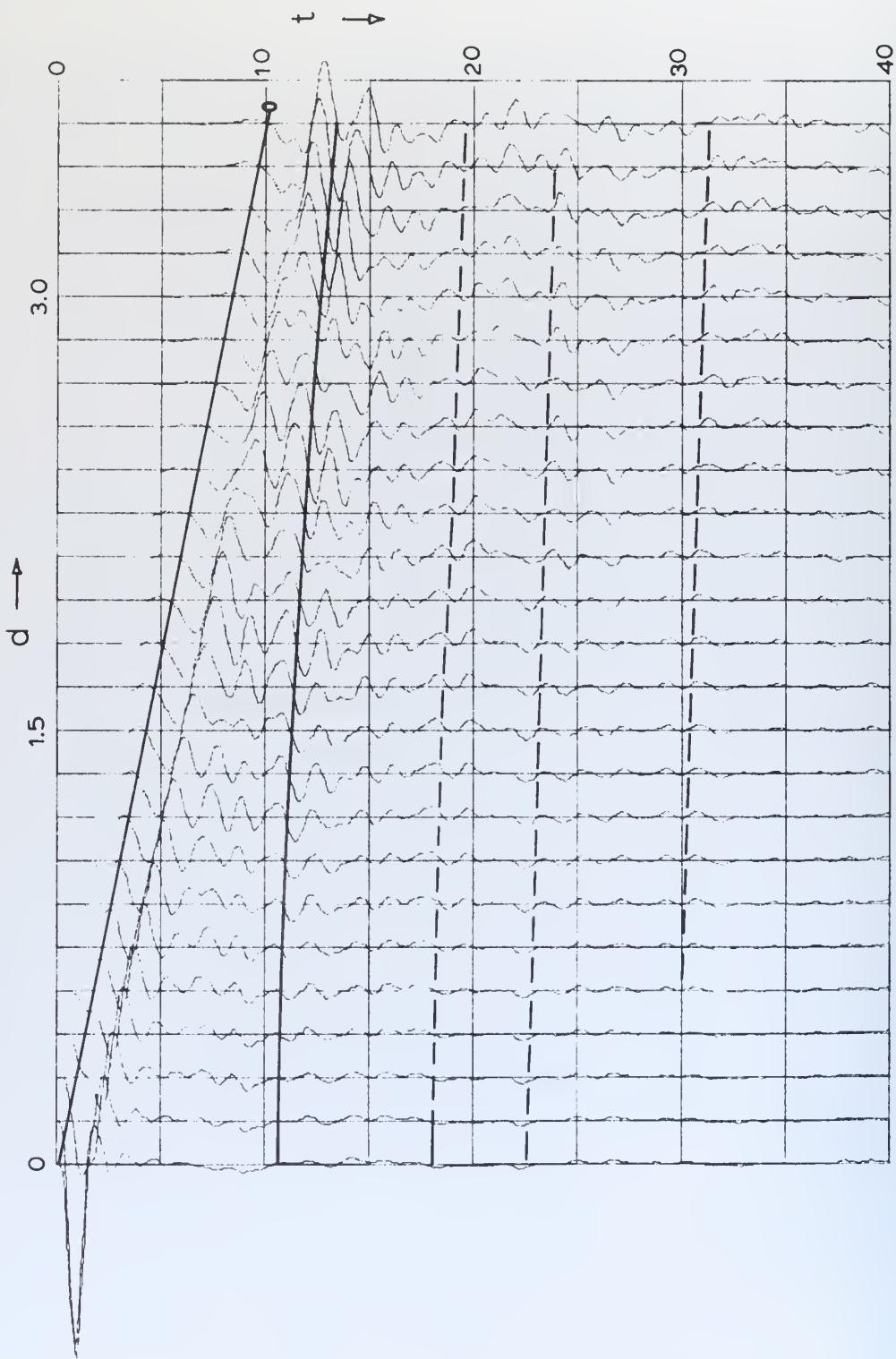
Figure 32B. Reflection Seismogram CA F5A B3 L2: Shear stress
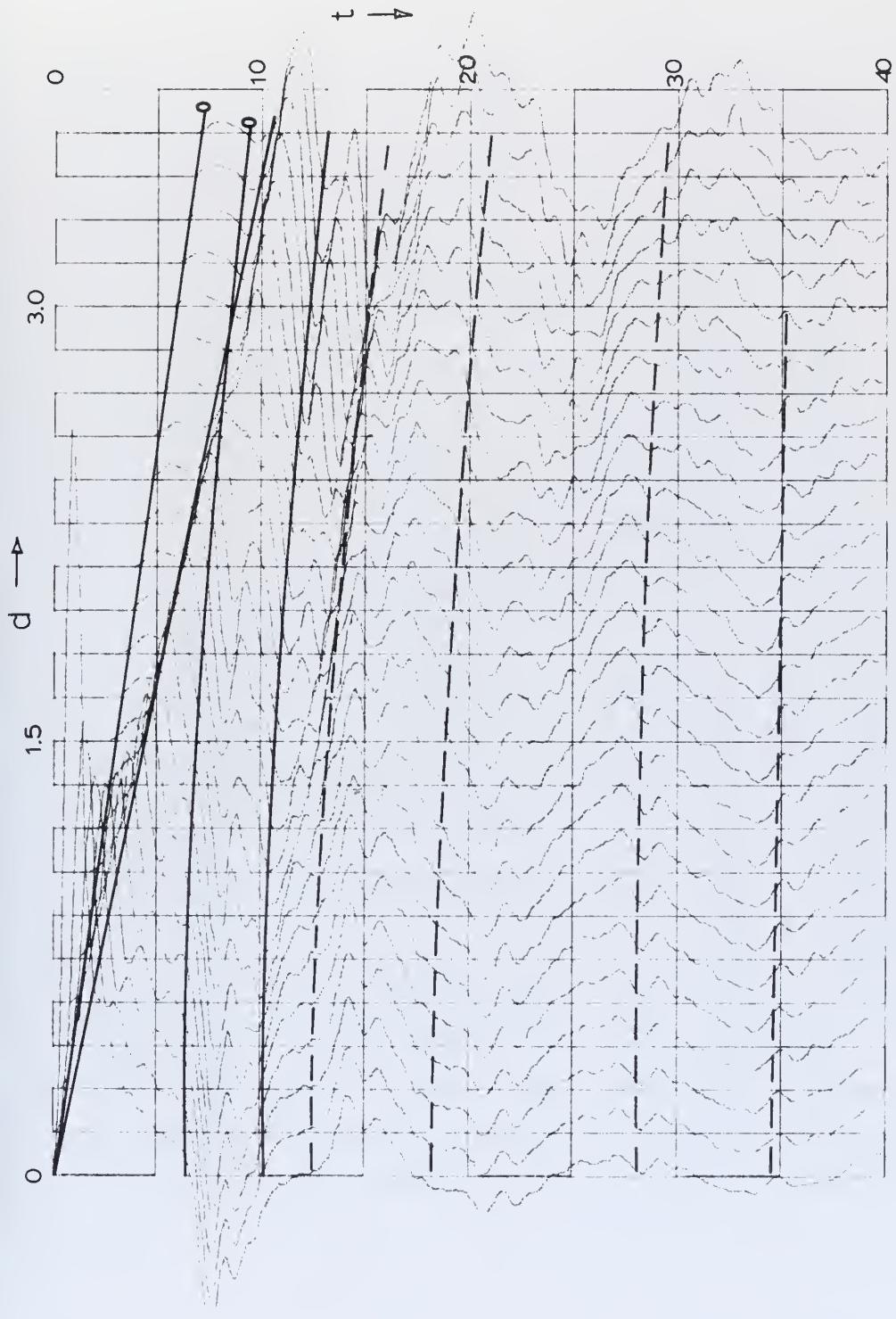
Figure 32C.   Reflection Seismogram CA F5A B3 L2:   Vertical Displacement
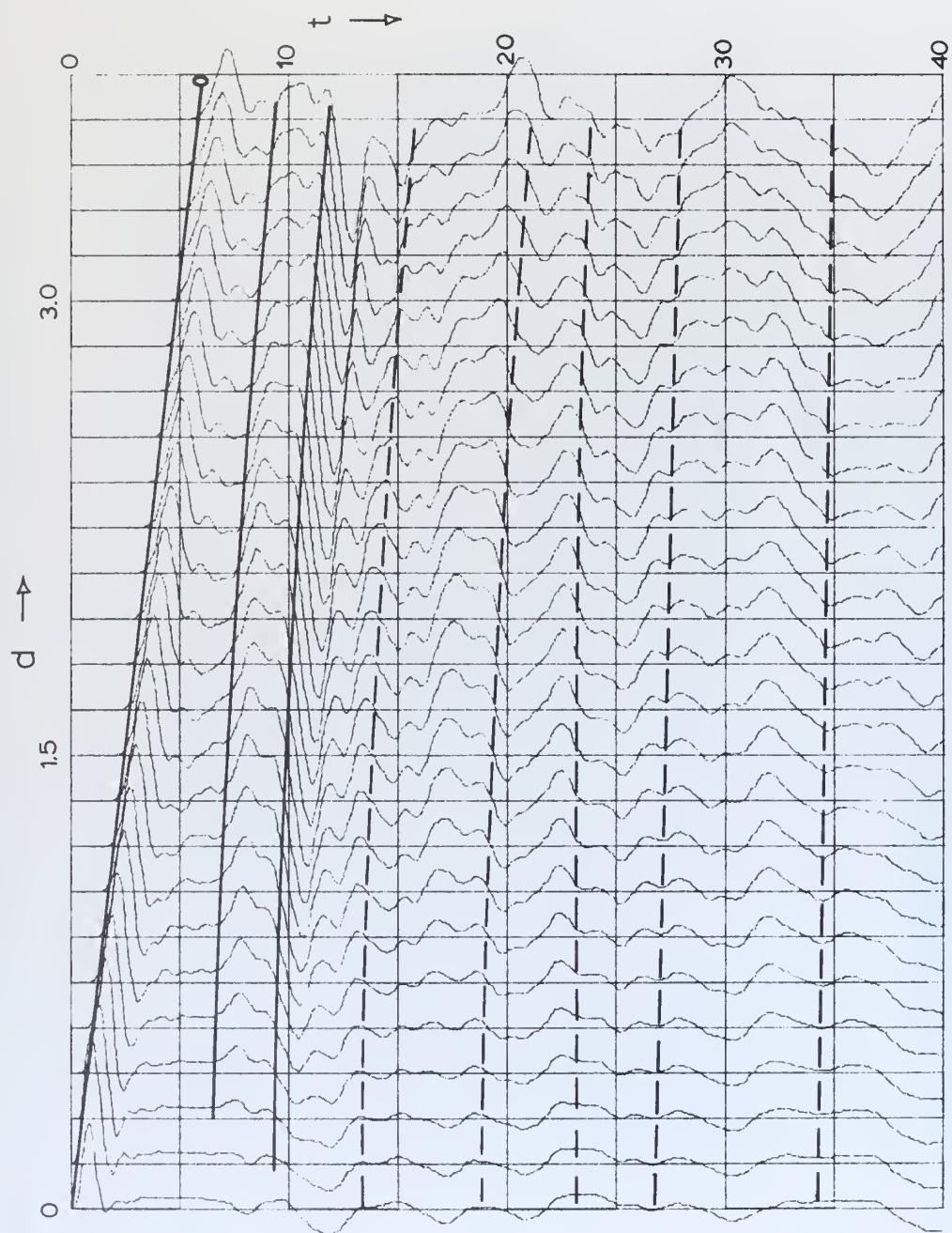
Figure 32D: Reflection Seismogram CA F5A B3 L2: Horizontal Displacement

Figure 33

Refraction seismogram CA F5A B3 L2

Shear stress

DX: 0.10   DY: 0.15   DT: 0.05

L: 71   M: 81   N: 800

IA: 2   ID: 1   JB: 22   JJ: 2

Horizontal distance (d)

versus

time (t)

——————o   Direct wave arrivals

——————   First reflections

—— – ——   Refracted arrivals
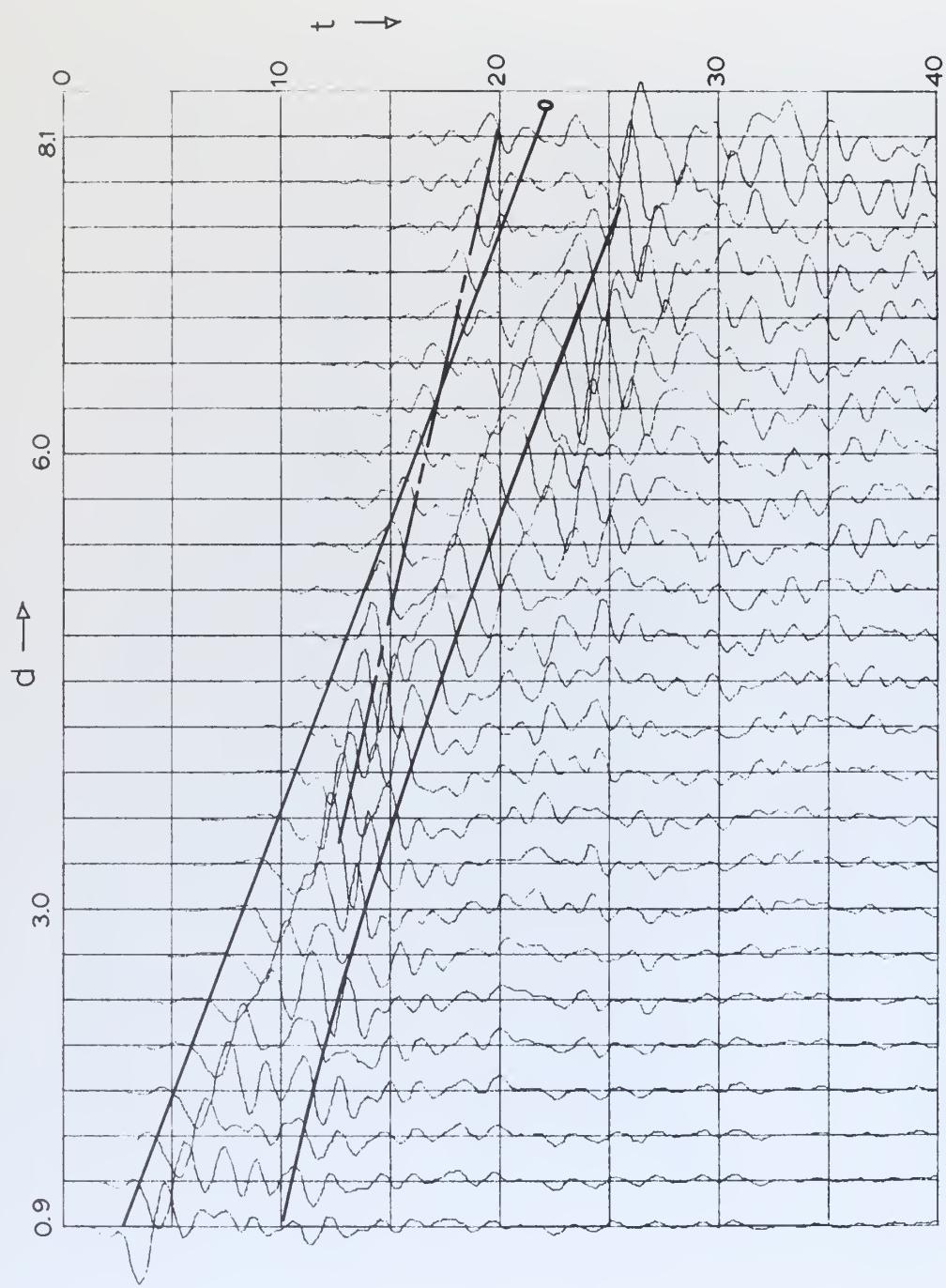
Figure 33. Refraction Seismogram CA F5A B3 L2: Shear Stress

Figure 34

Reflection seismogram CB F5A B3 L2

Dilatational stress

DX: 0.10   DY: 0.15   DT: 0.05

L: 71   M: 81   N: 800

IA: 2   ID: 1   JB: 16   JJ: 1

Horizontal distance (d)

versus

time (t)

————o   Direct wave arrivals

————   First reflections

— — —   Multiple reflections
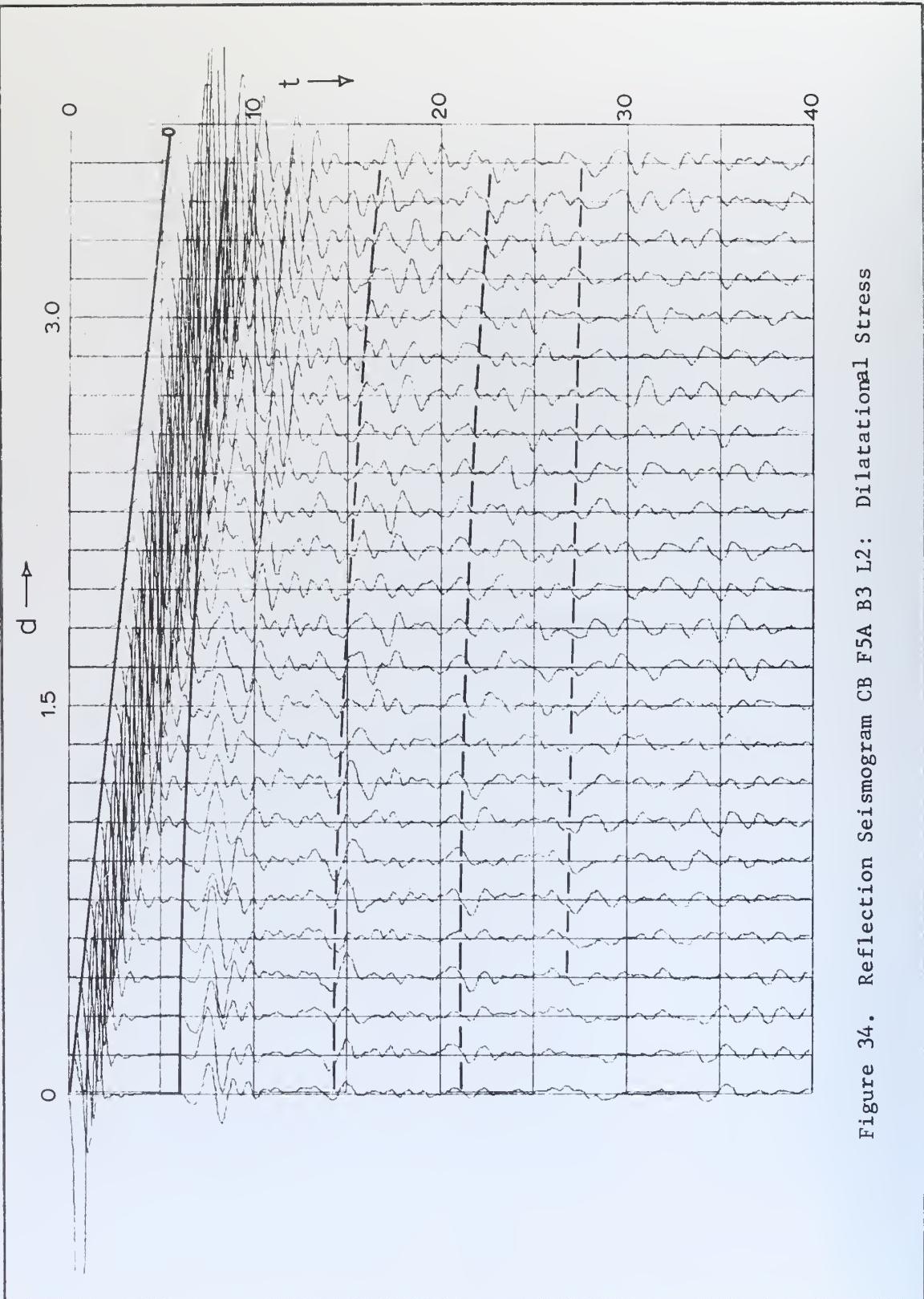
Figure 34. Reflection Seismogram CB F5A B3 L2: Dilatational Stress

Figure 35

Bottom detector seismogram CB F5A B3 L2

Dilatational stress

DX: 0.10   DY: 0.15   DT: 0.05

L: 71   M: 81   N: 800

IA: 20   ID: 20   JB: 16   JJ: 2

Horizontal distance (d)

versus

time (t)

————o   Direct wave arrivals

— — —   Surface reflected multiples

—— - ——   Interface wave conversion
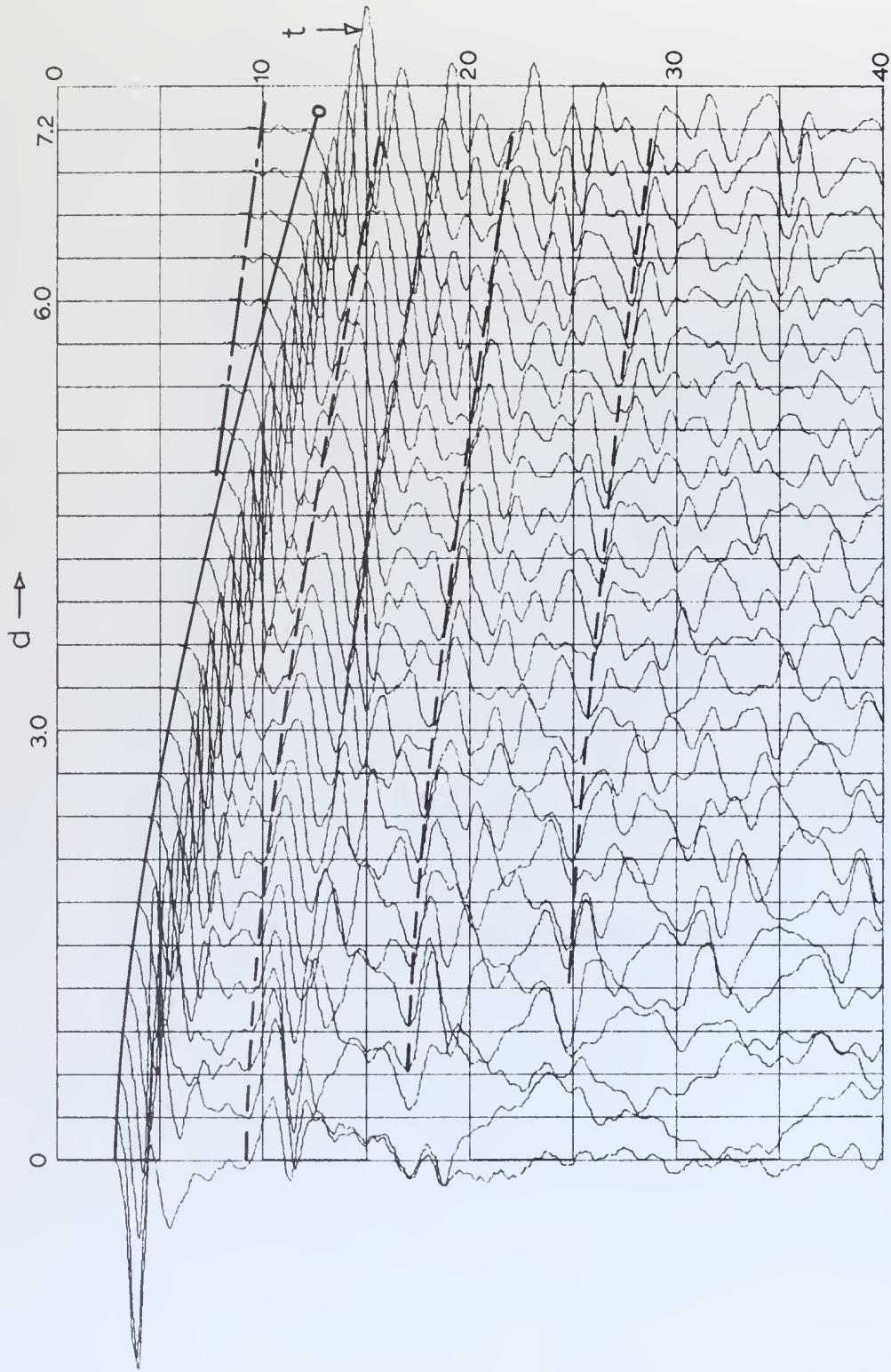
Figure 35. Bottom Detector Seismogram CB F5A B3 L2: Dilatational Stress

Figure 36

Reflection seismogram CC F5A B3 L2

Dilatational stress

DX: 0.10   DY: 0.15   DT: 0.05

L: 71   M: 81   N: 800

IA: 2   ID: 1   JB: 16   JJ: 1

Horizontal distance (d)

versus

time (t)

————o   Direct wave arrivals

————   First reflections

—— ——   Multiple reflections

—— - ——   Shear wave conversion
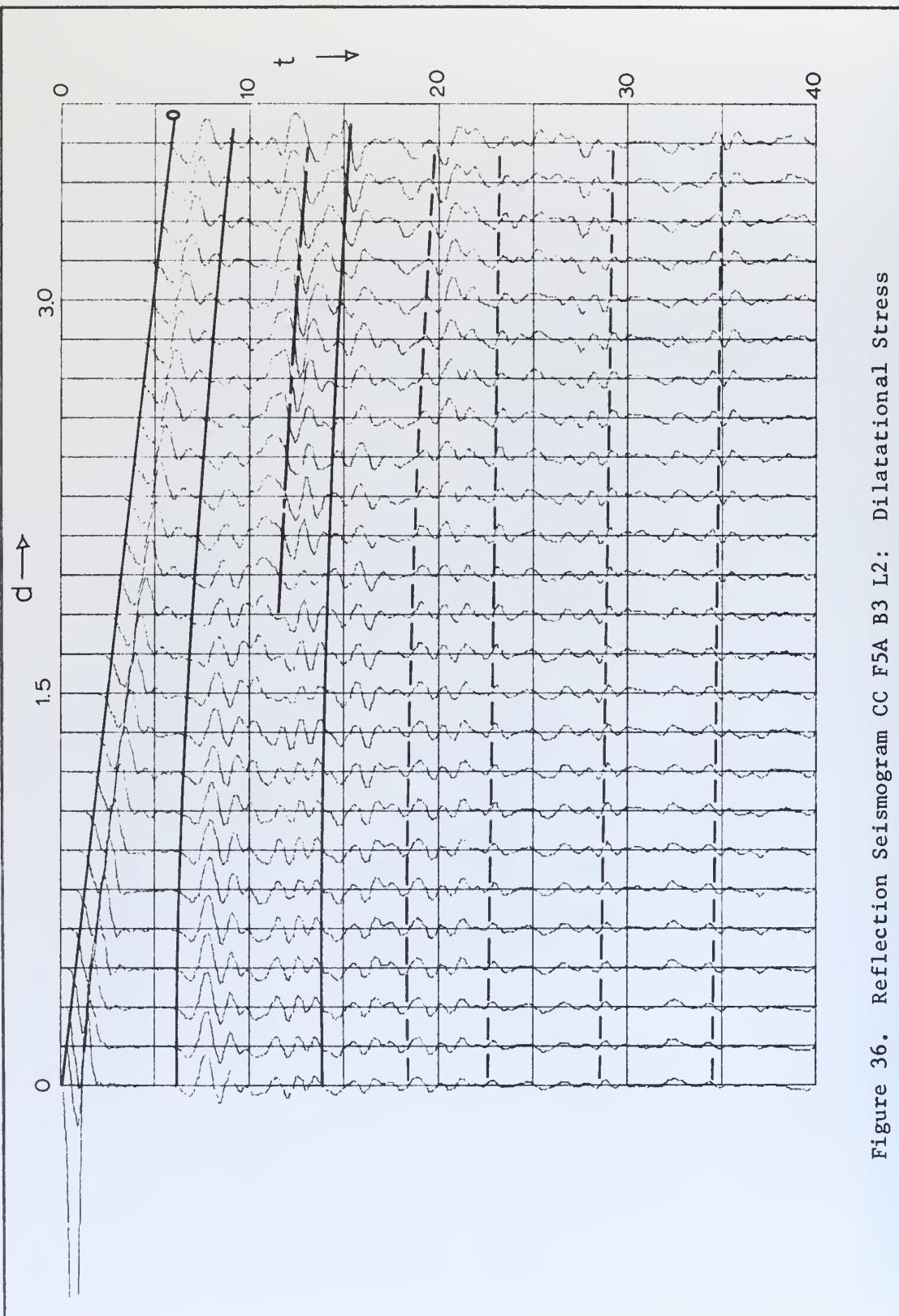
Figure 36. Reflection Seismogram CC F5A B3 L2: Dilatational Stress
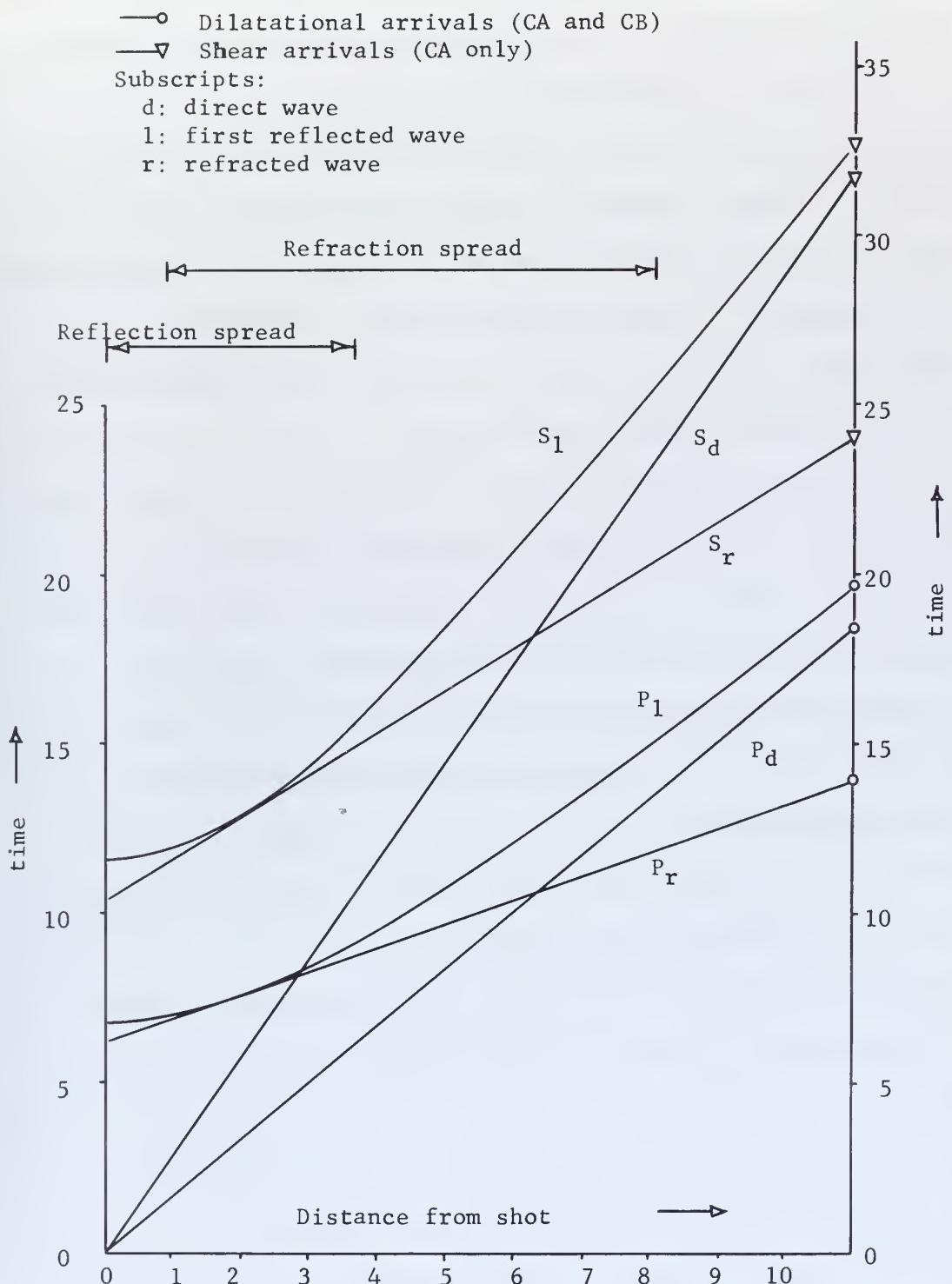
Figure 37. Theoretical time-distance curves for velocity structures CA and CB.

Elastic rebound is present, causing the development of a cyclic wave train. Phase reversal is observed for events reflected from the free surface on all records. These features are particularly apparent in the contour plots discussed in the next section.

Although no refracted arrivals are shown on any of the records of Fig. 32, a close examination of the traces revealed their presence after a refraction record was obtained. Figure 33 is the shear stress refraction record for velocity structure CA. The surface detector spread (shown in Fig. 27) extended across most of the solution space into the attenuation region on the right.

In addition to the arrival of the refracted shear wave, Fig. 33 shows the development of a small shear stress in advance of the first shear arrival. This is generated by the passage of the dilatational wave across the mesh, a result of the coarseness of the mesh relative to the wave velocity. As the dilatational wave passes a mesh point at an oblique angle relative to the x or y axis, shear strains are set up between mesh points. In fact, it is just this effect which causes the generation of the initial shear wave at the forcing function applica-tion point, or, more precisely, between one application point (where the applied dilatational stress causes some displacement) and the neighboring mesh point where displacements are different. The shear wave is then generated from two centers. For shot point location L2, these centers are (fictitious) mesh points $(\frac{1}{2}, 14\frac{1}{2})$ and $(\frac{1}{2}, 16\frac{1}{2})$.

Figure 34 is the dilatational stress reflection record for velocity structure CB. This structure (shown in Fig. 28) is identical to CA except that, in the upper layer, shear wave velocity (and hence, Lamé's constant μ) was set to zero. The record is, of course, very

90

similar to that obtained from structure CA except that the amplitudes

of the first arrivals are somewhat greater. This is caused by the lack

of rigidity in the upper layer leading to a loss of the attenuation

effect of shear strains on dilatational strains.

An example of a seismogram obtained with a spread of detectors

on the bottom of a water layer is shown in Fig. 35. Because of the

relationship between shot point location and detector location, the

only lineations available for correlation, except for the direct wave,

are multiple reflections between the bottom and the surface, and re-

fracted waves. An additional effect observed on this record is the

generation of a head wave in advance of the direct wave. This wave is

generated at the interface between the two layers by the dilatational

wave travelling through the lower medium at a high velocity.

A three-layer reflection seismogram is shown in Fig. 36. The

main feature of this record, not seen in the two-layer seismogram, is

the mutual interference between the first multiple from the first

transition zone and the reflected wave from the second transition zone.

As these two waves are out of phase with one another, the initial

effect is one of destructive interference. As distance from the shot

point is increased, the waves arrive from somewhat different directions,

altering the phase relationships, leading eventually to constructive

interference.

2. The Contour Output

An on-line printer contour plotting subroutine was developed so

that the reflection and transmission of elastic waves might be observed

in a qualitative manner. At chosen intervals, the values of horizontal

or vertical displacement, dilatational or shear stress or vorticity are

computed for each mesh point, converted to an alphabetic representation and printed as a rectangular contour plot. Figures 38 and 39 show portions of such plots, dilatational stress plotted for the problem CB F5A B4 L2 at time mesh levels K=16 and 91 respectively. Figure 38 shows the generation of the initial dilatational wave by the forcing function. Figure 39 shows the progress of the dilatational wave as it is reflected and transmitted at the transition zone. Some minor modification of the main two-dimensional program was necessary to produce this form of output. Examination of the subroutine shows what additional parameters were necessary. Table X shows the scaled values represented by the plotted characters.

An animated motion picture was made of dilatational and shear stress for this problem. This presentation enables the progress of wave fronts throughout the solution space to be readily observed, including phase changes where they occur. This output allowed the efficacy of the attenuation parameter to be determined quite easily during the development phase of the model. A copy of this motion picture on Super 8mm film is on file at the Naval Postgraduate School, Department of Oceanography (Code 58Ad), and is available to interested investigators on a loan basis.

Some effects were noted on the contour outputs before they were identified on the seismograms. The dilatational plots first showed the development of a head wave in the upper layer (Fig. 40). Other presentations clearly show the development of a shear wave in the lower medium due to the incidence of a dilatational wave against an elastic transition zone (Fig. 41) and the generation of an interface wave travelling along the fluid-elastic boundary in advance of the shear wave (Fig. 42).
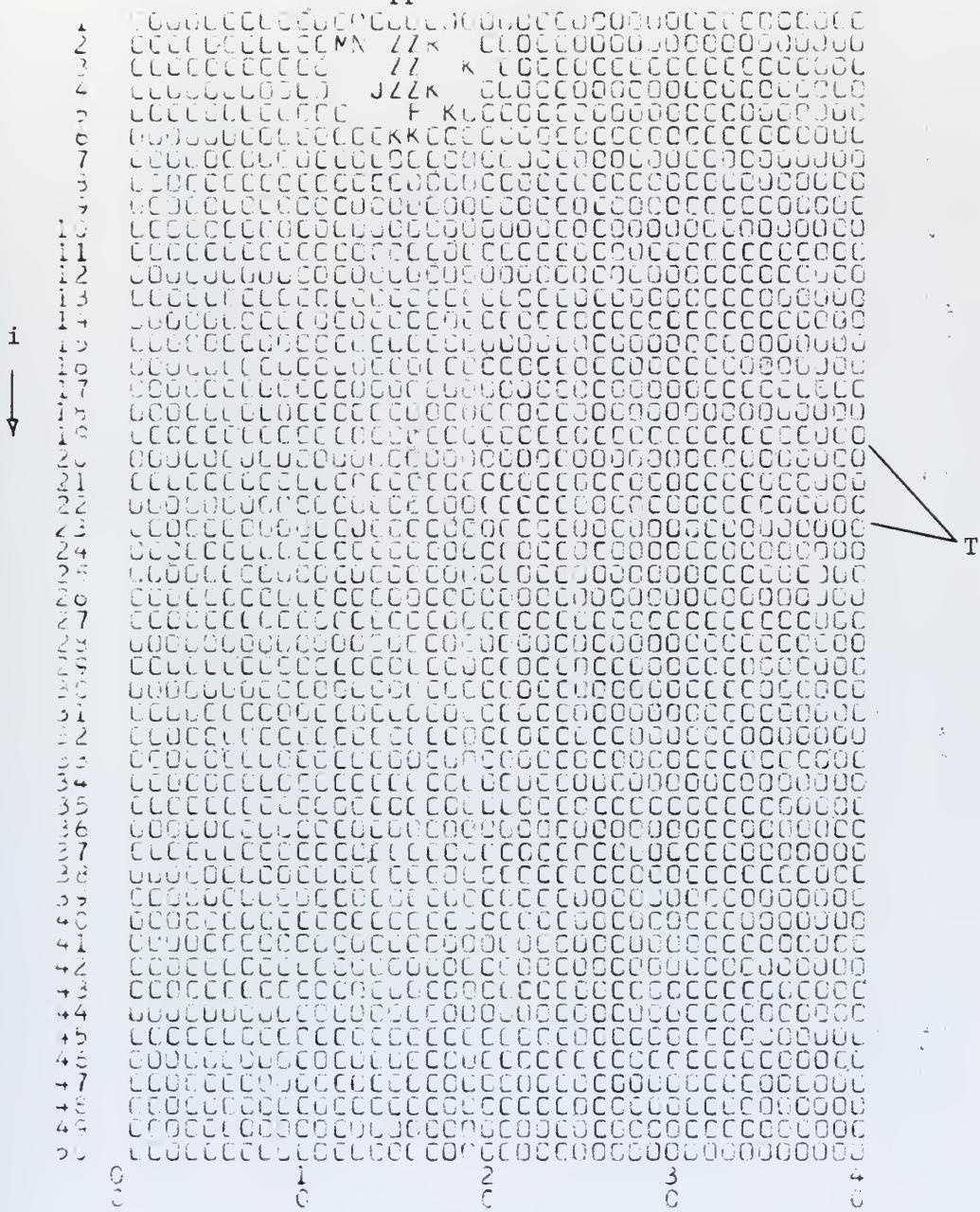
Figure 38. Portion of the printer contour plot showing
generation of the dilatational wave.
(see Table X for scaled values)

T   Transition zone
F   Forcing function application point

93

DILATATION: CB F5A B4 L2   K=91
FF

[contour plot figure]

i ↓

j →

T   Transition zone
F   Forcing function application point

Figure 39.   Portion of the printer contour plot
showing transmission of the dilatational
wave into the lower media
(see Table X for scaled values)

Table X.

SCALE OF CONTOURED QUANTITY

I	SYM(I)	VALUE
1	A	-0.0085417
2		-0.0081250
3	B	-0.0077083
4		-0.0072917
5	C	-0.0068750
6		-0.0064583
7	D	-0.0060417
8		-0.0056250
9	E	-0.0052083
10		-0.0047917
11	F	-0.0043750
12		-0.0039583
13	G	-0.0035417
14		-0.0031250
15	H	-0.0027083
16		-0.0022917
17	J	-0.0018750
18		-0.0014583
19	K	-0.0010417
20		-0.0006250
21	O	-0.0002083
22		0.0002083
23	M	0.0006250
24		0.0010417
25	N	0.0014583
26		0.0018750
27	P	0.0022917
28		0.0027083
29	Q	0.0031250
30		0.0035417
31	R	0.0039583
32		0.0043750
33	S	0.0047917
34		0.0052083
35	T	0.0056250
36		0.0060417
37	U	0.0064583
38		0.0068750
39	V	0.0072917
40		0.0077083
41	W	OVERSCALE
42	Z	UNDERSCALE

Figure 40. Portion of the printer contour plot showing the development of a dilatational head wave.
(see Table X for scaled values)

T Transition zone
H Head wave

SHEAR: CB F5A B4 L2   K=84
                         FF

```
 1  000C0G0CCC0C0CC00CGCCC00CC0C00000C00000000
 2  000000000000000000000000000000000000000000
 3  000C0C00C00C0C00C00C000000C000000000000000
 4  000000000000C0C0C0C00000000000000C0C00000G0
 5  0000000000000000000C00C0000000000C000000C00
 6  000C00000C0C00000000000000C00000000000000000
 7  0000000000000000000C00C0C0C00000000C00000000
 8  0000000000000000000C000C00C00000000000000000
 9  000CC00000C0C0000C0C0C0C00000000000000000000
10  00000000000000000000000000000000000000000000
11  C000000000C00000C0000000000000000C000000C00
12  00000000C00000C0000000C000000000000C00000000
13  000000000000000000000000000000000000000000
14  000000000C000C0C000C0C0C00C00000000C000000
15  00000000C000C0000C000C00C00000000000000000
16  0000000000000C000C0C000000000000000000000
17  000C00000000C00000000C0000C00000000000000
18  000C000000000000000C0000000000000000000000
19  00000C00000C00000C000C0000000000000000000
20  000000000000C000000000000C000000C000000000
21  000000   M  NNM K   JJ K   0000000000000000
22  00000C  MM  NM  KO JKJJ K   000000000000000
23  0000000        00 K0       0000000000000000
24  000000000  0 0 000 0      0000000000000000
25  00000000      C0000       0000000000000000
26  00000000      00000       0000000000000000
27  000C00000     00000      00000000000000000
28  000000000000 00000000 0CC00000000000000000
29  0000000000C0C0000000000000000000000000000
30  000000000C0000000000000C00C00000000000000
31  000C000000000C0000C000000C0000000000000000
32  0000000000C0C000C0000000000000000000000000
33  0000000000C0C00C00000000000000000000000000
34  000000000000000000000000000000000000000000
35  00000C00000000000000000000000000000000000
36  0000000000000C000000000000C00000C00000000
37  000000000000000000000000000000000C0000000
38  00000000C00C00C000C000000C000000000000000
39  000C00000C0C00C000C00C00C000000C00C0000000
40  00000000000000000000000000000000000000000
41  000C00000000C00000C00C0000000000000000000
42  000000000C00C00000C0000000000000000000000
43  000000000000000000000000000000000000000000
44  000000000000C0C000000C00C00000CC000000000
45  00000000C000000000C00C00000000000000000000
46  0000000000CC00000C0C00C00000000000000000
47  00000000000C0000C00C0C0C0000000CC000000000
48  000000000C0C000000000C000000000000000000
49  000C00C0C0C00000000C00C0000000000000000000
50  000000000C00000000000000000000000000000000
```

                    i ↓

      0   1   2   3   4
      0   0   0   0   0

                       j ⟶

                                                  T

        T   Transition zone
        F   Forcing function application point

Figure 41. Portion of the printer contour plot
            showing generation of a shear wave at
            the transition zone by the dilatational
            wave.
              (see Table X for scaled values)

SHEAR: CB F5A B4 L2   K=178

```
 1  CROCCCOCOOOOCOCOOOOOOOOOOOCOOOOOOOOOOOOOOOOOOOO
 2  OOOOOOOOOOOOOOOCOOOOOOOOOOOOOOOOOOOOOCOOOOOOOOO
 3  OOOOCOOOOOOOOOOOOOOOOOOOOOOOOOOOOOOOOOOOOOOOOOO
 4  COOOCOCOOOCOOOCOOOOOOOOOOOOOOOOOOOOOOCOOCCOOOOO
 5  OOOOOOOOOOOOOOOOOOOOOOOOOOOOOOOOOOOOOOCOOOOOOOO
 6  COOCCOCOOOOOCOCOOOOOOOOOOOOOOOOOOOOOOOOOOOOOOOO
 7  OOOOOOOOOOOOOOOOOOOOOOCOOCOOOOOOOOOOCOOOOOOOOOO
 8  OOOOCOCOOOOOOOOOOOOOOOOOOOOOOOOOOOOOOOOOOOOOOOO
 9  OOOCCOCOOOOOOOCOOOOOOOOOOCOOOOOOOOOOOOOOOOOOOOO
10  COOOCOCOOOOOOOOOOOOOOOOOOOOOOOOOOCOCOOOOOOOOOO
11  OOOOCOOOOOOOOOOOOOOOOOOOOOOOOOOOOOOOOOOOOOOOOOO
12  CCOCCOCOOOOOOOOOOOOOOOOOOOOOOOOOCCOOCCCOOOOCOOO
13  OOOOOOOOOOOOOOOOOOOOOOOOOOOOOOOOOOOOOOOOOOOOOOO
14  OCOOCCCOOOOOOOOCCOCOOOOCOOOOOOOOOOOOCOOOOOOOOOO
15  OOOOCOOOOOOOOOOOOOOOOOOOOOOOCOOOOOOOOOOOOOOOOOO
16  OOOOOOOOCOOOCOOOOOOOOOOOOOOOOOOOOOOOOOOOOOOOOOO
17  OOOOCOCOOOOCCOOOOOOOOOOOOOOOOOOOOOOOOOOOOOOOOOO
18  OOOOOOOOOOOOOOOOOOOOOOOOOOOOOOOOOOOOCCOOOOOOOO
19  CCOOOOOOOOOOOOOOOOOOOOOOOOOOOOOOOOOOOOOOOOOOOO
20  OOOOCOCOOOOOOCOOOOOOOOOOOOOOOOCOOOOCOOOOOOOOOC
21    O   OO   JKKJJK  JGD  ZACE  JK     OOOOOCOOOOO
22  G FFF   CNPQRR    NMMQ WWW R   MMMMM    C     OO
23  OOOOOOOOO   OKKO KJ O N      K   OOOCOOOOOOOO
24  OOOOCOOOO O O   OOO   O MMO   K  OOOOOOOOOOOOO
25  OOOOCOCC   OCC  COOOOO M O KK   OOOOOOOOOOOOOO
26  OOOOCOOO   OOO  OO OO    O KK   OOOOCOOOOOOOOO
27  COOOCOOO   OOO   O    O KK   OOOOOOOOOOOOOO
28  OOOOCOC   OCCOOO        O  KK   OOOOCOOOOOOOO
29  OOOOC      OOOOOO     O  O  KK   OOOOOOOOOOOOO
30  OOOO   O OOOOOOO M  OOOO  KK   OOOOOOOOOOOOO
31  OOOO   OOOOO   OO  M OOOOO  KK   OOOOOOOOOOO
32  COOOOOOOOO   OO  M OOOOO   K   OOOOOOOOOOOO
33  OOOOCOOOOC   OO     OOOOO   K   OOOOOOOOOOO
34  OOOOCOOOO    OOC   OOOOOO       OOOOOOOOOOOO
35  COOOCOOOO    OOO   O OOOO     OOOOOOOOOOOO
36  COOOCOOOO   OOCC  OO OOOO     OOOOOOOOOOOO
37  OOOOOOOOO   OOOO  OO OOOO     OOOOCOOOOOOOOC
38  OOOOOOCOOOOOOOCC   OOOOOOO    OOOOOOOOOOOO
39  OOOOCOOOOOOO  OO OOOOOOOO    OOOOOOOOOOOO
40  OOOOOOOOOOO   OO OOOOOOO    OOOOOOOOOOO
41  OOOOCOOOOOO OC   OOOOOOO     OOOOOOOOOOOO
42  OOOOCOOOOO  OO   OOOOOOO    OOOOOOOCOOCCOOO
43  COOOCOOOO   OO    OOOOOOO   OOOOOOOOOOOOO
44  OCOOCOOO OOO      OOOOOOOOOOOOOOOOOOOOOOOO
45  OOOOOOOOOO    OOOOOOOOOOOOOOOOOCOOOOOOO
46  OCOOCOOOO      OOOOOOOOOCOOOOOOOOOOOOOO
47  OOOOOOOO   OO  OOOOOOOOOO   OOOCOOCOOOOO
48  OOOOOO     OO  OOOOOOOOOO   OOOOOOOOOOOO
49  OCOO       OC OOOOOOOOOO    OOOOCOOOOOO
50  OOO      OOO  OOO OOOOOO    OOOOOOOOOOOO
      2         3         4         5         6
      0         0         0         0         0
```

i ↓

j ⟶

T   Transition zone
I   Interface wave

Figure 42.   Portion of the printer contour plot
             showing development of an interface
             shear wave.
             (see Table X for scaled values)

V. SUMMARY

The two seismic models presented here were developed primarily as
tools to assist in marine geophysical field exploration. The models
produce synthetic seismograms similar in format to that of actual field
records in order to facilitate direct comparison. Although both models
present two-dimensional records (horizontal distance versus time), the
reflection profiling model is made up of a series of one-dimensional
model solutions. The complete solution simulates a moving source of
vertically incident pulses where the velocity structure is slightly
altered between transmissions. In contrast, the reflection/refraction
model treats the propagation of energy in two dimensions. Each complete
solution simulates a single pulse travelling through the solution space.
The synthetic seismograms are produced as records from a series of
detectors in a horizontal array.

The models are based on numerical solutions to the wave equations
in one and two dimensions in bounded domains. The equations are
expressed in unsimplified forms which are not amenable to direct
analytical solution. The stability of these numerical solutions and
their convergence to the analytical solutions was investigated. Sta-
bility and convergence criteria were established in terms of mesh
ratios and wave velocities.

In order to provide a wide variability of physical simulation, the
solution domains are modeled by a number of easily varied non-dimen-
sional parameters. These parameters are used to set the size and sub-
division of the solution space as well as the distribution of elastic
parameters and the shape and extent of the forcing function.

The structures modeled in this paper were, in general, based upon realistic distributions of the non-dimensional elastic parameters in marine environments. Some of these models have inherent resonance with the type and width of the forcing function used and the mesh sizes. Records are produced with some features which reflect this resonance. In particular, there is some tuning of the pulses in the narrow transition zone in some of the models. Care should be taken when trying to extrapolate features found in these records to cover a more general case.

VI. <u>FUTURE WORK</u>

The applicability of these models to a wide variety of studies was
the primary consideration in their design. The interpretation of various
velocity structures in this study was limited to a gross overview of
simpler problems that might be encountered in field exploration. Al-
though a full presentation of the use of all of the variable parameters
was not attempted here, there are areas in both models where improvements
could be made which would increase their variability.

A first step in improvement of the one-dimensional model might be
the inclusion of a variable depth source. It was felt that this was not
warranted in the model due to the complexity of a forcing function at
depth that could not be included as part of one boundary condition.

The same improvement might be applied to the two-dimensional model.
However, this would involve an additional order of magnitude of com-
plexity and the model could no longer be called "simplified." A more
reasonable improvement could be made which would remove the requirement
that all transition zones be horizontal. The wave velocities and
density could be put into the model as two-dimensional arrays instead
of vectors. Terms involving the y-derivative of Lamé's constants and
of density would then be retained. This improvement would approximately
double the main core storage required (to 550K bytes) and increase the
main program run time by about one-third (to 24 min).

Although the attenuation parameters used in both models are con-
sidered adequate for the purpose for which they were included (elimi-
nation of boundary reflections), they are by no means definitive.

These models could be used to study the effects of various velocity attenuation functions by entering A(x) or B(x,y) as functions of other physical parameters (e.g. overburden pressure, Lame's constants or particle displacement).

Only a single forcing function is presented for each model. Several functions were examined in the development of the models including a flat-topped pulse, spike pulse and "sinc" function. The models could be used to study the reflection and/or refraction of a wide variety of forcing functions, limited only by the size of the time mesh increment (DT).

In Section III, it was noted that an interface wave was observed in shear stress on the contour plot output. This model could certainly be used to study the various classes of such waves under a variety of conditions. Some preliminary work was done in generating particle motion plots from the vertical and horizontal displacement outputs available. Although elliptical particle motions were observed as pre- dicted [Alterman and Rotenberg 1969], limitations of distance from the generating point did not permit identification of the interface phases.

Neither model is by any means limited to the homogeneous layer- transition zone structure presented in this paper. The velocity structure could consist entirely of transition regions of various gradients. This could be applicable to investigation of the effects of the gradients on reverberation.

A collection of records is on file at the Naval Postgraduate School, Department of Oceanography (Code 58Ad).

SEISMIC REFLECTION PROFILING MODEL

NUMERICAL METHOD OF ONE DIMENSIONAL SEISMIC MODELING.

THIS PROGRAM PRODUCES A ONE DIMENSIONAL SEISMIC MODEL FOR THE
TRANSMISSION OF A NORMALLY INCIDENT DILATATIONAL WAVE THROUGH
TRANSVERSELY ISOTROPIC MEDIA IN WHICH THE DILATATIONAL WAVE
VELOCITY AND THE AMOUNT OF VELOCITY ATTENUATION CAN BE
DESCRIBED AS COMBINATIONS OF LINEAR FUNCTIONS OF DISTANCE.

METHOD:

REPEATED NUMERICAL SOLUTION BY FINITE DIFFERENCES OF THE
HYPERBOLIC WAVE EQUATION:

$$(U)TT = (V(U)X)X + A(U)T$$

WHERE:

V IS THE SQUARE OF THE DILATATIONAL WAVE VELOCITY.
A IS THE VELOCITY ATTENUATION PARAMETER.

SUBJECT TO THE FOLLOWING COLLATERAL CONDITIONS:

B1: U(L,T) = 0. LOWER BOUNDARY IS PERFECTLY REFLECTIVE.

B2: DU/DX = F(T) ON X=0. VARIABLE STRESS APPLIED TO
                           THE UPPER BOUNDARY.

I1: U(X,0) = 0. INITIAL DISPLACEMENTS ARE ZERO.

I2: DU/DT = 0 ON T=0. INITIAL DISPLACEMENT VELOCITIES
                        ARE ZERO.

PARAMETER LIST:

U: WORKING ARRAY OF DISPLACEMENTS. DIMENSIONED (N,3)

D: OUTPUT VECTOR OF DILATATIONAL STRESSES. DIMENSIONED (M)

C: WAVE VELOCITY VECTOR. DIMENSIONED (N).

A: ATTENUATION PARAMETER VECTOR. DIMENSIONED (N)

F: FORCING FUNCTION VECTOR. DIMENSIONED (M).

DX: MESH SIZE IN THE X DIRECTION.

103

DT: MESH SIZE IN THE T DIRECTION.

DK: HORIZONTAL DISTANCE BETWEEN SUCCESSIVE SOLUTION
STATIONS.

N: NUMBER OF X MESH POINTS. N.LE.251

M: NUMBER OF TIME STEPS IN EACH SOLUTION, M.LE.2000

NC: NUMBER OF POINTS (CX,CT) DEFINING THE WAVE VELOCITY
C(I) POLYGON. NC.LE.20.

NA: NUMBER OF POINTS (AX,AT) DEFINING THE DAMPING PARAMETER
A(I) POLYGON. NA.LE.20.

MF: NUMBER OF POINTS (FT,FX) DEFINING THE FORCING FUNCTION
F(I) POLYGON. MF.LE.20.

IP: INDEX OF THE X MESH POINT AT WHICH THE OUTPUT STRESS
VECTOR IS COMPUTED.

NG: NUMBER OF HORIZONTAL STATIONS IN THE VELOCITY ARRAY.

EX: VECTOR OF HORIZONTAL STATION LOCATIONS OF THE
VELOCITY ARRAY. DIMENSIONED (NG).

EE: ARRAY OF VELOCITIES. GIVES DEPTH OF A PARTICULAR
VELOCITY AT EACH HORIZONTAL STATION. DIMENSIONED (NG,NC).

CT: INITIALIZING VECTOR OF VELOCITY VALUES. DIMENSIONED (NC).

EEE: HORIZONTAL DISTANCE TO FIRST SHOT POINT.

DS: SCALING FACTOR FOR THE PLOT OF THE STRESS VECTOR.

TS: TIME SCALE IN UNITS PER INCH USED IN THE OUTPUT PLOT.

XSP: SPACING IN INCHES BETWEEN TIME GRID LINES ON THE
SYNTHETIC SEISMOGRAM.

YSP: SPACING IN INCHES BETWEEN TRACES ON THE
SYNTHETIC SEISMOGRAM.

OUTPUT:

KK SUCCESSIVE GRAPHS OF STRESS VERSUS TIME.

```
      DATA GG/'U R2'/
      REAL TA/'TIME'/
      DIMENSION U(251,3),F(2000),CX(20),CT(20),AX(20),
     1AT(20),FX(20),FT(20),D(2000),T(2000),X(251),EE(10,13),
     2XG(250),YG(250),GTI(11),EX(11),ET(10),CC(50),CO(50,13),
     3BA(251),BB(251),BC(251),GTI(11),I=1,11)
      READ(5,102)(GTI(I),I=1,11)
      READ(5,103)N,M,NA,NC,NF,NG,LL,IP,NCT,KK
      READ(5,101)DX,DT,DK,DS,TS,EEE
      READ(5,100)XSP,YSP
      READ(5,104)(EX(I),I=1,NG)

      WRITE(6,999)      GTI
      WRITE(6,211)      GG
      WRITE(6,212)      N,M,NA,NC,NF,NG,LL,IP,NCT,KK
      WRITE(6,214)      DX,DT,DK,DS,TS,EEE
      WRITE(6,216)      XSP,YSP
      WRITE(6,215)(I,EX(I),I=1,NG)
      NM1=N-1
      MM1=M-1
      MM2=M-2
      R2=(DT/DX)**2
      TP=1.0
      TINC=1.0/TS
      V=M
      ST=V*DT*TS

      READ(5,105)((EE(I,J),I=1,NG),CT(J),J=1,NC)
      READ(5,100)(AX(I),AT(I),I=1,NA)
      READ(5,100)(FX(I),FT(I),I=1,NF)

      WRITE(6,999)      GTI
      WRITE(6,206)      GG
      WRITE(6,210)(J,(EE(I,J),I=1,NG),CT(J),J=1,NC)
      WRITE(6,999)
      WRITE(6,200)(I,AX(I),AT(I),I=1,NA)
      WRITE(6,200)(I,FX(I),FT(I),I=1,NF)

      CALL POLYG(N,DX,AX,AT,NA,0.0,A,LB)
      DO 13 J=1,M
   13 F(J)=0.0
      CALL POLYG(LL,DT,FX,FT,NF,0.0,F,LC)

      WRITE(6,203)      LB
      WRITE(6,202)(I,A(I),I=1,N,5)
      WRITE(6,204)      LC
```

```
      WRITE(6,202)(J,F(J),J=1,LL)
   18 WRITE(6,999)
      T(1) = 0.0
      X(1) = 0.0
      DO 19 I=1,N
      V=I-1
      X(I)=V*DX
   19 DO 20 J=1,M
      V=J-1
   20 T(J)=V*DT*TS
C
      DO 48 J=1,NC
      DO 49 I=1,NG
      ET(I)=EE(I,J)
   49 CONTINUE
      CALL PCLYG(KK,DK,EX,ET,NG,EEE,CC,LF)
      DO 51 I=1,KK
      CO(I,J)=CC(I)
   51 CONTINUE
   48 CONTINUE
      V=KK
      YMAX=V*YSP
      CALL GRID(0.0,ST,0.0,YMAX,XSP,YSP,XG,YG,KA,LD)
      CALL PLOTS
      CALL SYMBOL(1.0,1.0,0.14,GTI,00.0,44)
      CALL SYMBOL(1.0,0.00,0.14,'C D LODGE   BOX 96   B1',0.0,24)
      CALL AXIS(0.0,2.0,TA,NCT,ST,0.0,0.0,TINC)
      CALL PLOT(0.0,2.5,-3)
      CALL LINE(XG,YG,KA,1,1)
C
C
C     SETTING FIRST TWO ROWS TO ZERO:
C
      DO 14 KY=1,KK
      DO 10 I=1,N
      U(I,1)=0.0
      U(I,2)=0.0
   10 CONTINUE
      D(1)=0.0
      D(2)=0.0
      DO 52 I=1,NC
      CX(I)=CO(KY,I)
   52 CONTINUE
C
      VOX=KY-1
      VOX=VOX*DK
      WRITE(6,217) KY,VOX
      WRITE(6,211) GTI
```

```
      WRITE (6,200) (I,CX(I),CT(I),I=1,NC)
      CALL POLYG(N,DX,CX,CT,NC,0.0,C,LA)
C
      DC=C(2)-C(1)
      C2=C(1)**2
      BA(1)=1.0/(1.0-0.5*A(1)*DT)
      AB(1)=(-1.0-0.5*A(1)*DT)*BA(1)
      BC(1)=(2.0-2.0*C2*R2)*BA(1)
      BD(1)=C(1)*R2*DC
      BE(1)=(C2*R2+BD(1))*BA(1)
      BF(1)=(C2*R2-BD(1))*BA(1)
      DO 7 I=2,NM1
      DC=C(I+1)-C(I-1)
      C2=C(I)**2
      BA(I)=1.0/(1.0-0.5*A(I)*DT)
      BB(I)=(-1.0-0.5*A(I)*DT)*BA(I)
      BC(I)=(2.0-2.0*C2*R2)*BA(I)
      BD(I)=0.5*C(I)*R2*DC
      BE(I)=(C2*R2+BD(I))*BA(I)
    7 BF(I)=(C2*R2-BD(I))*BA(I)
C
C     COMPUTING FIRST AND LAST MEMBERS OF J+1 ROW:
C
      NN=1
    9 DO 11 J=3,M
    6 GO TO(1,2,3,5),NN
    1 LI=3
      L=2
      LJ=1
      GO TO 4
    2 LI=1
      L=3
      LJ=2
      GO TO 4
    3 LI=2
      L=1
      LJ=3
      GO TO 4
    5 NN=1
      GO TO 1
    4 U(1,LI)=BC(1)*U(1,L)+(BE(1)+BF(1))*U(2,L)-BF(1)*2.*DX*F(J)
     1+BB(1)*U(1,LJ)
      U(N,LI) = 0.0
C
C     COMPUTING ENTIRE J+1 ROW:
C
      DO 12 I=2,NM1
      U(I,LI)=BC(I)*U(I,L)+BE(I)*U(I+1,L)+BF(I)*U(I-1,L)+BB(I)*U(I,LJ)
```

107

```
   12 CONTINUE
      NN=NN+1
      D(J)=(0.50/DX)*DS*(U(IP+1,LI)-U(IP-1,LI))
   11 CONTINUE
C
      CALL LINE(T,D,M,1,1)
      CALL PLOT(0.0,YSP,-3)
   14 CONTINUE
      V=10.0
      CALL PLOT(0.0,V,-3)
      CALL PLOTE
      WRITE(6,205)
C
  100 FORMAT(2F10.0)
  101 FORMAT(6F10.0)
  102 FORMAT(11A4)
  103 FORMAT(10I5)
  104 FORMAT(F10.0)
  105 FORMAT(5F10.0)
  202 FORMAT(I7,2F15.5)
  203 FORMAT(I7,F12.5)
  204 FORMAT('1',9X,'LB =',I3//5X,'I',7X,'A(I)'//)
  205 FORMAT('0',9X,'LC =',I3//5X,'J',7X,'F(J)'//)
  206 FORMAT('0',15X,'END OF GRAM'//)
      FORMAT('0',15X,'VELOCITY DEFINING ARRAY'//30X,'DEPTHS',
     122X,'VELO'//)
  210 FORMAT('0',6X,I3,3X,10F5.1)
  211 FORMAT('0',10X,11A4/)
  212 FORMAT(13X,A4/)
  213 FORMAT('0',9X,'N',5X,'M',5X,'NA',4X,'NC',4X,'NF',4X,'NG',4X,
     1'LL',4X,'IP',4X,'NCT',3X,'KK'/6X,10I6)
  214 FORMAT('0',6X,'DX',10X,'DT',10X,'DK',10X,'DS',10X,'TS',10X,
     1'EE'/6F12.4)
  215 FORMAT('0',10X,'EX(I)'/6(I6,F10.4/))
  216 FORMAT('0',6X,'XSP',9X,'YSP'/2F12.4)
  217 FORMAT('1'//10X,'SHOT NR:',I3,10X,'DIST:',F8.3//)
   99 FORMAT('1')
C
      STOP
      END
```

108

SEISMIC REFLECTION/REFRACTION MODEL

NUMERICAL METHOD OF TWO DIMENSIONAL SEISMIC MODELING.

THIS PROGRAM PRODUCES A TWO DIMENSIONAL SEISMIC MODEL FOR THE
TRANSMISSION OF DILATATIONAL AND SHEAR WAVES THROUGH TRANSVERSELY
ISOTROPIC HORIZONTALLY LAYERED MEDIA IN WHICH THE WAVE VELOCITIES,
DENSITY AND VELOCITY CAN BE DESCRIBED AS COMBINATIONS OF LINEAR
FUNCTIONS OF DISTANCE.

PARAMETER LIST:

DISTRIBUTION PARAMETERS AND WORKING ARRAYS AND VECTORS:

U: WORKING ARRAY OF VERTICAL DISPLACEMENTS. DIMENSIONED (L,M,3).

V: WORKING ARRAY OF HORIZONTAL DISPLACEMENTS. DIMENSIONED (L,M,3)

B: ARRAY OF ATTENUATION PARAMETERS. DIMENSIONED (L,M).

C: VECTOR OF DILATATIONAL VELOCITIES. DIMENSIONED (L).

S: VECTOR OF SHEAR VELOCITIES. DIMENSIONED (L).

PH: VECTOR OF DENSITIES. DIMENSIONED (L).

F: ARRAY OF FORCING FUNCTIONS. DIMENSIONED (M,LL)

FI: FORCING FUNCTION INPUT VECTOR. DIMENSIONED (LL).

PD,PS,PR,PQ: OUTPUT VECTORS OF DILATATIONAL AND SHEAR STRESSES.
     VERTICAL AND HORIZONTAL DISPLACEMENTS. EACH DIMENSIONED (KK).

NUMERICAL PARAMETERS:
DX: MESH SIZE IN THE X DIRECTION.

DY: MESH SIZE IN THE Y DIRECTION.

DT: MESH SIZE IN THE T DIRECTION.

L: NUMBER OF X MESH POINTS. L.LE.71

M: NUMBER OF Y MESH POINTS. M.LE.81

N: NUMBER OF T MESH POINTS. N.LE.800

NC: NUMBER OF POINTS DEFINING THE WAVE VELOCITY AND DENSITY
     POLYGONS. NC.LE.20

NBA: NUMBER OF POINTS DEFINING THE VERTICAL ATTENUATION
     PARAMETER. NBA.LE.20

NBB: NUMBER OF POINTS DEFINING THE HORIZONTAL ATTENUATION
     PARAMETER, NBB.LE.20

NF: NUMBER OF POINTS DEFINING THE FORCING FUNCTION POLYGON. NF.LE.20

IA: INDEX OF THE X MESH POINT AT WHICH OUTPUT STRESSES ARE
    TO BE COMPUTED.

ID: INDEX OF THE X MESH POINT AT WHICH OUTPUT DISPLACEMENTS
    ARE TO BE COMPUTED.

KK: NUMBER OF OUTPUT STATIONS (DETECTORS) KK.LE.40

JB: INDEX OF THE Y MESH POINT OF THE FIRST DETECTOR LOCATION.

JJ: MESH POINT INCREMENT BETWEEN DETECTORS.

MA,MB: INCLUSIVE INDICES OF THE FORCING FUNCTION APPLICATION AREA.

SS: SCALING FACTOR FOR THE OUTPUT VALUES

OUTPUT:

     THE VALUES OF THE FOUR QUANTITIES (PD,PS,PR,PQ) ARE WRITTEN
     ON A STORAGE DEVICE (TAPE,DISK OR DRUM) FOR LATER RETREIVAL
     AND PLOTTING.

```
      DATA GG/6HUV11 /
      DIMENSION U(71,81,3),V(71,81,3),AX(20),AT(20),C(71),BA(71),
     1BB(81),FI(100),X(71),Y(81),T(800),B(71,81),F(81,100),S(71),
     2PD(40),PS(40),PR(40),GTI(11),AA(71),AB(71),AC(71),AD(71),
     3AE(71),AF(71),AH(71),AI(71),AJ(71),AK(71),AL(71),RH(71),
     4PQ(40)
      CALL CANCEL(2)
      READ(5,108)(GTI(I),I=1,11)
      READ(5,106) L,M,N,NC,NBA,NBB,NF,IA,LL,KK,JB,JJ,MA,MB,ID
      READ(5,107) DX,DY,DT,SS,TS
      WRITE(6,200)(GTI(I),I=1,11),GG,L,M,N,NC,NBA,NBB,NF,IA,
     1LL,KK,JB,JJ,MA,MB,ID
      WRITE(6,201) DX,DY,DT,SS,TS
      WRITE(1)(GTI(I),I=1,11),GG,L,M,N,NC,NBA,NBB,NF,IA,LL,
     1KK,JB,JJ,MA,MB,ID
      WRITE(1) DX,DY,DT,SS,TS
      NM1=N-1
```

```
      NM2=N-2
      LM1=L-1
      RA=(DT/DX)**2
      RB=0.25*(DT**2)/(DX*DY)
      RC=(DT/DY)**2
      READ(5,100)(AX(I),AT(I),I=1,NC)
      CALL POLYG(L,DX,AX,AT,NC,0.0,RH,KR)
      WRITE(6,110)(I,AX(I),AT(I),I=1,NC)
      READ(5,100)(AX(I),AT(I),I=1,NC)
      CALL POLYG(L,DX,AX,AT,NC,0.0,S,KS)
      WRITE(6,110)(I,AX(I),AT(I),I=1,NC)
      READ(5,100)(AX(I),AT(I),I=1,NC)
      CALL POLYG(L,DX,AX,AT,NC,0.0,C,KC)
      WRITE(6,110)(I,AX(I),AT(I),I=1,NC)
      READ(5,100)(AX(I),AT(I),I=1,NBA)
      CALL POLYG(L,DX,AX,AT,NBA,0.0,BA,KB)
      XL=AX(2)
      READ(5,100)(AX(I),AT(I),I=1,NBB)
      CALL POLYG(M,DY,AX,AT,NBB,0.0,BR,KZ)
      READ(5,100)(AX(I),AT(I),I=1,NF)
      CALL POLYG(100,DT,AX,AT,NF,0.0,FI,KF)
      DO 1 I=1,L
      Z=I-1
      X(I)=Z*DX
      IF(X(I).GT.XL) GO TO 3
      DO 2 J=1,M
    2 B(I,J)=RB(J)
      GO TO 1
    3 DC 4 J=1,M
      IF(BA(I).GT.BB(J)) GO TO 5
      B(I,J)=BB(J)
      GO TO 4
    5 B(I,J)=BA(I)
    4 CONTINUE
    1 CONTINUF
      WRITE(6,101)KC
      WRITE(6,102)(I,X(I),C(I),I=1,L)
      WRITE(6,120)KS
      WRITE(6,102)(I,X(I),S(I),I=1,L)
      WRITE(6,121)KR
      WRITE(6,102)(I,X(I),RH(I),I=1,L)
      WRITE(6,103)KB
      WRITE(6,102)(I,X(I),BA(I),I=1,L)
      DO 6 J=1,M
      Z=J-1
      Y(J)=Z*DY
      DO 7 K=1,LL
      IF(J.LT.MA.OR.J.GT.MB) GO TO 8
```

111

```
      F(J,K)=FI(K)
      GO TO 7
8     F(J,K)=0.0
7     CONTINUE
6     CONTINUE
      TM=RH(IA)*(S(IA)**2)
      TL=RH(IA)*((C(IA)**2)-2.0*TM
      TK=TL+(2.0*TM)/3.0
      C2=C(1)**2
      S2=S(1)**2
      AAA=C2*RC
      AAB=S2*RC
      AAC=2.0*C(1)*(C(2)-C(1))
      AAD=2.0*S(1)*(S(2)-S(1))
      AAF=S2*RC
      DM=(2.0*AAD+S2)*RH(1)
      DL=(2.0*AAC+C2)*RH(1)-2.0*DM
      AA(1)=2.0*(1.0-AAA-AAB)
      AB(1)=AAA+0.25*(DL+2.0*DM)*RA
      AC(1)=AAA-0.25*(DL+2.0*DM)*RA
      AD(1)=AAB
      AE(1)=DL*RB
      AF(1)=(C2-S2)*RB
      AH(1)=2.0*(1.0-AAE-AAF)
      AI(1)=AAF+0.25*DM*RA
      AJ(1)=AAF-0.25*DM*RA
      AK(1)=AAE
      AL(1)=DM*RB
      DO 17 I=2,LM1
      C2=C(I)**2
      S2=S(I)**2
      AAA=C2*RA
      AAB=S2*RC
      AAC=C(I)*(C(I+1)-C(I-1))
      AAD=S(I)*(S(I+1)-S(I-1))
      AAF=C2*RA
      AAG=RH(I+1)-RH(I-1)
      DM=2.0*RH(I)*AAD+S2*AAG
      DL=2.0*RH(I)*AAC+C2*AAG-2.0*DM
      AA(I)=2.0*(1.0-AAA-AAB)
      AB(I)=AAA+0.25*(DL+2.0*DM)*RA
      AC(I)=AAA-0.25*(DL+2.0*DM)*RA
      AD(I)=AAB
      AE(I)=DL*RB
      AF(I)=(C2-S2)*RB
      AH(I)=2.0*(1.0-AAE-AAF)
```

```fortran
      AI(I)=AAF+0.25*DM*RA
      AJ(I)=AAF-C.25*DM*RA
      AK(I)=AAF
   17 AL(I)=DM*RB
      DO 10 K=1,3
      DO 10 I=1,L
      DO 10 J=1,M
      U(I,J,K)=0.0
      V(I,J,K)=0.0
   10 LOS=10
      NN=1
      DO 20 J=1,KK
      PD(J)=C.0
      PS(J)=0.00
      PQ(J)=0.00
   20 PR(J)=0.0
      DO 21 I=1,2
      DO 21 J=1,KK
   21 WRITE(1)PD(J),PS(J),PQ(J),PR(J)
      DO 12 K=3,N
  506 GO TO(601,6C2,603,604),NN
  601 LI=3
      LJ=2
      LK=1
      GO TO 605
  602 LI=1
      LJ=3
      LK=2
      GO TO 605
  603 LI=2
      LJ=1
      LK=3
      GO TO 605
  604 NN=1
      GO TO 606
  605 DO 13 J=1,M
      IF(J.EQ.1.OR.J.EQ.M) GO TO 15
      IF(K.GT.LL) GO TO 600
      UA=2.0*DX*(F(J+1,K)-F(J-1,K))
      AG=2.0*DX*F(J,K)
      GO TO 607
  600 UA=0.0
      AG=0.0
  607 BP=0.50*B(1,J)*DT
      BM=1.-BP
      BP=1.+BP
      U(1,J,LI)=(U(1,J,LJ)*AA(1)+U(2,J,LJ)*AB(1)+AC(1))-AG*AC(1)
     1+(U(1,J+1,LJ)+U(1,J-1,LJ)-V(1,J-1,LJ))*AD(1)+(V(1,J+1,LJ)-V(1,J-1,LJ))*AE(1)
```

```
      2-U(I,J,LK)*RP)/BM
      V(I,J,LI)=(V(I,J,LJ)+U(2,J,LJ)*AH(I)+V(2,J,LJ)*(AI(I)+AJ(I))
     1+(V(I,J+1,LJ)+V(I,J-1,LJ))*AK(I)+(U(1,J+1,LJ)-U(1,J-1,LJ))*AL(I))
     2+UA*AF(I)-V(I,J,LK)*BP)/BM
      DC 14 I=2,LCS
      BP=0.50*B(I,J)*DT
      BM=1.-BP
      BP=1.+BP
      UA=U(I+1,J+1,LJ)+U(I-1,J-1,LJ)-U(I-1,J+1,LJ)-U(I+1,J-1,LJ)
      VA=V(I+1,J+1,LJ)+V(I-1,J-1,LJ)-V(I-1,J+1,LJ)-V(I+1,J-1,LJ)
      U(I,J,LI)=(U(I,J,LJ)+U(I,J,LJ)*AA(I)+U(I+1,J,LJ)*AB(I)+U(I-1,J,LJ)*AC(I)
     1+(U(I,J+1,LJ)+U(I,J-1,LJ))*AH(I)+V(I+1,J,LJ)-V(I-1,J,LJ))*AE(I)
     2+VA*AF(I)-U(I,J,LK)*BP)/BM
      V(I,J,LI)=(V(I,J,LJ)+V(I,J,LJ)*AH(I)+V(I+1,J,LJ)*AI(I)+V(I-1,J,LJ)*AJ(I)
     1+(V(I,J+1,LJ)+V(I,J-1,LJ))*AK(I)+(U(I,J+1,LJ)-U(I,J-1,LJ))*AL(I)
     2+UA*AF(I)-V(I,J,LK)*BP)/BM
   14 CONTINUE
      U(L,J,LI)=0.0
      V(L,J,LI)=0.0
      GO TO 13
   15 DO 16 I=1,L
      U(I,J,LI)=0.0
   16 V(I,J,LI)=0.0
   13 CONTINUE
      JA=JB
      DO 28 J=1,KK
      PXX=(U(IA+1,JA,LI)-U(IA-1,JA,LI))*(0.5/DX)
      PXY=(U(IA,JA+1,LI)-U(IA,JA-1,LI))*(0.5/DY)
      PYX=(V(IA+1,JA,LI)-V(IA-1,JA,LI))*(0.5/DY)
      PYX=(V(IA,JA+1,LI)-V(IA,JA-1,LI))*(0.5/DX)
      PD(J)=(PXX+PYY)*SS*TK
      PS(J)=(PYX+PXY)*SS*TM
      PQ(J)=U(ID,JA,LI)*SS
      PR(J)=V(ID,JA,LI)*SS
      WRITE(1) PD(J),PS(J),PQ(J),PR(J)
   28 JA=JA+JJ
      NN=NN+1
      IF(LOS.EQ.LM1) GO TO 12
      LCS=LOS+1
   12 CCNTINUE
   25 DO 26 K=1,N
      Z=K-1
   26 T(K)=Z*DT*TS
      WRITE(6,104)KZ
      WRITE(6,102)(J,Y(J),BB(J),J=1,M)
      WRITE(6,105)KF
      WRITE(6,102)(K,T(K),FI(K),K=1,LL)
  100 FORMAT(2F10.0)
```

114

```fortran
101   FORMAT(1H1,6X,'KC=',I7//)
102   FORMAT(10X,I4,2F15.5)
103   FORMAT(1H1,6X,'KB=',I7///)
104   FORMAT(1H1,6X,'KZ=',I7///)
105   FORMAT(1H1,6X,'KF=',I7///)
106   FORMAT(15I5)
107   FORMAT(5F10.0)
108   FORMAT(11A4)
110   FORMAT('0',10X,I4,2F10.3/)
120   FORMAT(1H1,6X,'KS=',I7//)
121   FORMAT(1H1,6X,'KR=',I7//)
200   FORMAT('1',10X,11A4,6X,'A4//20X,'L:',I5/20X,'M:',I5/20X,'N:',I5/
     120X,'NC:',I4/20X,'NBA:',I3/20X,'NBB:',I3/20X,'NF:',I4/20X,'IA:',I5/
     2I4/20X,'LL:',I4/20X,'KK:',I4/20X,'JB:',I4/20X,'JJ:',I4/20X,
     3'MA:',I4/20X,'MB:',I4/20X,'ID:',I4//)
201   FORMAT(20X,'DX:',F10.5/20X,'DY:',F10.5/20X,'DT:',F10.5/20X,
     1'SS:',F8.3/20X,'TS:',F8.3//)
      STOP
      END
```

```
C      SEISMOGRAM PLOTTING PROGRAM
C      THIS PROGRAM IS USED IN CONJUNCTION WITH THE TWO DIMENSIONAL
C      SEISMIC MODEL TO PRODUCE THE SYNTHETIC SEISMOGRAMS. THE DATA
C      IS READ FROM THE STORAGE DEVICE (TAPE, DISK OR DRUM) CONVERTED
C      TO VECTOR FORMAT AND PLOTTED ON THE CALCOMP 765 PLOTTER.
C
C      PARAMETER LIST:
C
C      PS:   SCALING FACTOR FOR THE PLOTTED VALUES.
C
C      BT:   SPACE IN INCHES BETWEEN SEPARATE SEISMOGRAMS.
C
C      TT:   TIME AXIS SCALE IN UNITS PER INCH.
C
C      YSP:  SPACING IN INCHES BETWEEN INDIVIDUAL TRACES.
C
C      XSP:  SPACING IN INCHES BETWEEN TIME GRID LINES.
C
C      TID,TIS,TIQ,TIR: TITLES FOR THE FOUR SEISMOGRAMS, LIMITED
C      TO 24 CHARACTERS. ADDITIONALLY, THE TITLE GTI FROM THE
C      MAIN PROGRAM IS WRITTEN ON THE TRACES.
C
       DATA TI/'TIME'/
       DIMENSION D(25,800),GTI(11),T(800),P(800),
      1TID(6),TIS(6),TIR(6),TIR(11),I=1,11),XG(100),YG(100),TIQ(6)
      1READ(1)(GTI(I),I=1,11),GG,L,M,N,NC,NRA,NBB,NF,IA,LL,
      1KK,JB,JJ,MA,MB,ID
       READ(1)DX,DY,DT,SS,TS
       READ(5,100) PS,BT,TT,YSP,XSP
       READ(5,101)(TID(I),I=1,6)
       READ(5,101)(TIS(I),I=1,6)
       READ(5,101)(TIQ(I),I=1,6)
       READ(5,101)(TIR(I),I=1,6)
       WRITE(6,200)(GTI(I),I=1,11),GG,L,M,N,NC,NBA,NBB,NF,IA,
      1LL,KK,JB,JJ,MA,MB,ID
       WRITE(6,201) DX,DY,DT,SS,TS
       WRITE(6,202) PS,BT,TT,YSP,XSP
       DO 1 K=1,N
       DO 2 J=1,KK
       READ(1) D(J,K),DD,DD,DD
     2 CONTINUE
     1 REWIND 1
       NN=1
       DO 3 K=1,N,2
       V=K-1
       T(NN)=V*DT*TT
       NN=NN+1
     3 V=KK
```

```
YLG=V*YSP
V=N
XLG=V*DT*TT
XPP=XLG+0.4C
XPO=XPP+0.5C
TINC=1.0/TT
CALL GRID(C.O,XLG,0.0,YLG,XSP,YSP,XG,YG,KA,LO)
WRITE(6,220)KA
WRITE(6,221)(I,XG(I),YG(I),I=1,KA)
CALL PLOTS
CALL SYMBOL(1.0,-2.,14,'C.D.LODGE  BOX 96  QT',0.0,20)
CALL PLOT(0.1,0.,-3)
CALL LINE(XG,YG,KA,1,1)
CALL SYMBOL(XPP,0.,0.14,TID,90.0,74)
CALL SYMBOL(XPP,3.,14,GTI,90.,44)
CALL SYMBOL(XPO,0.1,0.14,GG,90.0,4)
DO 5 J=1,KK
NN=1
DO 6 K=1,N,2
P(NN)=D(J,K)*PS
IF(ABS(P(NN)).LT.1.0) GO TO 6
WRITE(6,225) P(NN)
P(NN)=1.0
WRITE(6,224) TID,K,NN,J
NN=NN+1
6 NN=NN-1
5 CALL LINE(T,P,NN,1,1)
CALL PLOT(0.0,YSP,-3)
CALL PLOTE
31 WRITE(6,603) TID
1KK,JB,JJ,MA,MB,ID
READ(1)(GTI(I),I=1,11),GG,L,M,N,NC,NBA,NBB,NF,IA,LL,
READ(1)DX,DY,DT,SS,TS
DO 13 K=1,N
14 READ(1) DD,D(J,K),DD,DD
DO 14 J=1,KK
13 CONTINUE
REWIND 1
CALL PLOTS
CALL SYMBOL(1.0,-2.,14,'C.D.LODGE  BOX 96  QT',0.0,20)
CALL PLOT(0.1,0.,-3)
CALL LINE(XG,YG,KA,1,1)
CALL SYMBOL(XPP,0.0,0.14,TIS,90.0,24)
CALL SYMBOL(XPP,3.,14,GTI,90.,44)
CALL SYMBOL(XPO,0.1,0.14,GG,90.0,4)
DO 7 J=1,KK
NN=1
```

```
      DO 8 K=1,N,2
      P(NN)=D(J,K)+PS
      IF(ABS(P(NN)).LT.1.0) GO TO 8
      WRITE(6,225) P(NN)
      P(NN)=1.0
      WRITE(6,224) TIS,K,NN,J
    8 NN=NN+1
      NN=NN-1
    7 CALL LINE(T,P,NN,1,1)
      CALL PLOT(0.0,YSP,-3)
      CALL PLOT(0.0,BT,-3)
      CALL PLOTE
      WRITE(6,603) TIS
      READ(1)(GTI(I),I=1,11),GG,L,M,N,NC,NBA,NRB,NF,IA,LL,
     1KK,JB,JJ,MA,MB,ID
      READ(1)DX,DY,DT,SS,TS
      DO 15 K=1,N
   16 READ(1) DD,DD,D(J,K),DD
   15 CONTINUE
      REWIND 1
      CALL PLOTS
      CALL SYMBOL(1.0,-2.,14,'C.D.LODGE   BOX  96  QT',0.0,20)
      CALL PLOT(0.1,0.,-3)
      CALL LINE(XG,YG,KA,1,1)
      CALL SYMBOL(XPP,0.0,0.14,TIQ,90.0,24)
      CALL SYMBOL(XPP,3.1,14,GTI,90.,44)
      CALL SYMBOL(XPO,0.1,0.14,GG,90.0,4)
    9 J=1,KK
      NN=1
   10 DO 10 K=1,N,2
      P(NN)=D(J,K)*0.5*PS
      IF(P(NN).LT.10.0) GO TO 10
      WRITE(6,225) P(NN)
      P(NN)=0.0
      WRITE(6,224) TIQ,K,NN,J
   10 NN=NN+1
      NN=NN-1
    9 CALL LINE(T,P,NN,1,1)
      CALL PLOT(0.0,YSP,-3)
      CALL PLOT(0.0,BT,-3)
      CALL PLOTE
      WRITE(6,603) TIQ
      READ(1)(GTI(I),I=1,11),GG,L,M,N,NC,NBA,NBB,NF,IA,LL,
     1KK,JB,JJ,MA,MB,ID
      READ(1)DX,DY,DT,SS,TS
      DO 17 K=1,N
   18 DO 18 J=1,KK
```

```fortran
18  READ(1) DD,CD,DD,D(J,K)
17  CONTINUE
    REWIND 1
    CALL PLOTS
    CALL SYMBOL(1.0,-2.,.14,'C,D,LODGE   BOX 96 QT',0.0,20)
    CALL PLOT(0.,1.,-3)
    CALL LINE(XG,YG,KA,1,1)
    CALL SYMBOL(XPP,0.0,.14,TIR,90.0,24)
    CALL SYMBOL(XPP,3.,.14,GTI,90.,44)
    CALL SYMBOL(XPO,0.,1.0,.14,GG,90.0,4)
    DO 11 J=1,KK
    NN=1
    DO 12 K=1,N,2
    P(NN)=D(J,K)*0.5*PS
    IF(P(NN).LT.10.0) GO TO 12
    WRITE(6,225) P(NN)
    P(NN)=0.0
    WRITE(6,224) TIR,K,NN,J
    NN=NN+1
12  NN=NN-1
11  CALL LINE(T,P,NN,1,1)
    CALL PLOT(0.0,YSP,-3)
    CALL PLOTE(0.0,BT,-3)
    WRITE(6,603) TIR
100 FORMAT(6A4)
101 FORMAT(5F10.0)
200 FORMAT(1.,10X,11A4,6X, A4//20X,'L:',I5/20X,'M:',I5/20X,'N:',I5/
   120X,'NC:',I4/20X,'NBA:',I3/20X,'NBB:',I3/20X,'NF:',I4/20X,'IA:',I5/
   214/20X,'LL:',I4/20X,'KK:',I4/20X,'JR:',I4/20X,'JJ:',I4/20X,
   3'MA:',I4/20X,'MB:',I4/20X,'ID:',I4//)
201 FORMAT(20X,'DX:',F10.5/20X,'DY:',F10.5/20X,'DT:',F10.5/20X,
   1'SS:',F8.3/20X,'TS:',F8.3)
202 FORMAT(20X,'PS:',F7.3/20X,'BT:',F8.3/20X,'TT:',F8.3/20X,
   1'YSP:',F7.3/20X,'XSP:',F7.3/20X,'KA=',I4//)
220 FORMAT(I6,2F12.5)
221 FORMAT(I6,2F12.5)
224 FORMAT(10X,6A4,3I7)
225 FORMAT(3X,F20.3)
601 FORMAT(1X,'C:',I4,2X,12F10.5)
602 FORMAT(1X,'R:',I4,2X,12F10.5)
603 FORMAT('0'//6X,6A4,'GRAM COMPLETE'/)
    STOP
    END
```

```
C      SUBROUTINE POLYG(N,DX,F,G,NS,XI,P,L)
C
C      PURPOSE
C            TO EVALUATE A FUNCTION APPROXIMATED BY A POLYGON OF 20 OR
C            LESS STRAIGHT LINE SEGMENTS
C
C            THE ORDINATES ARE GENERATED BY ADDING MULTIPLES OF AN
C            INCREMENT DX TO A BASE VALUE XI.
C
C            THE OUTPUT ARRAY OF ABCISSAE IS GENERATED BY REPEATED
C            SOLUTION OF :  P = AX + B.
C
C      DESCRIPTION OF PARAMETERS:
C
C      N:    NUMBER OF POINTS AT WHICH P IS TO BE DETERMINED.  N.LE.900.
C
C      DX:   SIZE OF X INCREMENT.
C
C      F:    ARRAY OF X-COORDINATES OF THE POINTS THROUGH WHICH THE
C            APPROXIMATING POLYGON PASSES.
C
C      G:    ARRAY OF Y-COORDINATES OF THE POINTS THROUGH WHICH THE
C            APPROXIMATING POLYGON PASSES.
C
C      NS:   NUMBER OF POLYGONAL POINTS.  NS.LE.20.
C
C      XI:   INITIAL X-COORDINATE.  XI.GE.F(1).
C
C      P:    OUTPUT ARRAY OF Y-COORDINATES ON THE POLYGON CORRESPONDING
C            TO X-COORDINATES OF I*DX; WHERE  I = 1,N
C
C      L:    OUTPUT PARAMETER INDICATING SUCCESS OF COMPLETION OF THE
C            SUBROUTINE
C            L=0   SUBROUTINE SUCCESSFULLY COMPLETED.
C            L=1   SUBROUTINE TERMINATED PRIOR TO COMPLETION.
C
       SUBROUTINE POLYG(N,DX,F,G,NS,XI,P,L)
       DIMENSION A(20),B(20),F(20),G(20),X(900),P(900),C(20),D(20)
       L=0
       NSM = NS-1
       EPS=0.001
       IF(XI.LT.F(1)) GO TO 2
       IF(N.GT.900) GO TO 2
       II=0
       DO 1 I=1,NSM
```

```
      GG=F(I+1)-F(I)
      IF(ABS(GG).LT.EPS) GO TO 1
      II=II+1
      C(II)=F(I)
      D(II)=G(I)
    1 CONTINUE
      C(II+1)=F(NS)
      D(II+1)=G(NS)
      DO 5 I=1,II
      GG=C(I+1)-C(I)
      GM=D(I+1)-D(I)
      A(I)=GM/GG
    5 B(I)=(C(I+1)*D(I)-C(I)*D(I+1))/GG
      DO 11 I=1,N
      Z = I-1
      X(I)=XI+Z*DX
   11 CONTINUE
      K=1
    4 DO 3 I=1,II
      IF(X(K).GT.C(I+1)) GO TO 3
      P(K)=A(I)*X(K)+B(I)
      K=K+1
      IF(K.GT.N) GO TO 6
      GO TO 4
    3 CONTINUE
    6 RETURN
    2 L=1
      RETURN
      END
```

```
SUBROUTINE GRID(XMIN,XMAX,YMIN,YMAX,GX,GY,X,Y,KA,L)
  THIS SUBROUTINE GENERATES A SEQUENCE OF POINTS (X,Y)
  WHICH MAY BE USED TO PLOT A GRID ON A CALCOMP PLOTTER
  GRAPH

  DESCRIPTION OF PARAMETERS:

    INPUT PARAMETERS:

      XMIN:  MINIMUM VALUE OF THE X COORDINATE TO BE
             GRIDDED.  IN INCHES.

      XMAX:  MAXIMUM VALUE OF THE X COORDINATE TO BE
             GRIDDED.  IN INCHES.

      YMIN:  MINIMUM VALUE OF THE Y COORDINATE TO BE
             GRIDDED.  IN INCHES.

      YMAX:  MAXIMUM VALUE OF THE Y COORDINATE TO BE
             GRIDDED.  IN INCHES.

      GX:    HORIZONTAL (X) GRID SPACING.  IN INCHES.

      GY:    VERTICAL (Y) GRID SPACING.  IN INCHES.

    OUTPUT PARAMETERS:

      X:     VECTOR OF ORDINATES.  DIMENSIONED .LE.500.

      Y:     VECTOR OF ABCISSAE.  DIMENSIONED .LE.500.

      KA:    NUMBER OF GRID POINTS (X,Y PAIRS) GENERATED.
             KA.LE.500.

      L:     PARAMETER INDICATING SUCCESS OF SUBROUTINE:

             L=0   SUBROUTINE SUCCESSFULLY COMPLETED.
             L=1   SUBROUTINE NOT FULLY COMPLETED.
             L=2   KA OUT OF RANGE.

  NOTE:  A 6 BY 10 INCH GRID OF ONE INCH SQUARES REQUIRES
         36 POINTS.
         AN 8 BY 60 INCH GRID OF HALF INCH SQUARES REQUIRES
         280 POINTS.
```

```
      SUBROUTINE GRID(XMIN,XMAX,YMIN,YMAX,GX,GY,X,Y,KA,L)
      DIMENSION X(500),Y(500)
      L=1
      A=0.0
      I=1
1     X(I)) = XMIN
      Y(I)) = YMIN + A*GY
      X(I+1)) = XMAX
      Y(I+1)) = YMIN + A*GY
      KA=I+2
      IF(KA.GT.500) GO TO 5
      IF(Y(I+1).GE.YMAX) GO TO 2
      X(I+2)) = XMAX
      Y(I+2)) = YMIN + (A+1.0)*GY
      X(I+3)) = XMIN
      Y(I+3)) = YMIN + (A+1.0)*GY
      KA=I+4
      IF(KA.GT.500) GO TO 5
      IF(Y(I+3).GE.YMAX) GO TO 2
      I=I+4
      A=A+2.0
      GO TO 1
2     A=0.0
      I=KA
3     X(I)) = XMIN + A*GX
      Y(I)) = YMAX
      X(I+1)) = XMIN + A*GX
      Y(I+1)) = YMIN
      KA=I+2
      IF(KA.GT.500) GO TO 5
      IF(X(I+1).GE.XMAX) GO TO 4
      X(I+2)) = XMIN + (A+1.0)*GX
      Y(I+2)) = YMIN
      X(I+3)) = XMIN + (A+1.0)*GX
      Y(I+3)) = YMAX
      KA=I+3
      IF(KA.GT.500) GO TO 5
      IF(X(I+3).GE.XMAX) GO TO 4
      I=I+4
      A=A+2.0
      GO TO 3
4     L=0
      RETURN
5     L=2
      RETURN
      END
```

```
C     SUBROUTINE CONPLT(L,M,K,NH,DX,DY,GS)
C
C     THIS SUBROUTINE IS USED IN COMMON WITH THE TWO DIMENSIONAL
C     SEISMIC MODEL TO GENERATE A PRINTER CONTOUR PLOT OF A SELECTED
C     VARIABLE OVER THE ENTIRE MESH. THE CALLING PROGRAM MUST PROVIDE
C     PRINTER PAGINATION AND TITLE IF DESIRED. THE SUBROUTINE ACCEPTS
C     HORIZONTAL AND VERTICAL DISPLACEMENT VALUES AND COMPUTES VALUES
C     AS REQUIRED. WHEN STRESSES OR VORTICITY ARE DESIRED, THE SUBROUTINE
C     REDUCES THE MATRIX BY ONE ROW AND COLUMN AND PRINTS 0'S ALONG THE
C     TOP AND LEFT BORDERS OF THE MATRIX.
C
C     PARAMETER LIST:
C
C     K:    MATRIX LEVEL TO BE CONTOURED (K=1,2 OR 3).
C
C     SYM:  VECTOR OF 42 ALPHA-NUMERIC CHARACTERS TO BE USED TO
C           REPRESENT THE VALUES CONTOURED.
C
C     GS:   SCALING FACTOR TO BE APPLIED TO THE CONTOURED QUANTITY.
C
C     NH:   INPUT PARAMETER SPECIFYING THE OUTPUT VARIABLE
C           ZZ WHICH IS PLOTTED BY THE SUBROUTINE.
C
C              NH=1:  VERTICAL DISPLACEMENT.
C              NH=2:  HORIZONTAL DISPLACEMENT.
C              NH=3:  DILATATION.
C              NH=4:  SHEAR.
C              NH=5:  ROTATION.
C
C     ALL OTHER PARAMETERS ARE DISCUSSED IN THE CALLING PROGRAM.
C
      SUBROUTINE CONPLT(L,M,K,NH,DX,DY,GS)
C
      COMMON U,V,SYM,ZZ,C,S,RH
      DIMENSION U(71,81,3),V(71,81,3),SYM(42),ZZ(81),RH(71),
     1C(71),S(71)
      DO 500 I=1,L
      TM=RH(I)*(S(I)**2)
      TL=RH(I)*(C(I)**2)-2.0*TM
      TK=TL+(2.0*TM)/3.0
      DO 501 J=1,M
      GO TO (505,511,506,507,512),NH
  505 KO=(U(I,J,K)*GS+2.05)*10.0+1.0
      IF(KO.LT.1) GO TO 502
      IF(KO.GT.41) GO TO 503
      GO TO 504
```

124

```
506   IF(I.EQ.1.OR.J.EQ.1) GO TO 510
      D=((U(I,J,K)-U(I-1,J,K))/DX+(V(I,J,K)-V(I,J-1,K))/DY)*TK
      KC=(D*GS+2.05)*10.0+1.0
      GO TO 509
510   KC=21
      GO TO 504
511   KO=(V(I,J,K)*GS+2.05)*10.0+1.0
      GO TO 509
507   IF(I.EQ.1.OR.J.EQ.1) GO TO 508
      D=((V(I,J,K)-V(I-1,J,K))/DX+(U(I,J,K)-U(I,J-1,K))/DY)*TM
      KC=(D*GS+2.05)*10.0+1.0
      GO TO 509
508   KO=21
      GO TO 504
512   IF(I.EQ.1.OR.J.EQ.1) GO TO 513
      D=((V(I,J,K)-V(I-1,J,K))/DX-(U(I,J,K)-U(I,J-1,K))/DY)*TM
      KC=(D*GS+2.05)*10.0+1.0
      GO TO 509
513   KO=21
      GO TO 504
502   ZZ(J)=SYM(42)
      GO TO 501
503   ZZ(J)=SYM(41)
      GO TO 501
504   ZZ(J)=SYM(KC)
501   CONTINUE
      WRITE(6,402)(I,(ZZ(J),J=1,M))
500   CONTINUE
      WRITE(6,410)
      WRITE(6,411)
402   FORMAT(10X,I2,2X,81A1)
410   FORMAT(...12X,'0',9X,'1',9X,'2',9X,'3',9X,'4',9X,'5',9X,
     1'6',9X,'7',9X,'8')
411   FORMAT(13X,'0',8(9X,'0'))
      RETURN
      END
```

LIST OF REFERENCES

Alterman, Z.S. and Karal, F.C., 1968, Propagation of Elastic Waves in Layered Media by Finite Difference Methods, Bulletin of the Seismological Society of America, v. 58, n. 1, pp. 367-398.

Alterman, Z.S. and Rotenberg, A., 1969, Seismic Waves in a Quarter Plane, Bulletin of the Seismological Society of America, v. 59, n. 1, pp. 347-368.

Bullen, K.E., 1959, An Introduction to the Theory of Seismology, Cambridge University Press.

Constantino, C.J., 1969, Two Dimensional Wave Propagation through Non-linear Media, Journal of Computational Physics, v. 4, n. 3, pp. 147-170.

Dobrin, M.B., 1960, Introduction to Geophysical Prospecting, McGraw-Hill.

Forsythe, G.E. and Wasow, W.R., 1967, Finite Difference Methods for Partial Differential Equations, John Wiley.

Fox, L., and others, 1962, Numerical Solution of Ordinary and Partial Differential Equations, Pergamon Press.

Grant, F.S. and West, G.F., 1965, Interpretation Theory in Applied Geophysics, McGraw-Hill.

Gupta, R.N., 1966a, Reflection of Elastic Waves from a Linear Transition Layer, Bulletin of the Seismological Society of America, v. 56, n. 2, pp. 511-526.

_____, 1966b, Reflection of Plane Elastic Waves from Transition Layers with Arbitrary Variation of Velocity and Density, Bulletin of the Seismological Society of America, v. 56, n. 3, pp. 633-642.

Officer, C.B., 1958, Introduction to the Theory of Sound Transmission, McGraw-Hill.

Sengbush, R..L., Lawrence, P.L. and McDonal, F.J., 1961, Interpretation of Synthetic Seismograms, Geophysics, v. 26, n. 2, pp. 138-157.

Smith, G.D., 1965, Numerical Solution of Partial Differential Equations, Oxford University Press.

Takeuchi, H., 1966, Theory of the Earth's Interior, Blaisdell.

Tooley, R.D., Spencer, T.W. and Sagoci, H.F., 1965, Reflection and Transmission of Plane Compressional Waves, Geophysics, v. 30, n. 4, pp. 552-570.

United States Naval Postgraduate School Computer Facility, 1969, Technical Note 0211-03, Plotting Package for NPGS IBM 360/67, by P. C. Johnson.

Wolf, A., 1937, The Reflection of Elastic Waves from Transition Layers of Variable Velocity, Geophysics, v. 2, n. 4, pp. 357-363.

INITIAL DISTRIBUTION LIST

No. Copies

1. Defense Documentation Center   20
    Cameron Station
    Alexandria, Virginia 22314

2. Library, Code 0212   2
    Naval Postgraduate School
    Monterey, California 93940

3. Professor R. S. Andrews   5
    Department of Oceanography
    Naval Postgraduate School
    Monterey, California 93940

4. Department of Oceanography   3
    Naval Postgraduate School
    Monterey, California 93940

5. Oceanographer of the Navy   1
    The Madison Building
    732 N. Washington Street
    Alexandria, Virginia 22314

6. LCDR C. D. Lodge   2
    P.O. Box 274
    Pebble Beach, California 93953

7. Professor J. J. von Schwind   1
    Department of Oceanography
    Naval Postgraduate School
    Monterey, California 93940

DOCUMENT CONTROL DATA - R & D

Security classification of title, body of abstract and indexing annotation must be entered when the overall report is classified)

1 ORIGINATING ACTIVITY (Corporate author)	2a. REPORT SECURITY CLASSIFICATION
Naval Postgraduate School	Unclassified
Monterey, California 93940	2b. GROUP

3 REPORT TITLE

Simplified Numerical Models for the Generation of Synthetic Reflection Profiling Seismograms and Synthetic Reflection/Refraction Seismograms

4 DESCRIPTIVE NOTES (Type of report and inclusive dates)

Master's Thesis; (April 1970)

5 AUTHOR(S) (First name, middle initial, last name)

Charles David Lodge

6 REPORT DATE	7a. TOTAL NO. OF PAGES	7b. NO. OF REFS
April 1970	128	17
8a. CONTRACT OR GRANT NO.	9a. ORIGINATOR'S REPORT NUMBER(S)	
b. PROJECT NO		
c.	9b. OTHER REPORT NO(S) (Any other numbers that may be assigned this report)	
d.		

10 DISTRIBUTION STATEMENT

This document has been approved for public release and sale; its distribution is unlimited.

11 SUPPLEMENTARY NOTES	12. SPONSORING MILITARY ACTIVITY
	Naval Postgraduate School
	Monterey, California 93940

13 ABSTRACT

Two numerical models were developed which generate synthetic seismograms in formats similar to those of records obtained in field exploration. The models solve the hyperbolic wave equations in one and two dimensions by finite difference approximations in initially undeformed solution domains of transversely-isotropic layered media subjected to a time varying, dilatational forcing stress applied at the surface. A velocity attenuation term was included in the models to inhibit strong boundary reflections.

The one-dimensional model produces synthetic reflection profiling seismograms for arbitrary horizontal or dipping layers. The two-dimensional model generates synthetic reflection/refraction seismograms for horizontal layered media with arbitrary distribution of wave velocities, Poisson's ratio and density. Several sample records were produced for some representative velocity structures. The synthetic seismograms were interpreted and gross correlation was carried out as if they were actual field records.

A-31408

14 KEY WORDS	LINK A		LINK B		LINK C	
	ROLE	WT	ROLE	WT	ROLE	WT
Numerical						
Seismic						
Model						

DD FORM 1473 (BACK)
1 NOV 65

S/N 0101-807-6821